

# Dual Readout Method in Calorimetry

Roberto Ferrari  
INFN Pavia

CERN, 7 June 2024

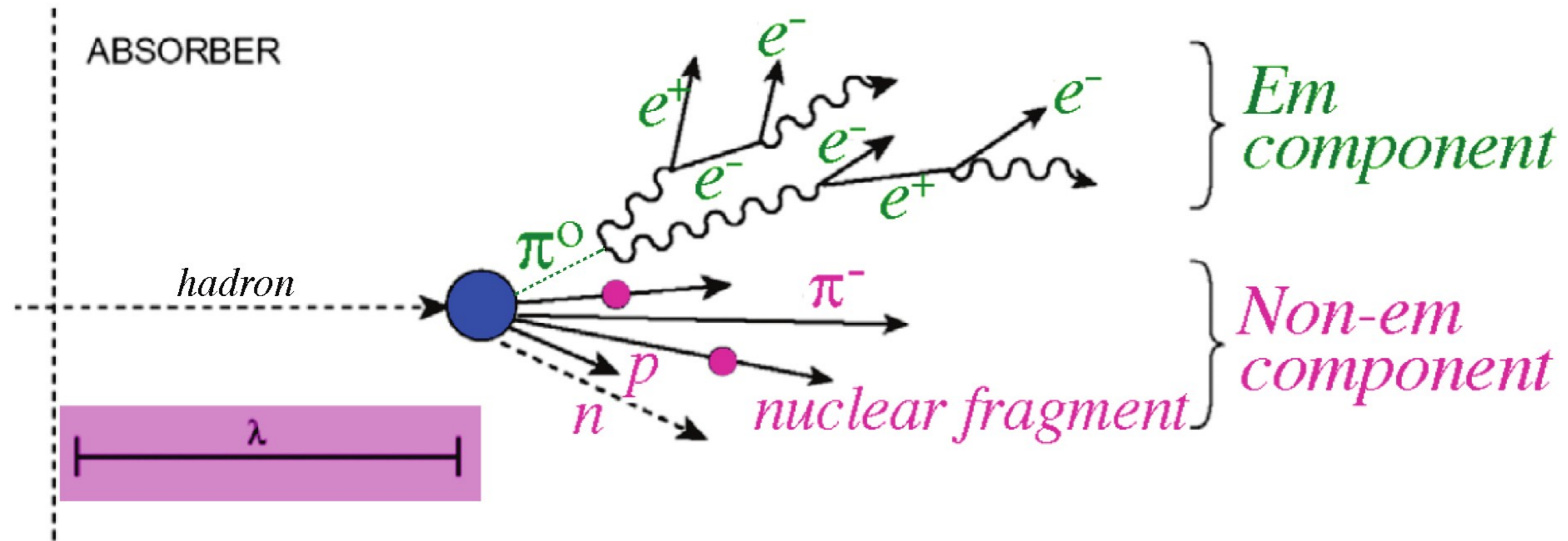
1. Hadron calorimetry issues
2. Dual-readout calorimetry
3. Few DREAM/RD52 results
4. Dual readout goes granular ( IDEA fibre calorimeter )
5. Exploit timing and DNNs
6. Crystal option (IDEA++) and pPFA
7. Next steps

---

# 1. Hadron calorimetry issues

# hadron calorimetry

Due to  $\pi^0$  and  $\eta$  production, hadronic showers develop 2 main components:



hadronic component:  $p$ ,  $n$ ,  $\pi^\pm$ , nuclear fission, ... delayed photons, ...

shower typical size:  $\lambda_1 \sim 35 \text{ g/cm}^2 \cdot A^{1/3}$



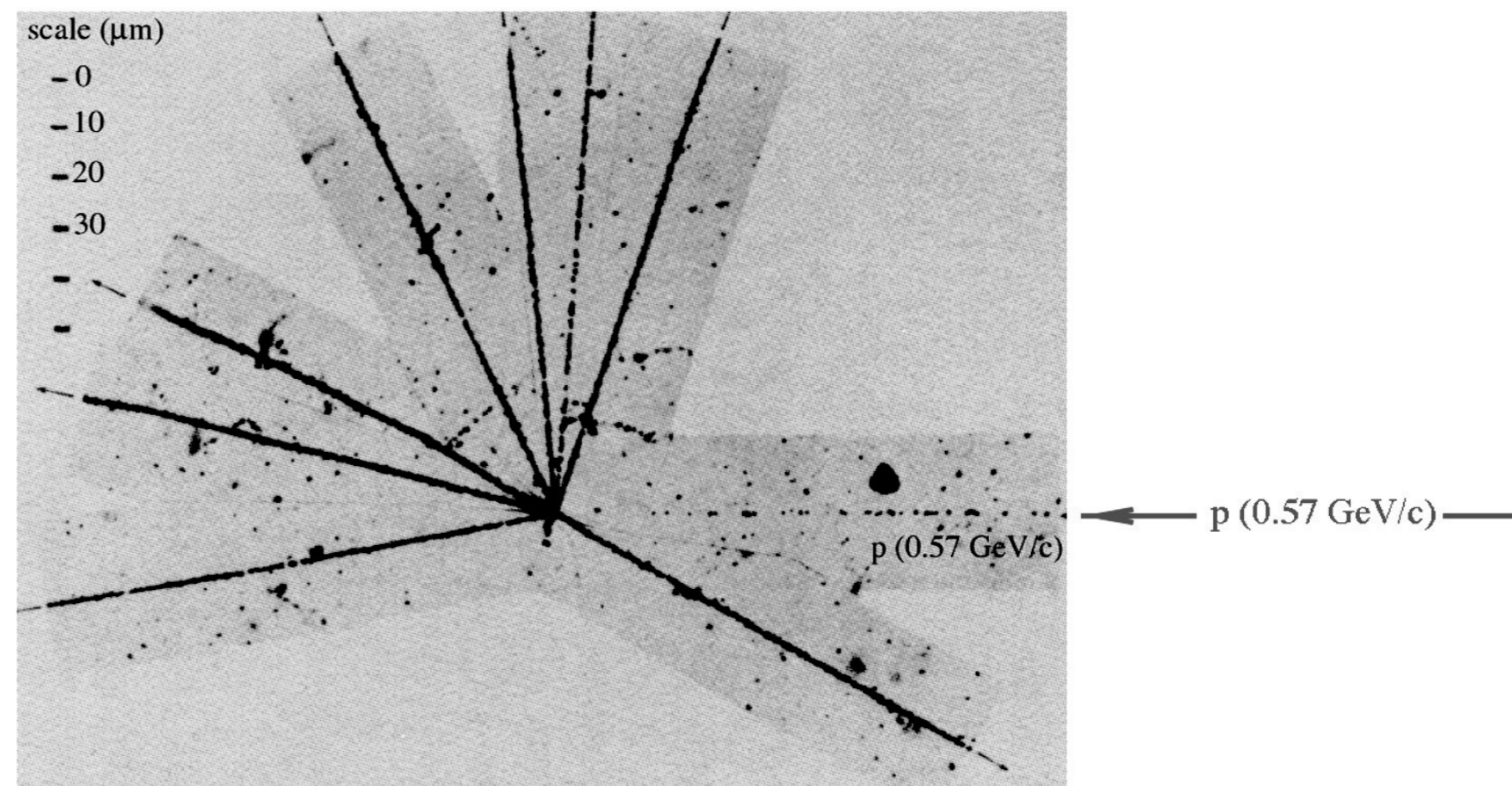
# hadronic showers

- **Electromagnetic (em) component**

- electrons, photons

- **Hadronic (non-em) component**

- charged mesons  $\pi^\pm$ ,  $K^\pm$  [ ~ 20% ]
- nuclear fragments, p [ ~ 25% ]
- neutrons, soft  $\gamma$ 's [ ~ 15% ]
- break-up of nuclei ("invisible") [ ~ 40% ]



average values ... issue: fluctuations!

Many components w/ large fluctuations in relative yield

1. Large non-gaussian fluctuations in em/non-em energy sharing
2. Increase of *em* component with energy
3. Large, non-gaussian fluctuations in "invisible" energy losses

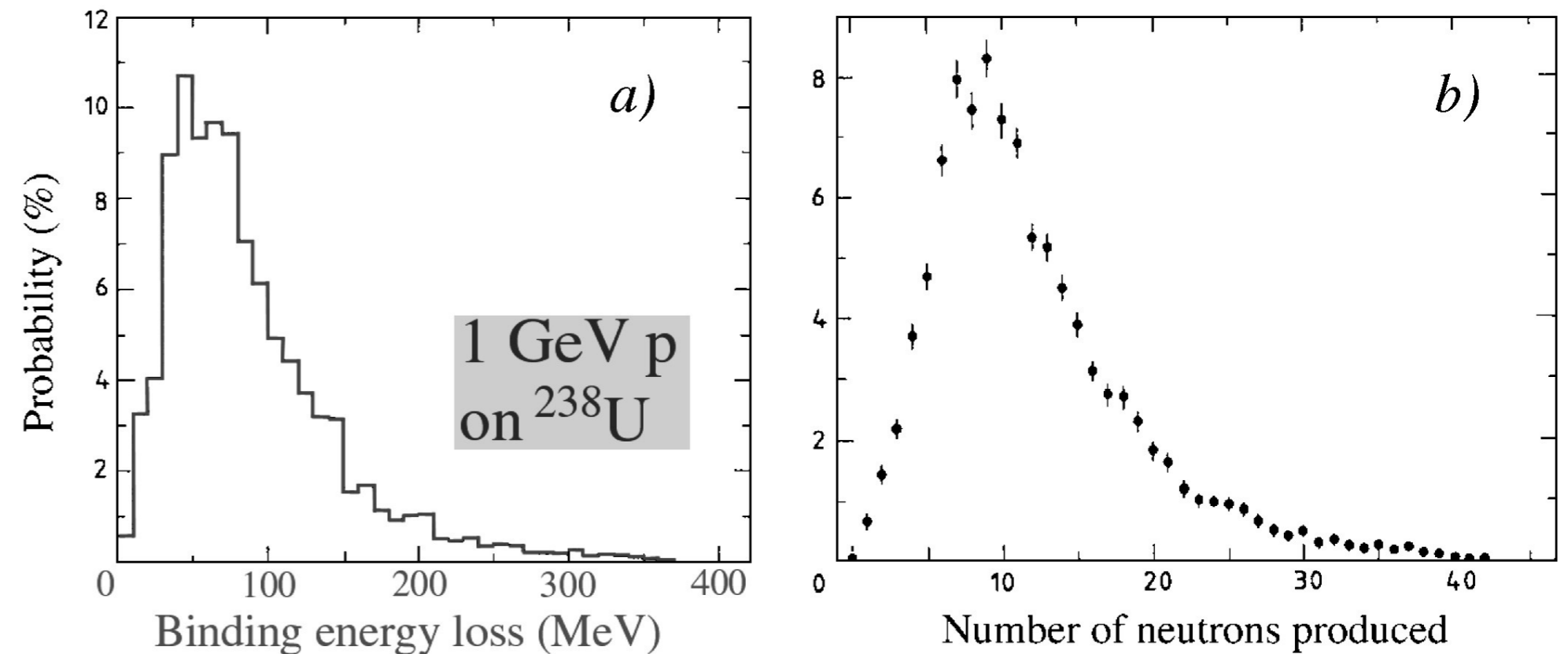
# invisible energy

- ◆ in nuclear reactions, energy lost (binding energy) to free protons and neutrons
- ◆ no measurable signal (invisible energy)
- ◆ on average about 30-40% of non-em shower energy

Large event-by-event fluctuations limit resolution

Correlation between invisible energy and kinetic energy carried by released nucleons

Evaporation nucleons: soft spectrum, mostly neutrons (2-3 MeV)



Wigmans, NIM A259, 389

# em fraction $f_{em}$

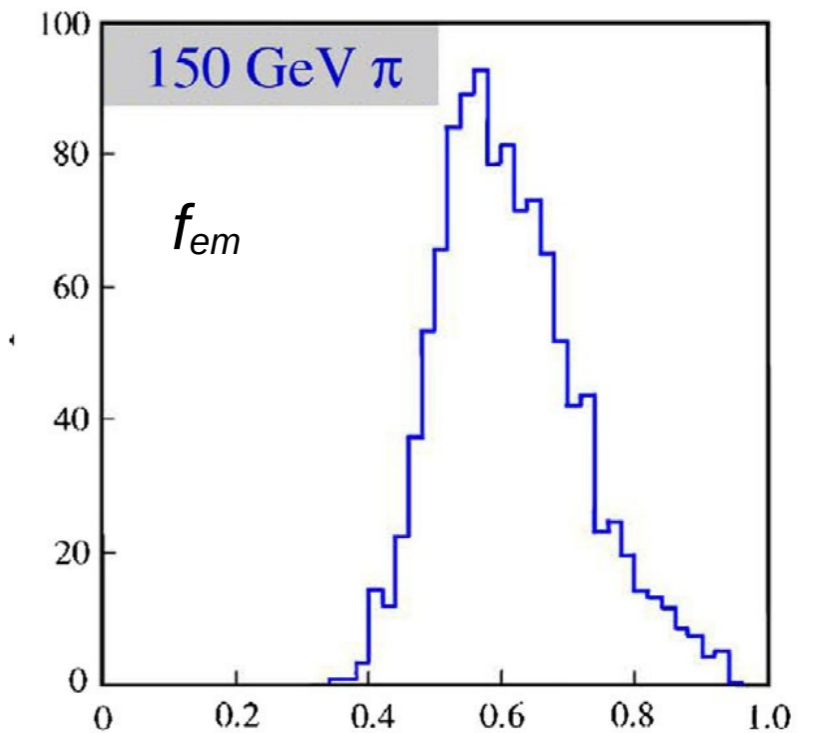
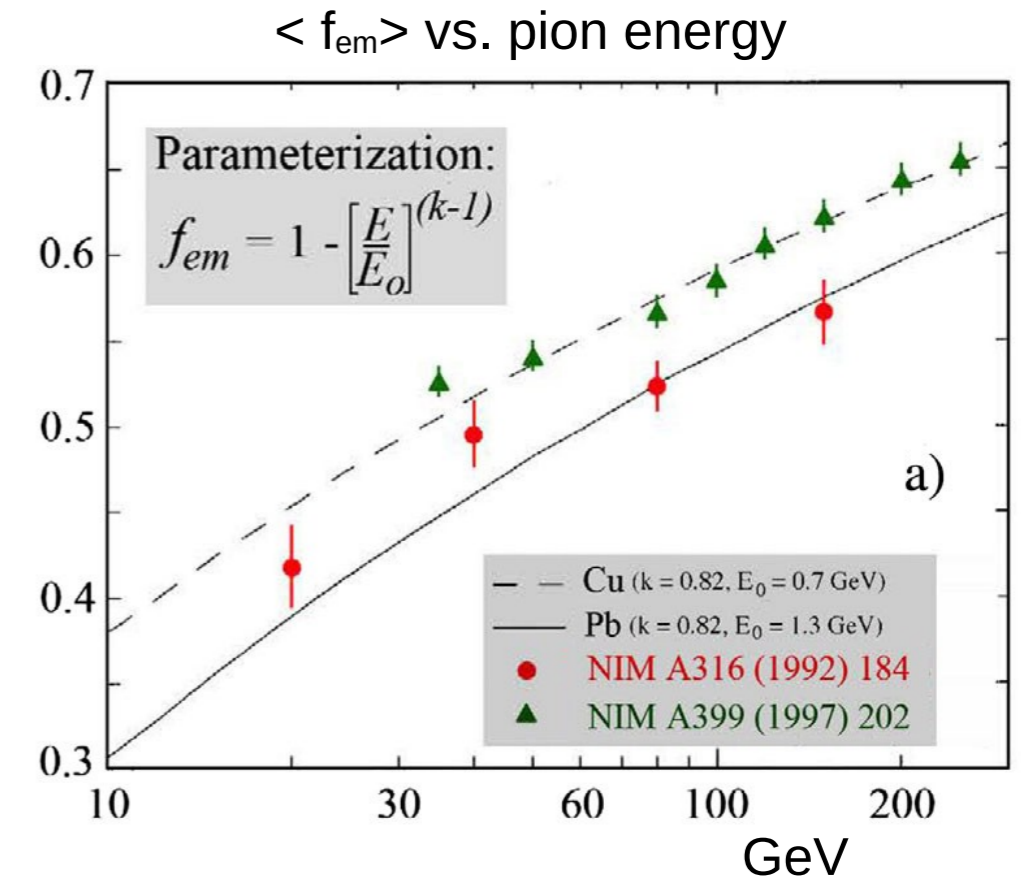
Shower energy fraction mainly carried by  $\pi^0$  (but also  $\eta$ ) mesons  
For shower initiated by charged pions:

$$\langle f_{em} \rangle = 1 - \left( \frac{E}{E_0} \right)^{(k-1)}$$

$E_0$ : average energy for single  $\pi^0$  production,  $k \approx 0.8 < \sim 1$

$\langle f_{em} \rangle$  large and energy dependent

fluctuations in  $f_{em}$  large and non-poissonian



DOI: 10.1103/RevModPhys.90.025002

# detector response

---

Response:

detected signal per unit energy deposit

e.g. number of scintillating (or Cherenkov) p.e. / deposited GeV

Hadronic showers:

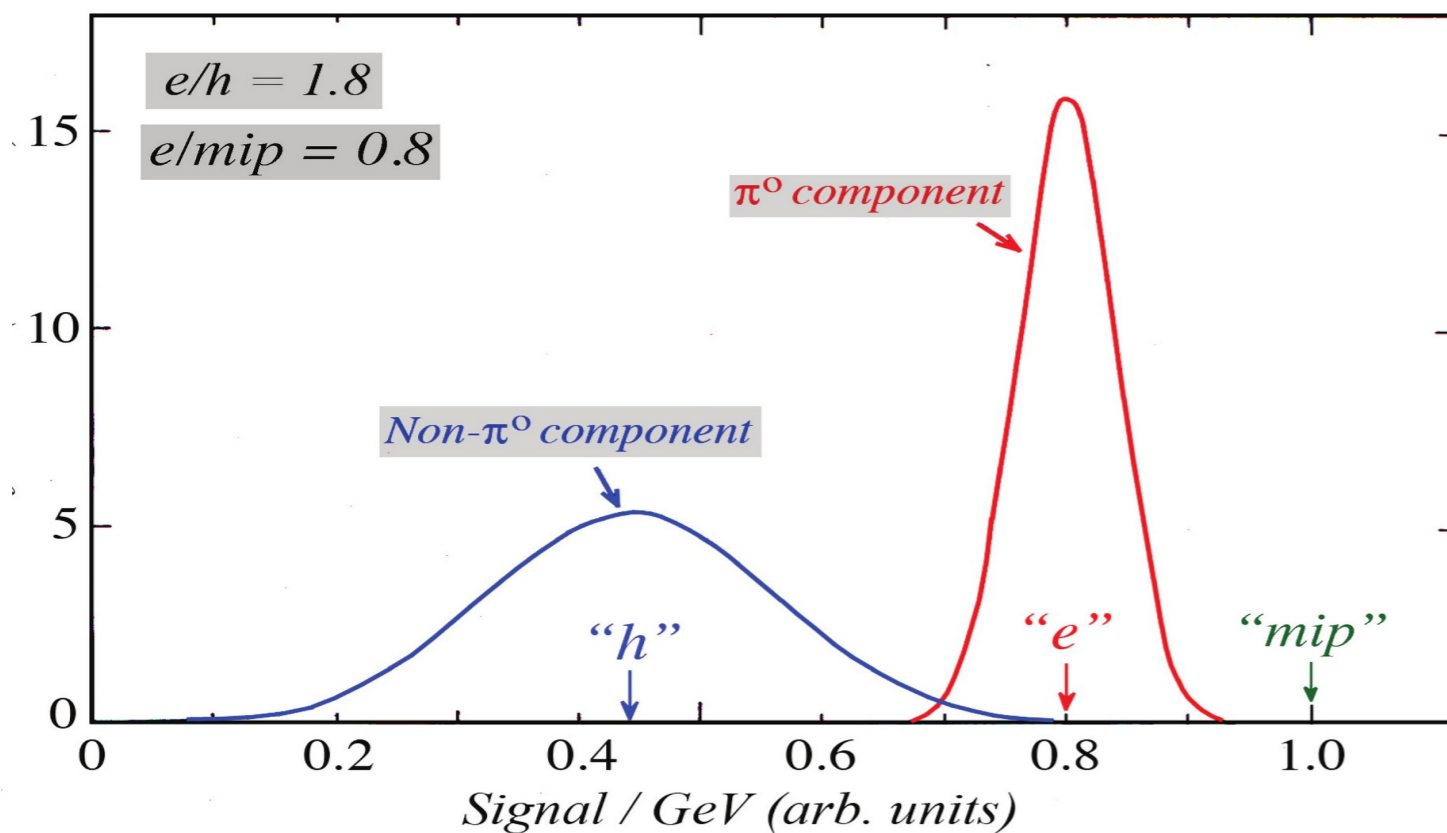
em component → response e

hadronic component → response h

what about relative ratio (e/h) ?



# detector response to hadronic showers



$e \neq h$

e.g. (left plot):

only  $1/1.8 \approx 56\%$  of non- $\pi^0$  energy accounted by signal

$e/h$  ratio: detector characteristic

typically,  $\sim 2$  for crystals, in range 1-1.8 for sampling calorimeters

Nevertheless:

- 1)  $e/\pi$  depends on energy ( $f_{em}$  depends on  $E$  and shower “age”)
- 2)  $\langle f_{em} \rangle$  different for  $\pi$ ,  $K$ ,  $p$   $\rightarrow$  response depends on particle type

# response to hadronic showers

---

Response to protons ?

Average signal for protons:  $S_p = e \cdot \langle f_{em}(p) \rangle \cdot E + h \cdot (1 - \langle f_{em}(p) \rangle) \cdot E$

→ Response:  $R_p = S_p / E \equiv p, \quad \langle f_{em}(p) \rangle \equiv f_p = f_p(E)$

→  $p = e \cdot f_p + h \cdot (1 - f_p) = h \cdot (1 + f_p \cdot (e/h - 1))$

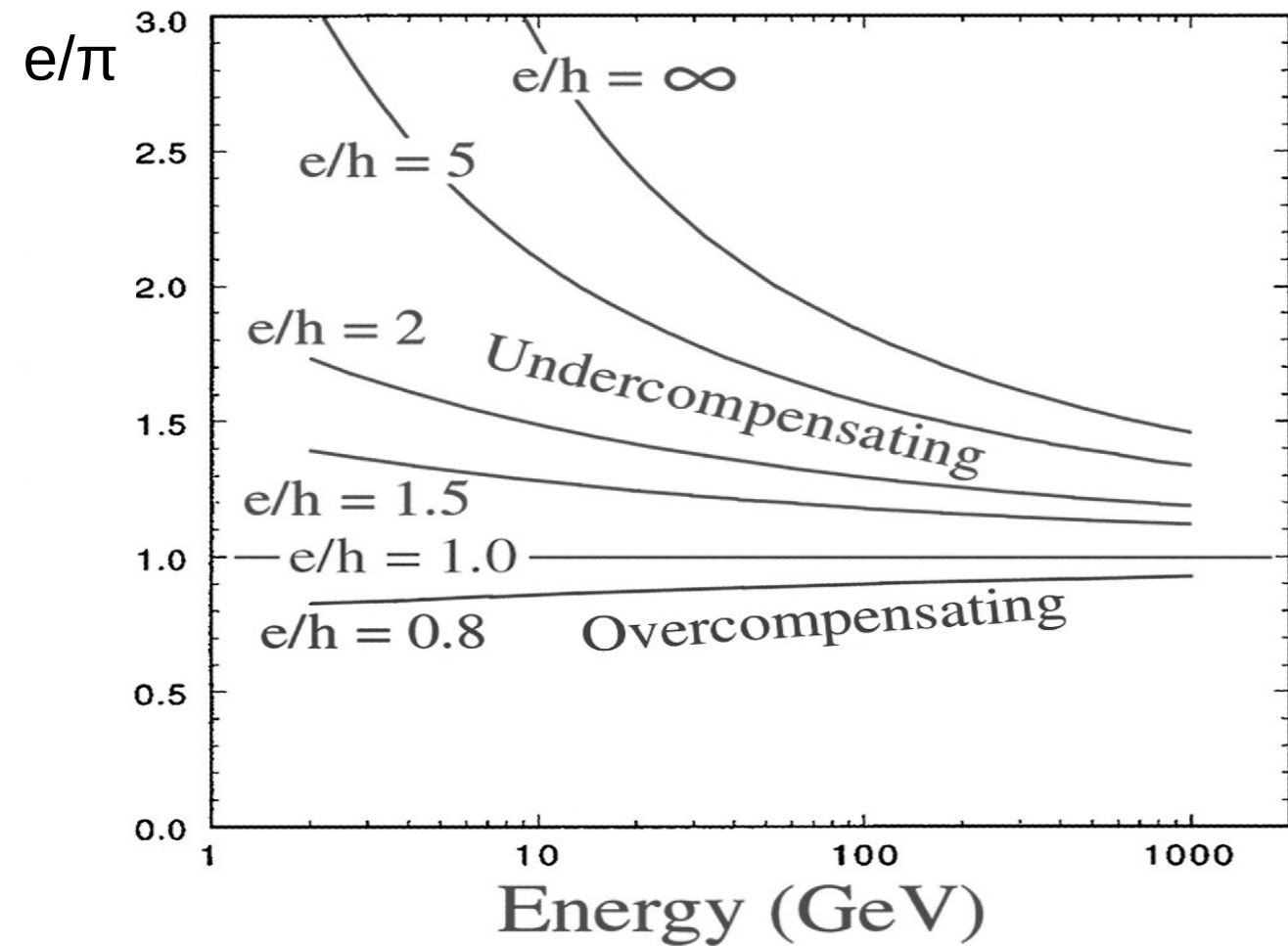
$e/p = e/h / (1 + f_p \cdot (e/h - 1)) \rightarrow$  do we have a problem ?

# e/π ratio

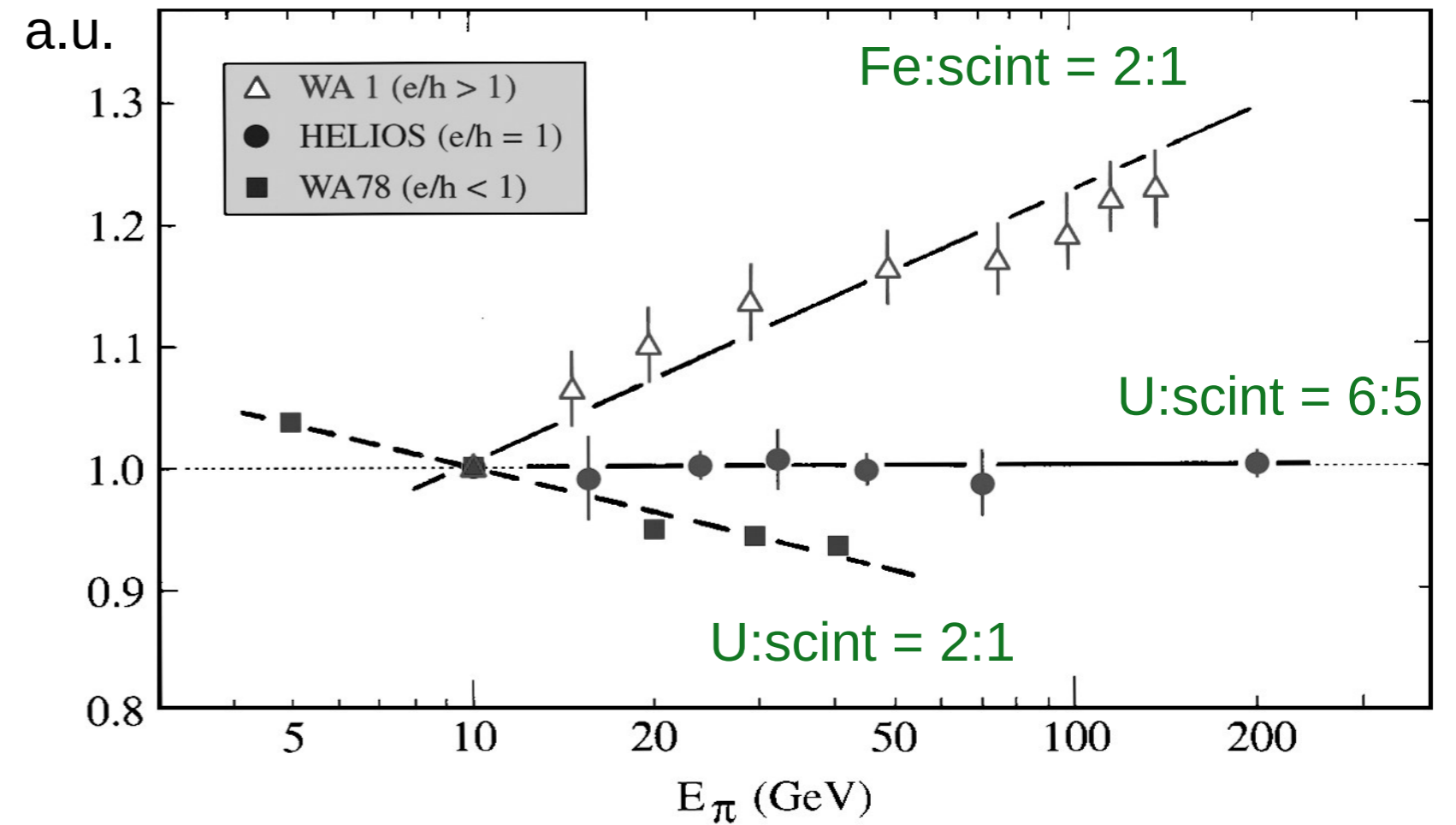
As well, calorimeter response to charged pions: π

$$e/\pi = e/h / ( 1 + f_{\pi} \cdot ( e/h - 1 ) ) \quad f_{\pi} \equiv \langle f_{em}(\pi) \rangle \neq f_p$$

e/π as function of E



Response to π as function of E



response to π as function of E

# compensation in hadron calorimetry

---

$e/h = 1 \rightarrow$  compensating calorimeter

1) increase  $h \rightarrow$  boost hadron response

e.g. by adding hydrogen or Uranium, both acting as “neutron converters”

$\rightarrow$  large integration volume and time

2) decrease  $e \rightarrow$  decrease em sampling fraction or frequency  $\rightarrow$  spoil em performance

$\rightarrow$  tune active / passive material ratio



# e/mip ratio

---

mip : minimum ionising particle → only ionisation

dE/dx (mip) :

lead ~ 12.6 MeV/cm → 7 MeV/X<sub>0</sub>

copper ~ 12.7 MeV/cm → 18 MeV/X<sub>0</sub>

( PMMA ~ 2.3 MeV/cm → 78 MeV/X<sub>0</sub> )

Moreover in high-Z absorbers :

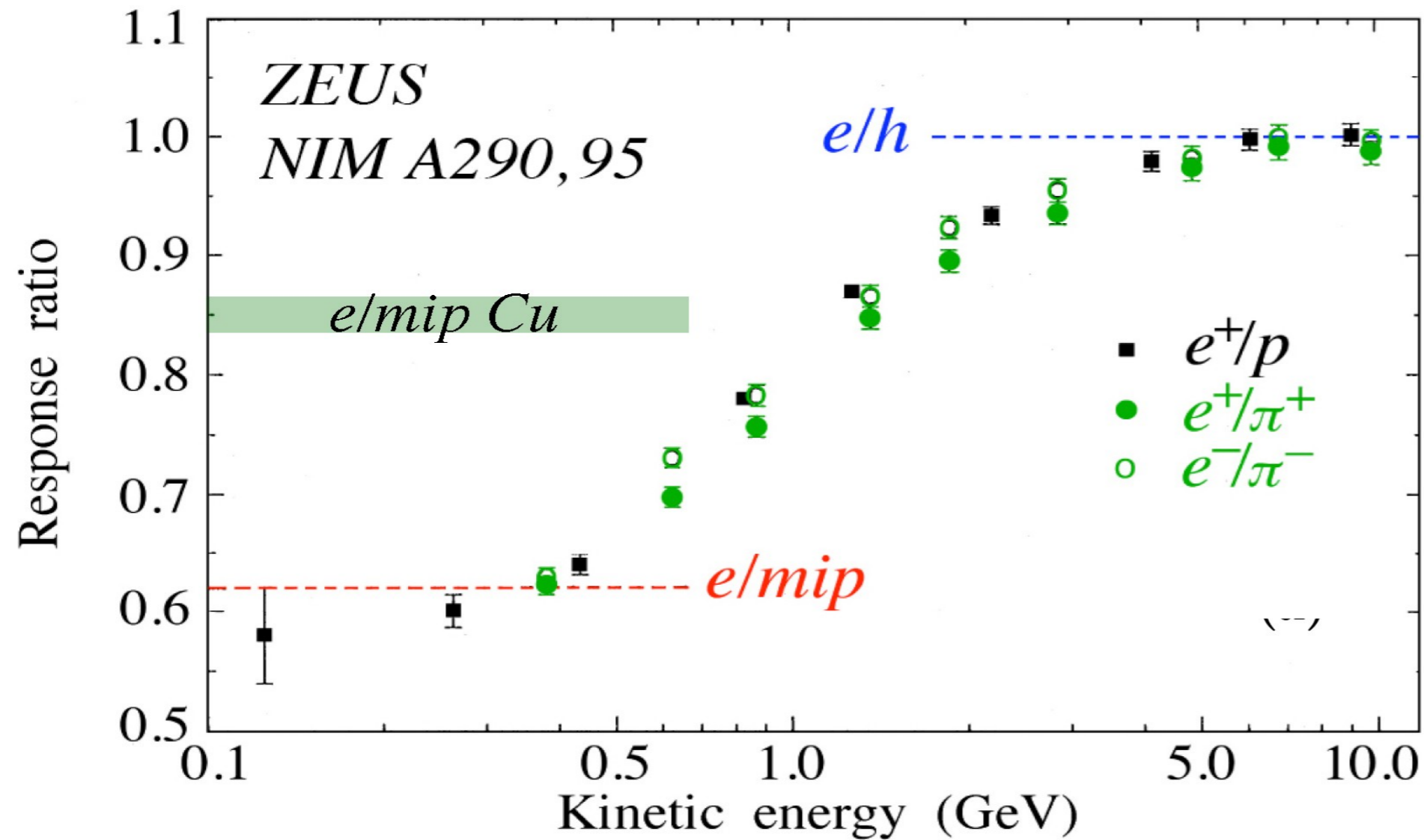
**Z<sup>5</sup> dependence of photoelectric effect** → most soft-γ interact in absorber

**photoelectrons have very short range** → contribute to signal only close to boundaries

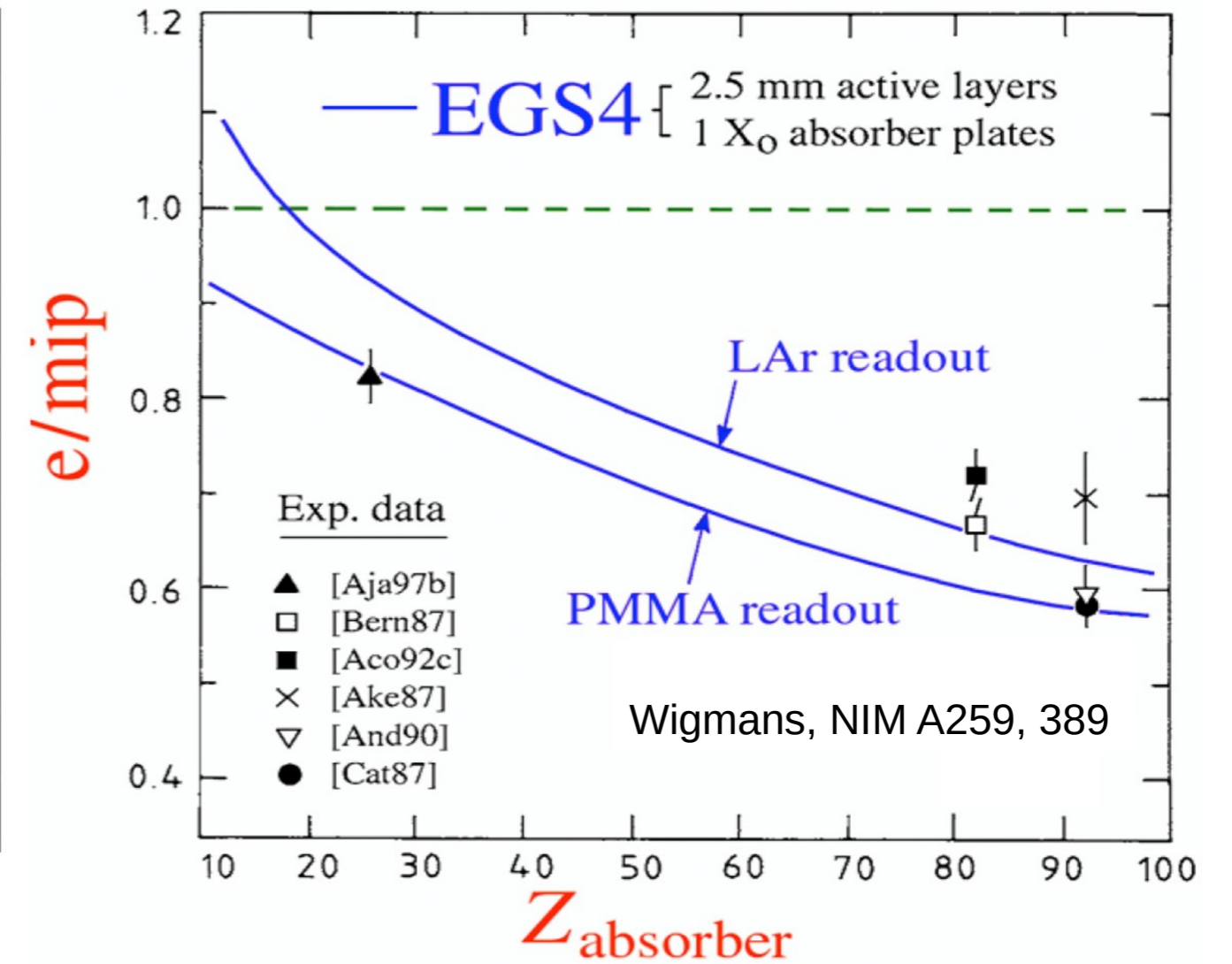
→ response to em showers suppressed wrt. mips

# e/mip ratio

Low-energy response ( compensating calorimeter! )



Non-linearity at low energy with high-Z absorbers (U, Pb)



Mitigated with low-Z absorbers (Cu)

Relevant for jet detection ... should we really care about ?

# what compensation does and does not

---

- ◆ NO guarantee for high resolution

- ◆ fluctuations in  $f_{em}$  are canceled but others may be very large

- ◆ Has drawbacks

- ◆ high-Z absorber required → small e/mip → non linearity @ low energy

- ◆ low sampling fraction required → em resolution limited

- ◆ relies on neutrons → integration over large volume and time

- ◆ SPACAL: to get  $30\%/√E$  ~15 tonnes of lead and ~50 ns integration time

- 

- ◆ high-res em and high-res hadron calorimetry mutually exclusive:

- ◆ good jet energy resolution ⇒ compensation

- ⇒ small sampling fraction (~3%) ⇒ poor em resolution

- ◆ good em resolution ⇒ high sampling fraction (100% crystals, 20% LAr)

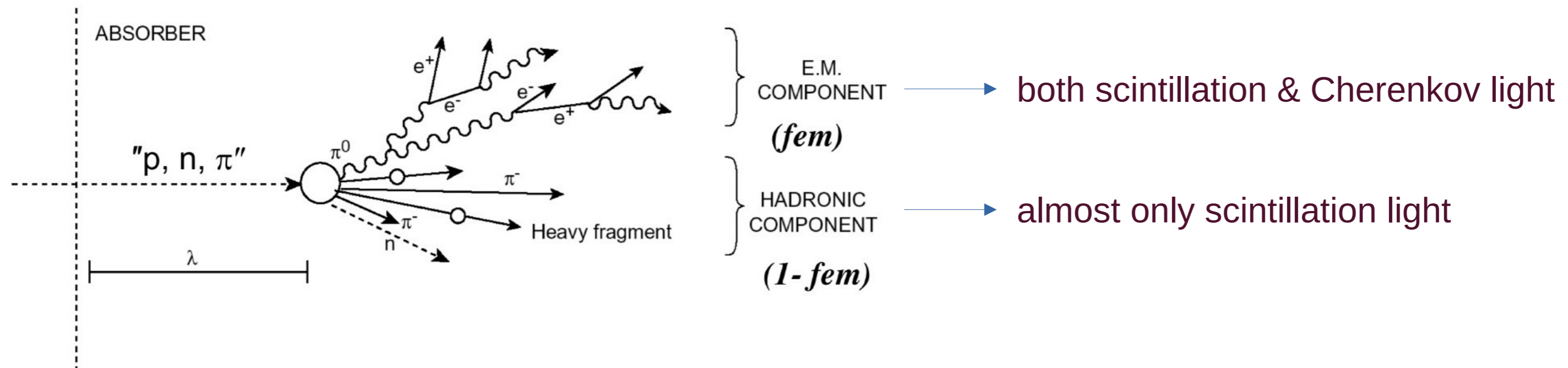
- ⇒ large non compensation ⇒ poor jet resolution

---

## 2. Dual-readout calorimetry

# dual-readout calorimetry

Disentangle relativistic (i.e. electromagnetic) and non relativistic (i.e. nuclear) components of hadronic shower



→ get (compensate for)  $f_{em}$  event by event

# dual-readout algebra

$$S = E \times [ f_{em} + s \times (1 - f_{em}) ]$$

$$C = E \times [ f_{em} + c \times (1 - f_{em}) ]$$

$f_{em}$  = electromagnetic shower fraction

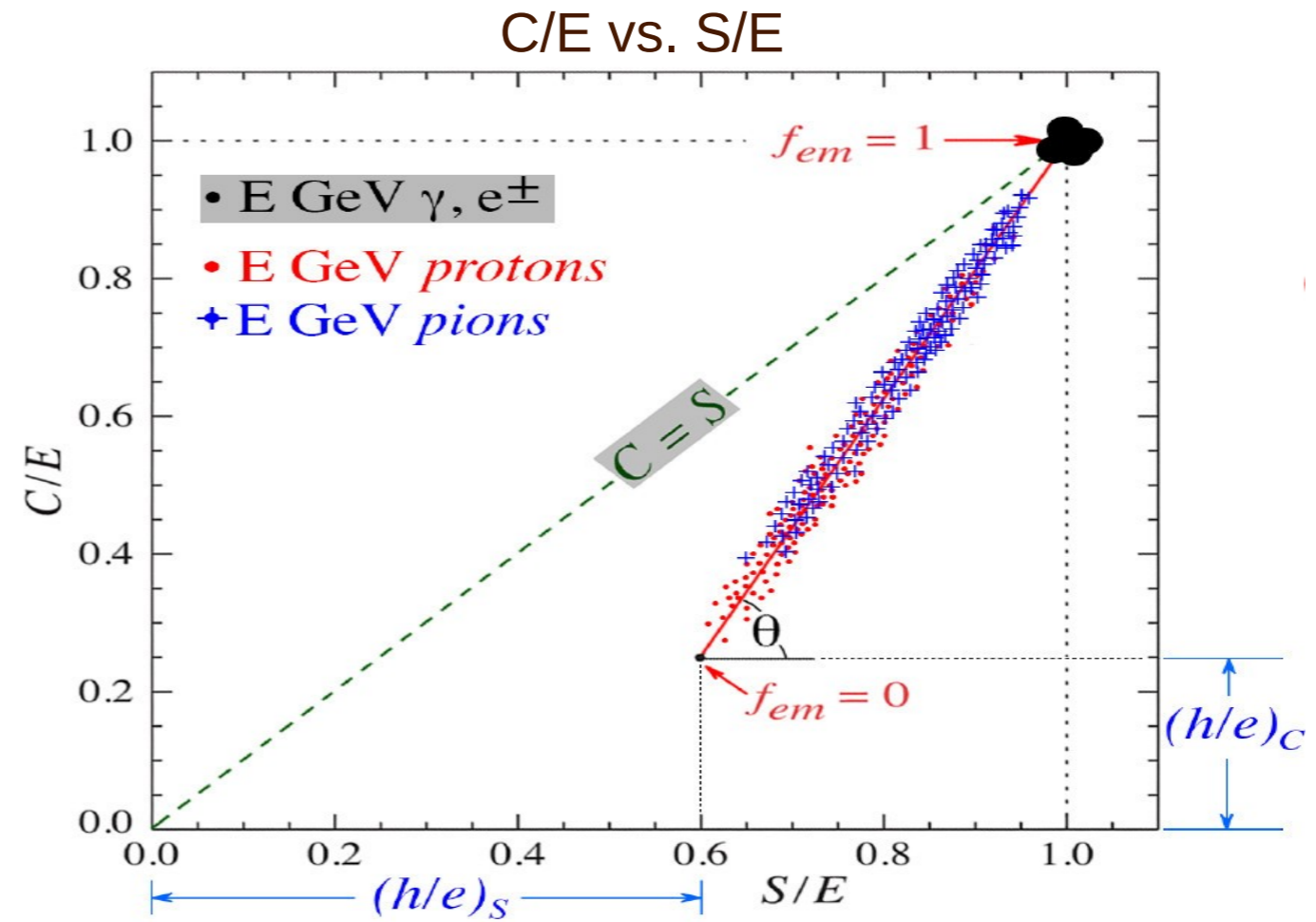
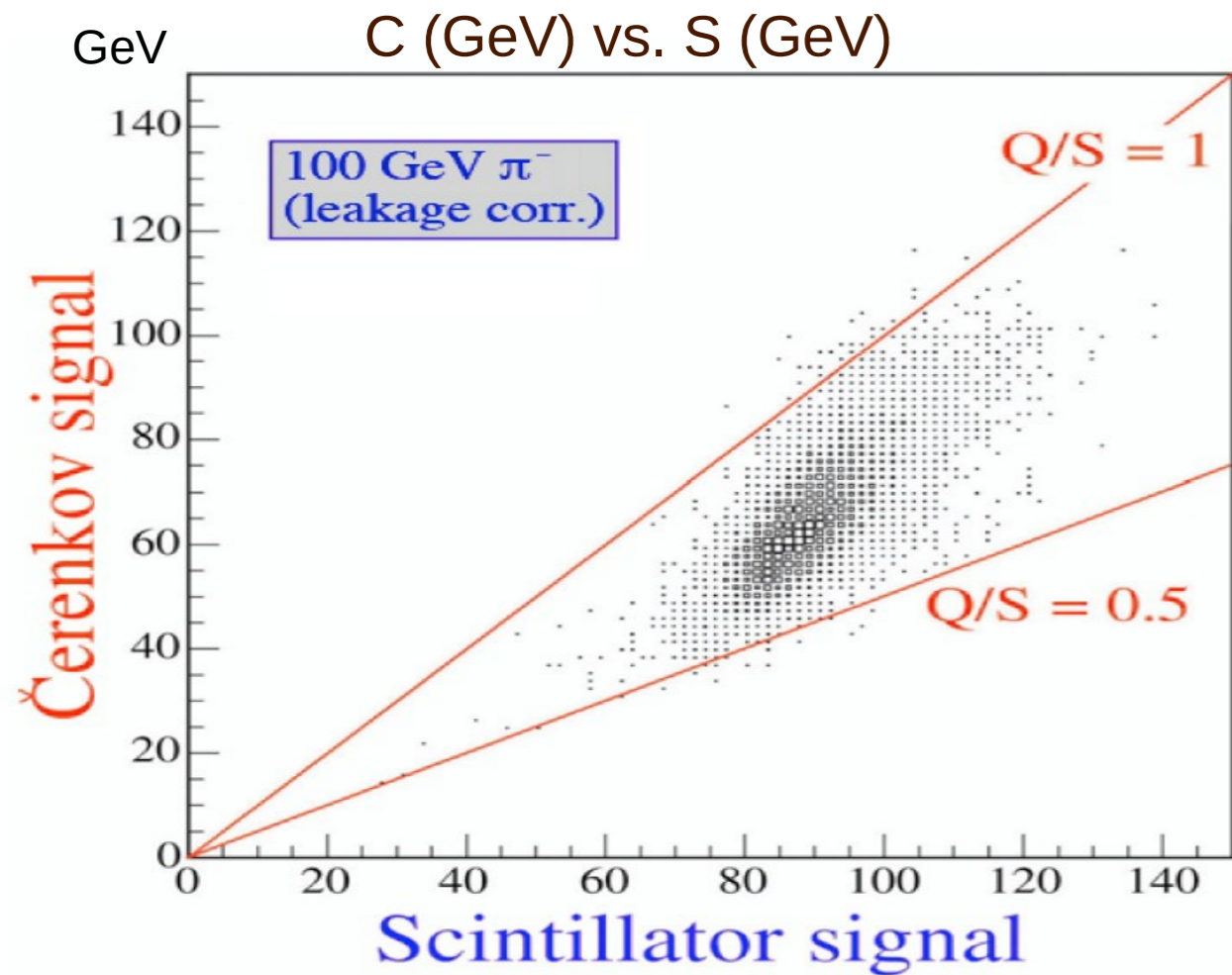
$s = (h/e)_s$  ,  $c = (h/e)_c$  : detector-specific constants

by solving the system, both  $E$  and  $f_{em}$  can be reconstructed

$E$  measured at em energy scale



# applying dual-readout formulae



Hadronic data points (S, C) located nearby straight lines

NIM A 537 (2005) 537

$$E = \frac{S - \chi C}{1 - \chi}$$

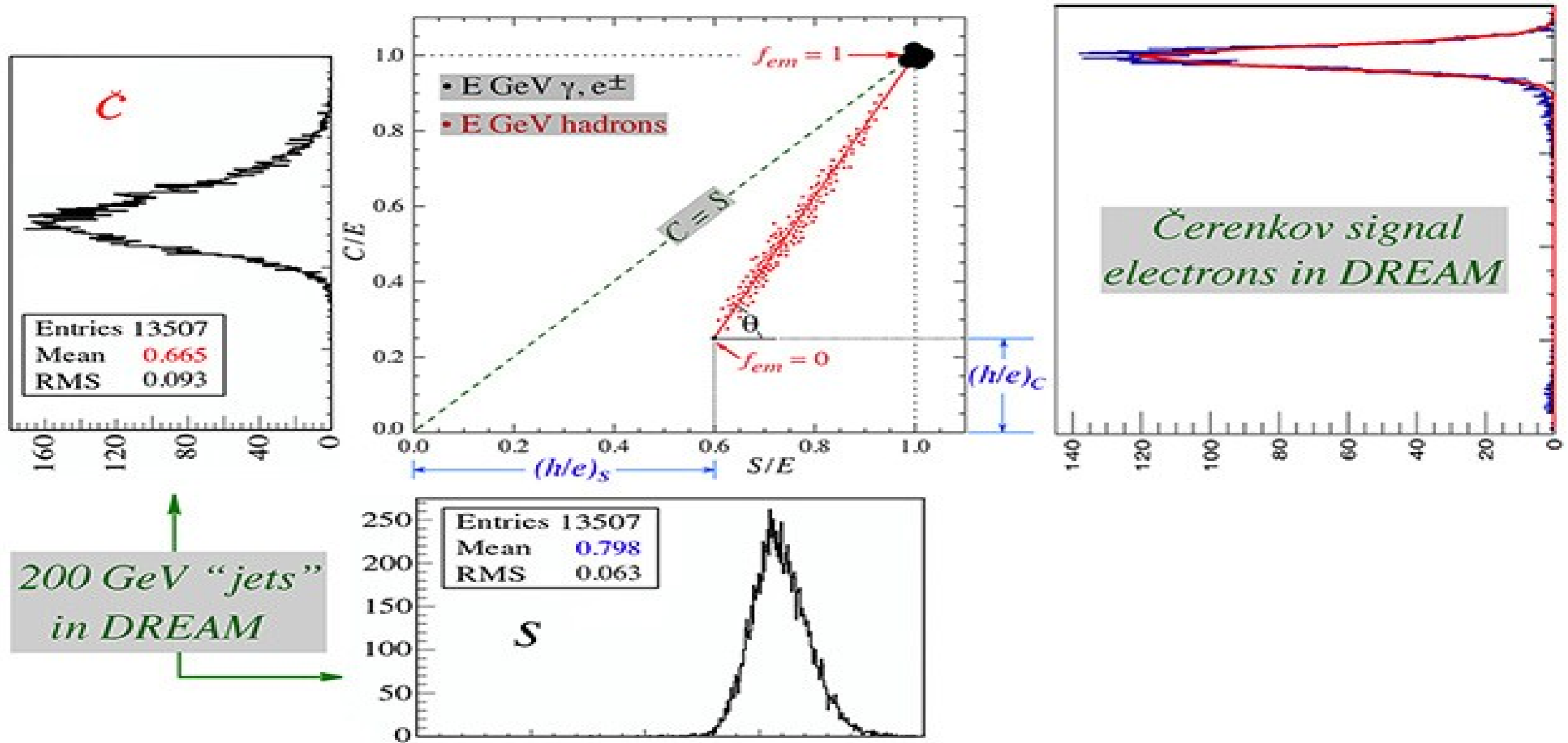
*is universally valid*

$$\cot \theta = \frac{1 - (h/e)_s}{1 - (h/e)_c} = \chi$$

$\theta, \chi$  independent of both:

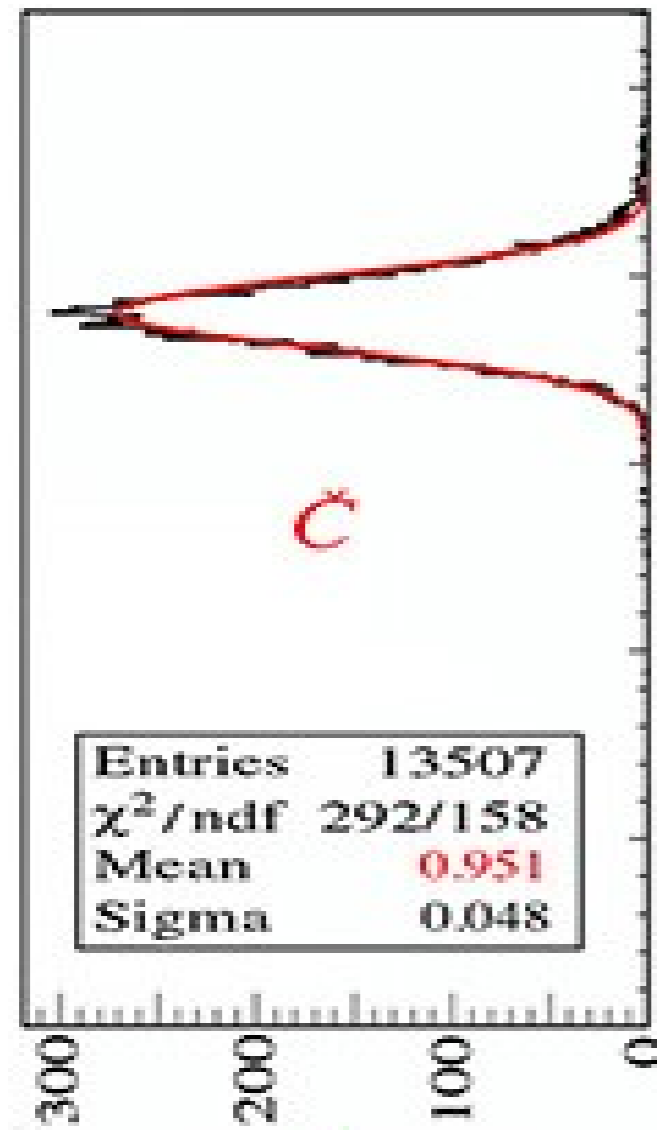
- i) energy (!)
- ii) type of hadron (!!)

# before dual-readout correction

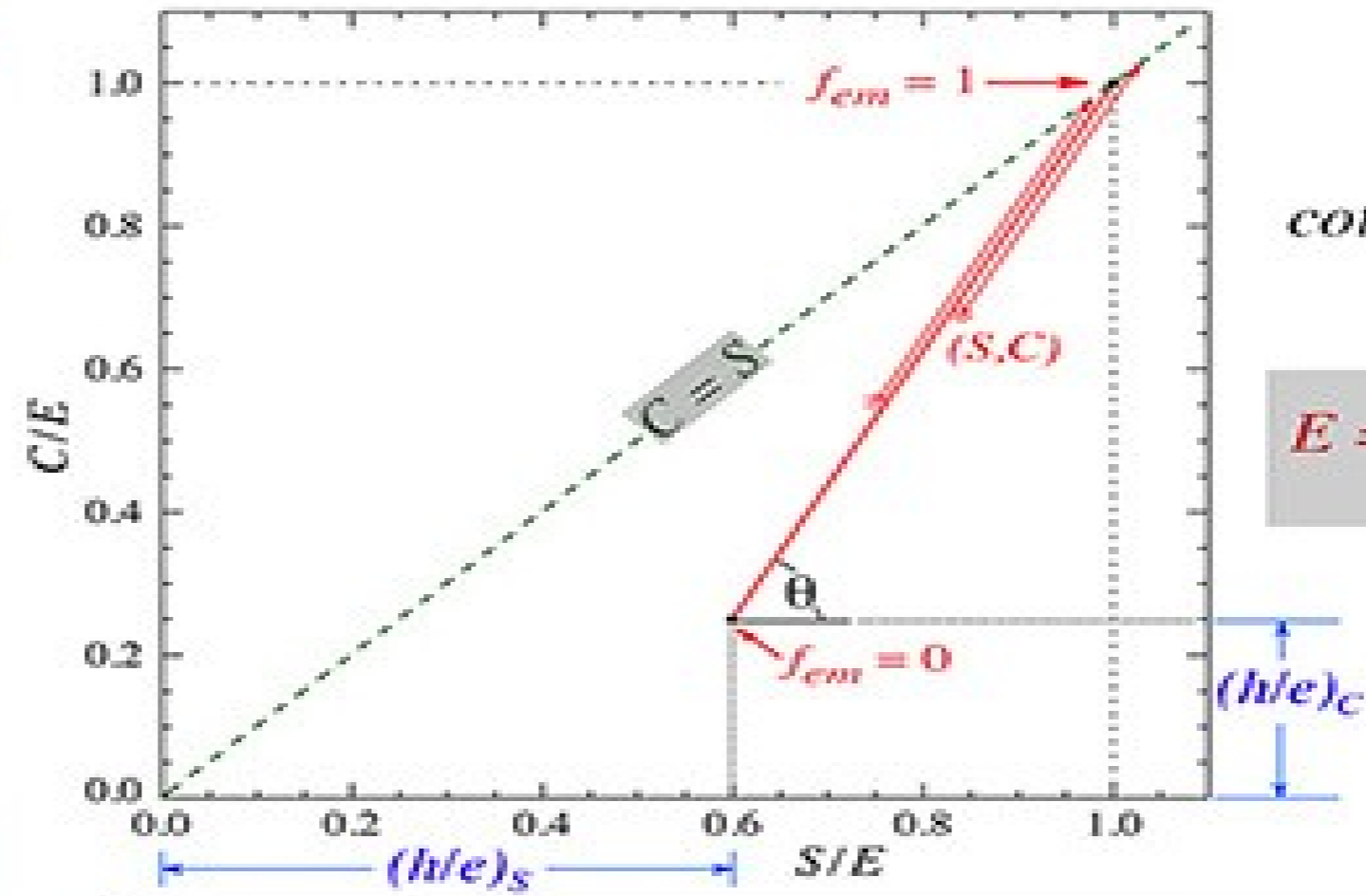




# after dual-readout correction

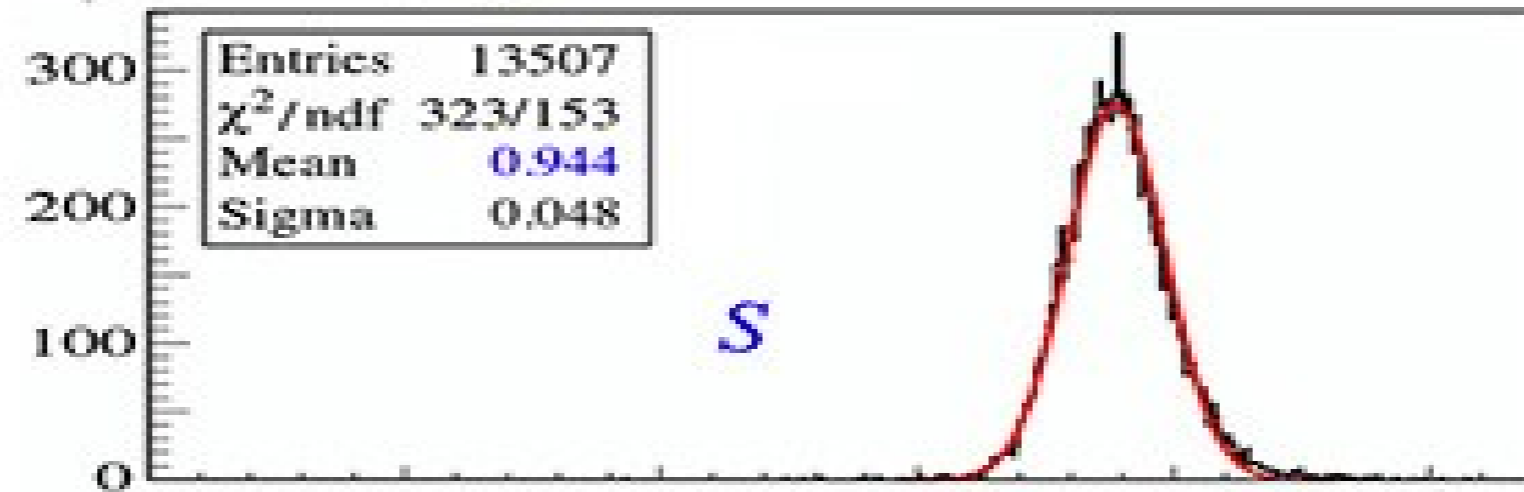


200 GeV "jets"  
in DREAM



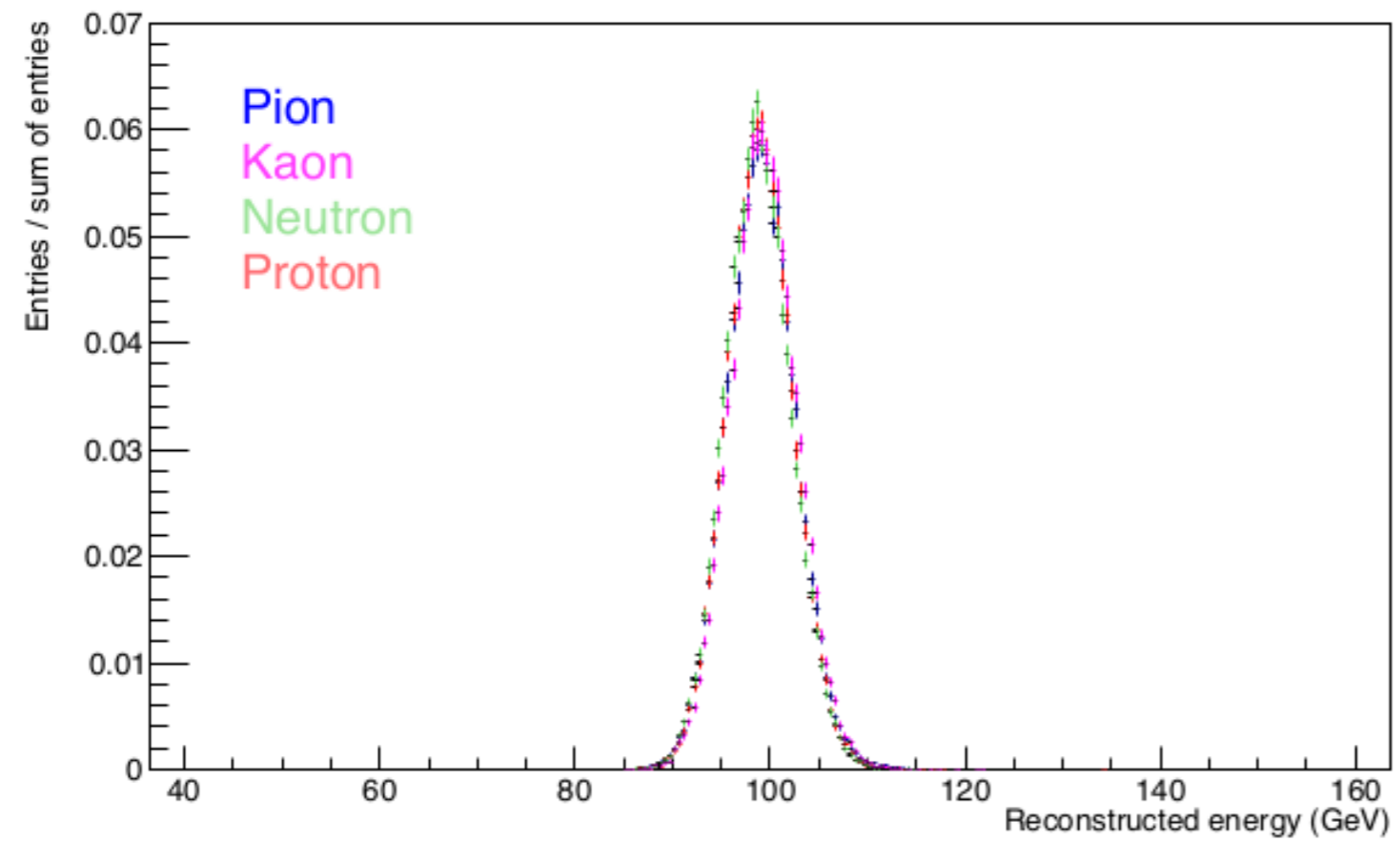
$$\cot \theta = \frac{1 - (h/e)_s}{1 - (h/e)_c} = \chi$$

$$E = \frac{S - \chi C}{1 - \chi}$$

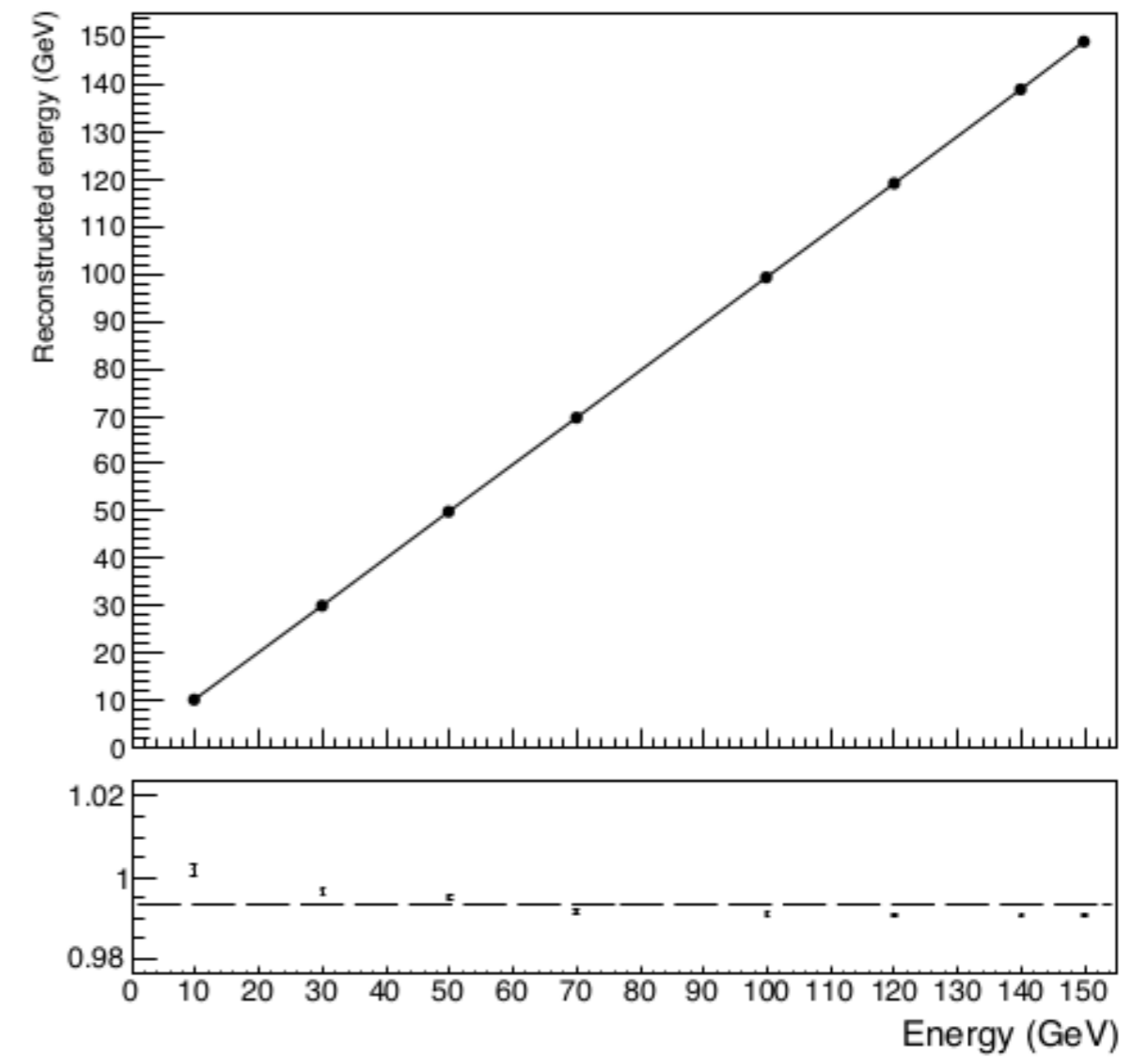


# Geant4 simulations

100 GeV hadrons



10-150 GeV  $\pi^-$



$$C/S = [ f_{em} + s \times (1 - f_{em}) ] / [ f_{em} + c \times (1 - f_{em}) ]$$

→ C/S depends only on  $f_{em}$  so that

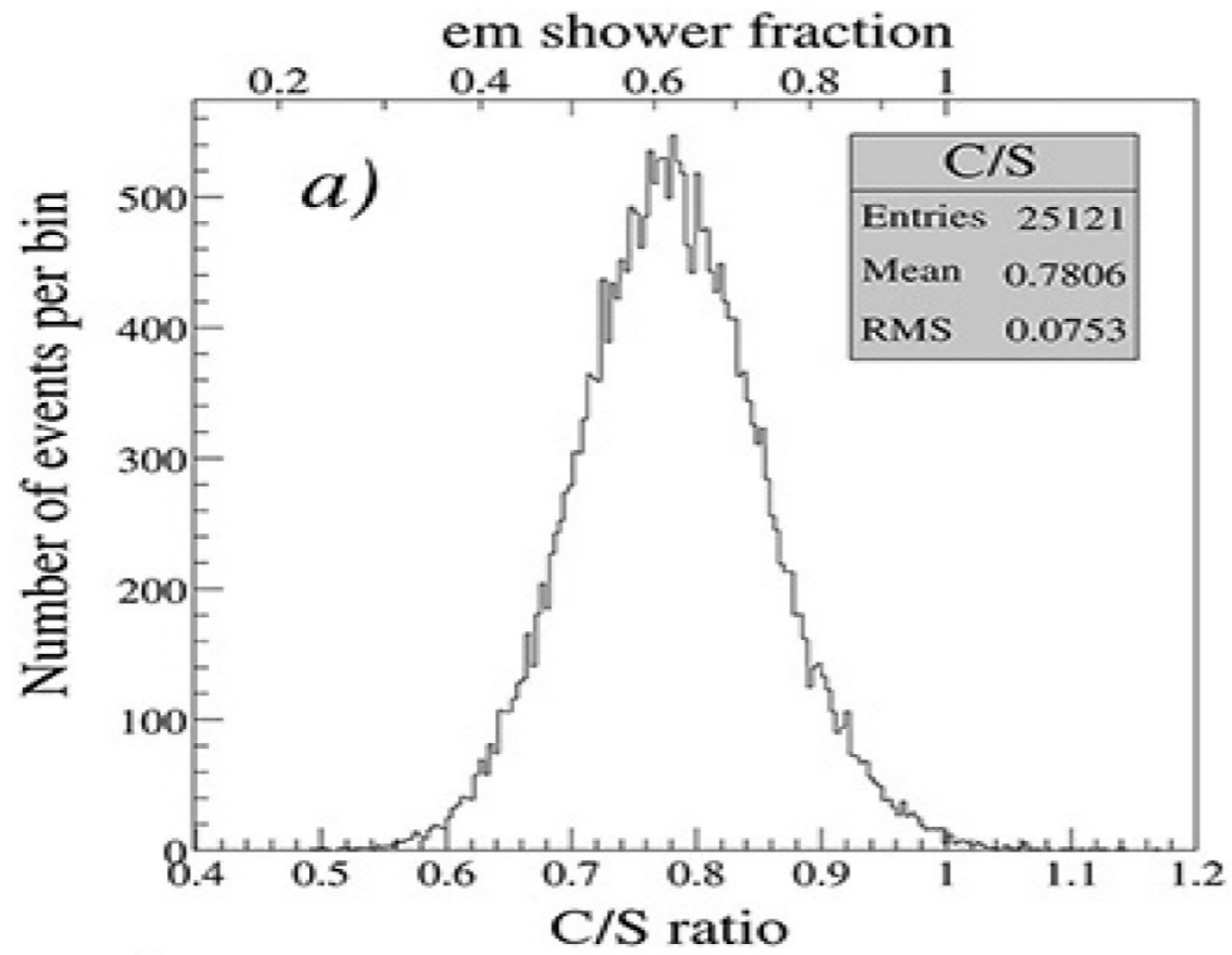
$$f = \frac{c - s(C/S)}{(C/S)(1 - s) - (1 - c)}$$

→  $f_{em}$  depends only on C/S → can use C/S to select  $f_{em}$  subsamples

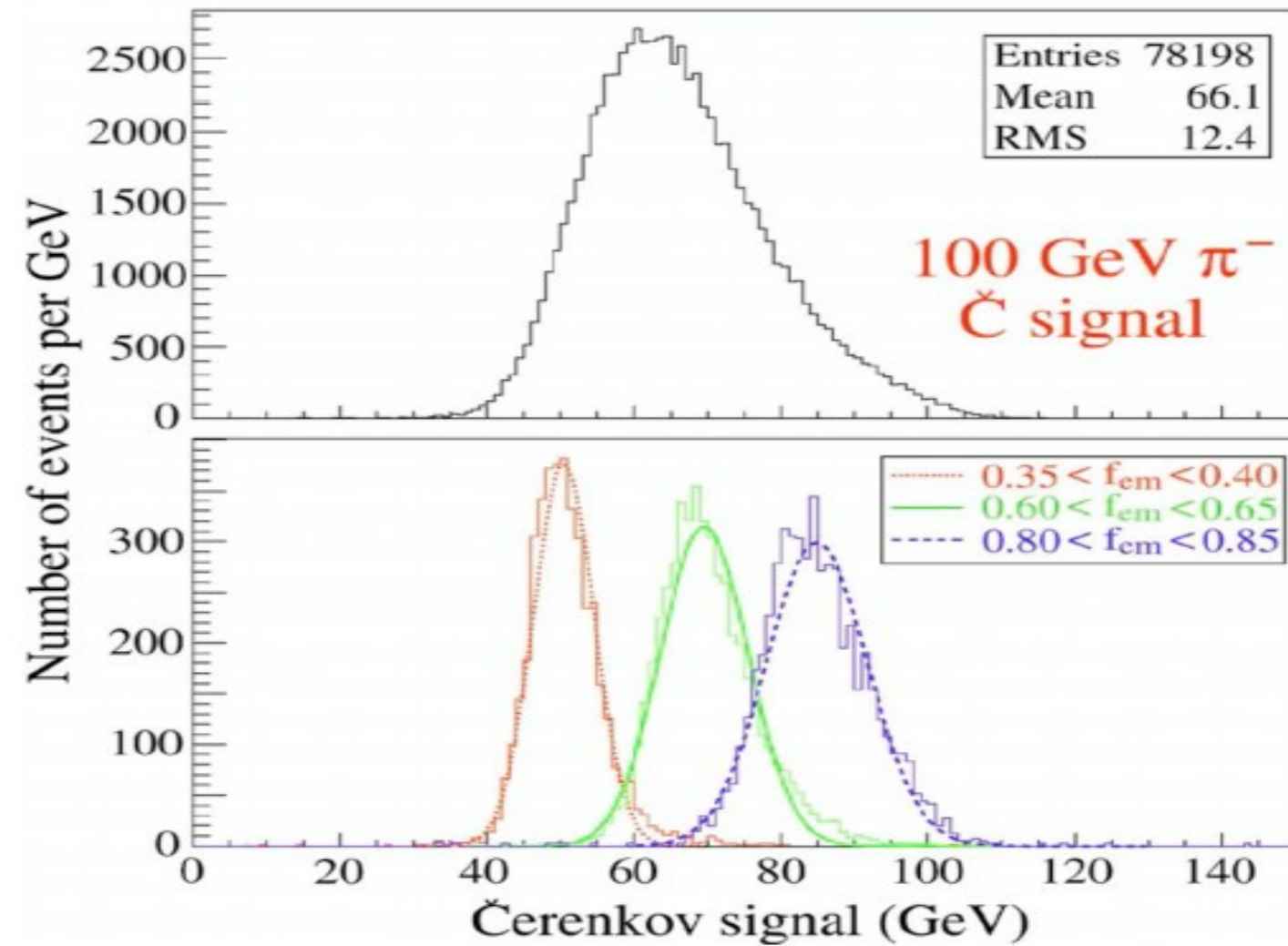
to get  $f_{em}$  absolute value, at least one of (h/e) factors needs to be known

[ or extracted e.g. by fitting  $\langle C/E \rangle$  as function of E ]

# $f_{em}$ fluctuations



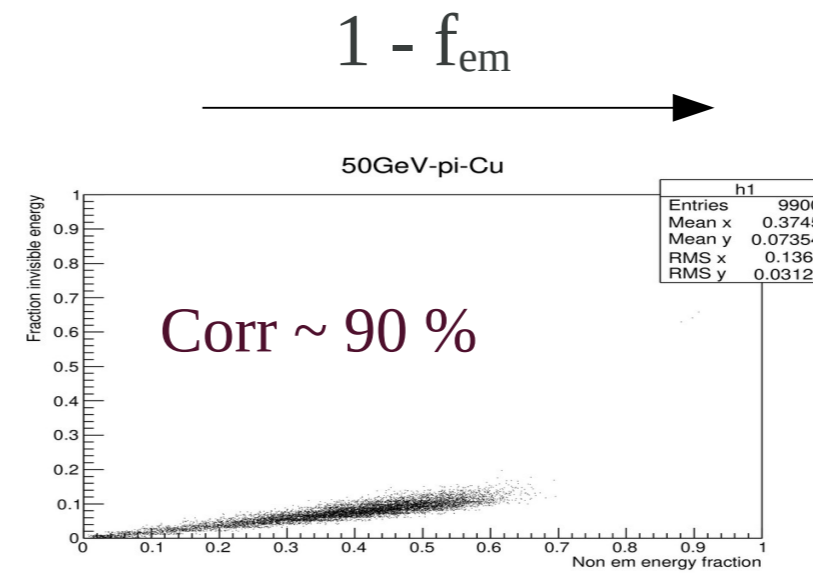
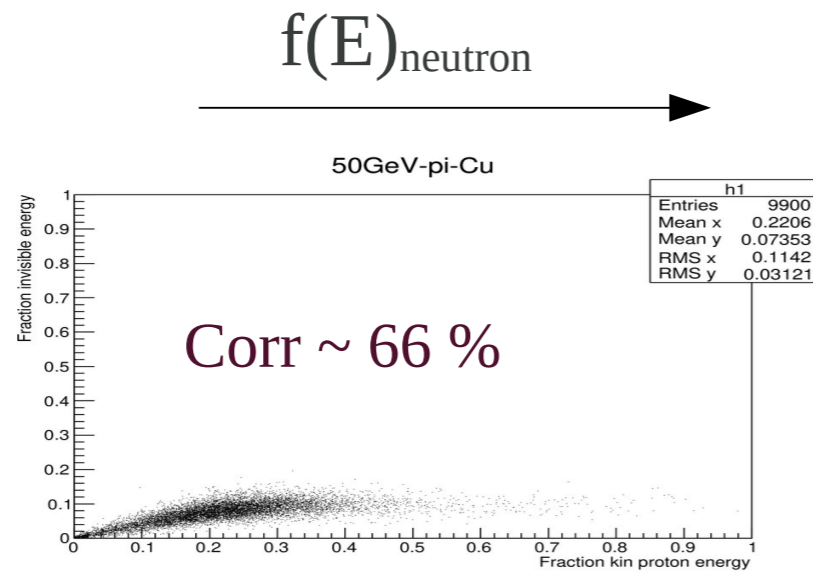
## DREAM: Effect of event selection based on $f_{em}$



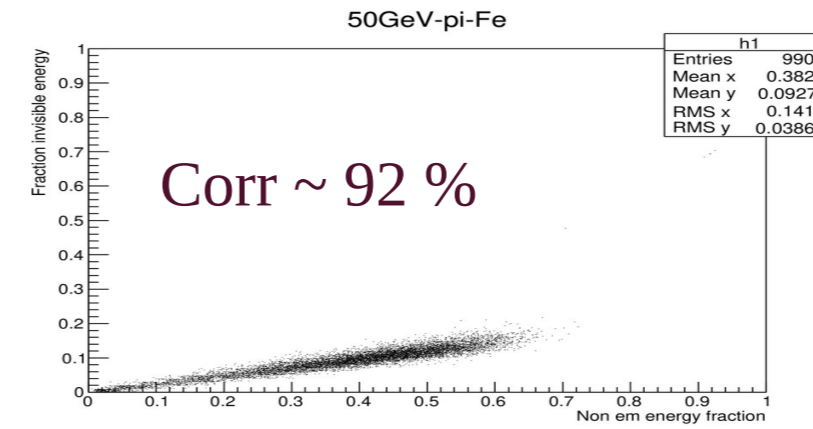
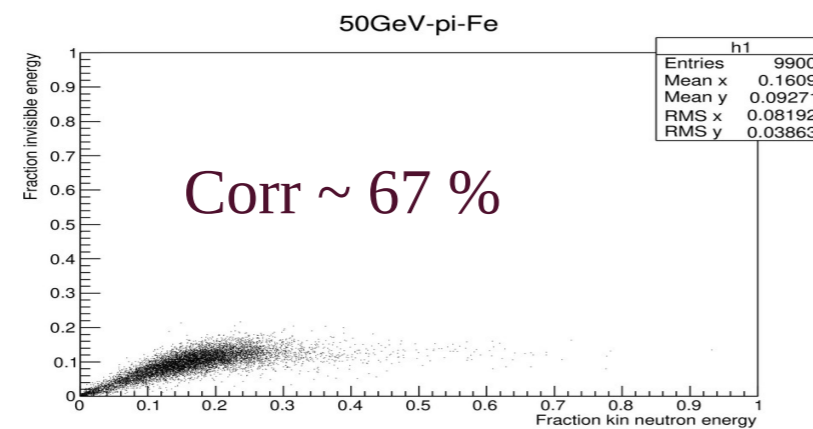
NIM A 537 (2005) 537

# invisible energy fraction – Geant4 simulations

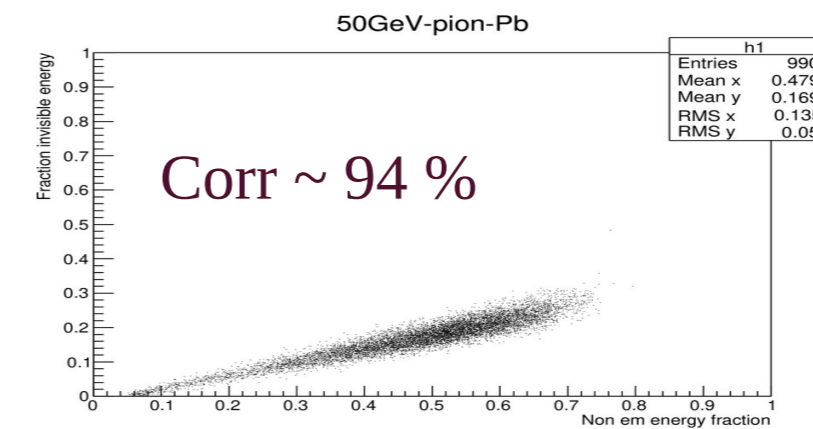
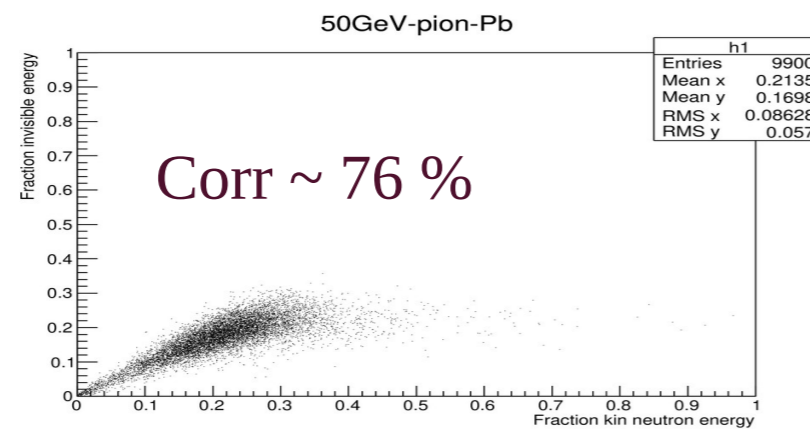
*Copper*



*Iron*



*Lead*



$f_{\text{inv}}$

# back to dual-readout formulae ...

$$E = \frac{S - \chi \cdot C}{1 - \chi}$$

measurable event by event, if  $\chi$  known

$$1 - f_{em} = \frac{1}{1 - \left(\frac{h}{e}\right)_c} \cdot \frac{S - C}{S - \chi \cdot C}$$

measurable if  $\chi$  known

(1-f<sub>em</sub>) can be reconstructed within (unknown) constant factor (>) O(1)

$$\chi = \frac{1 - \left(\frac{h}{e}\right)_s}{1 - \left(\frac{h}{e}\right)_c} = \frac{E - S}{E - C}$$

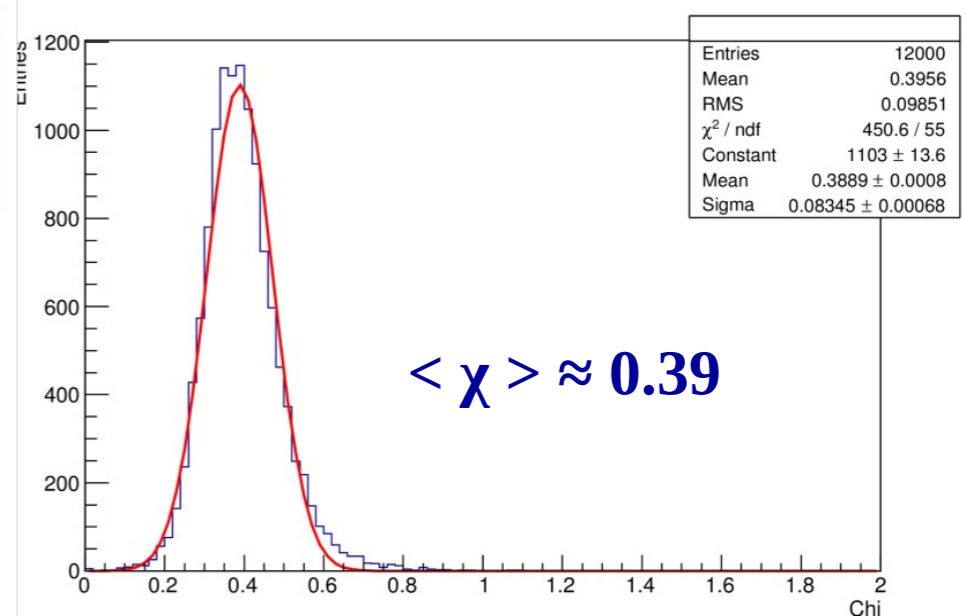
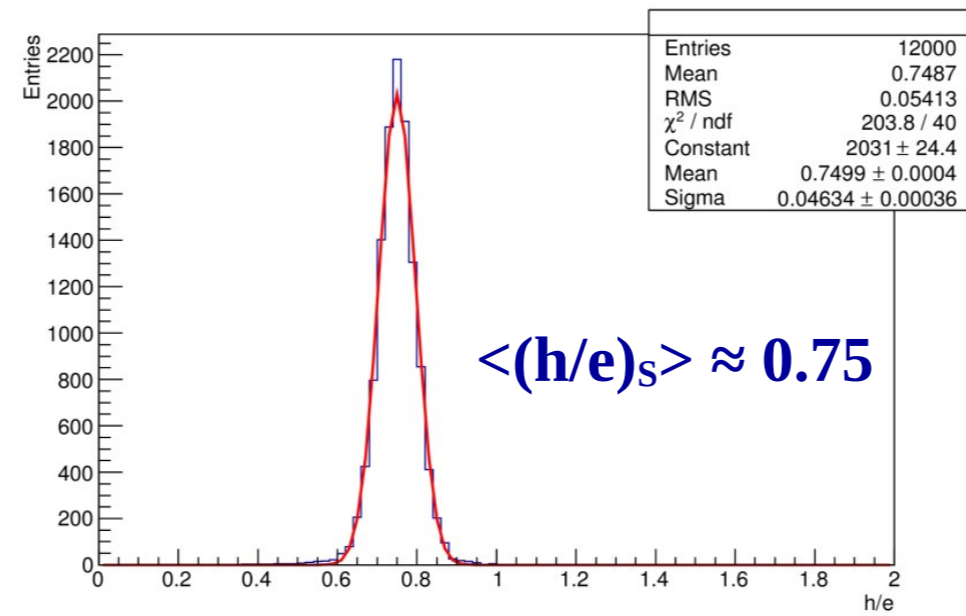
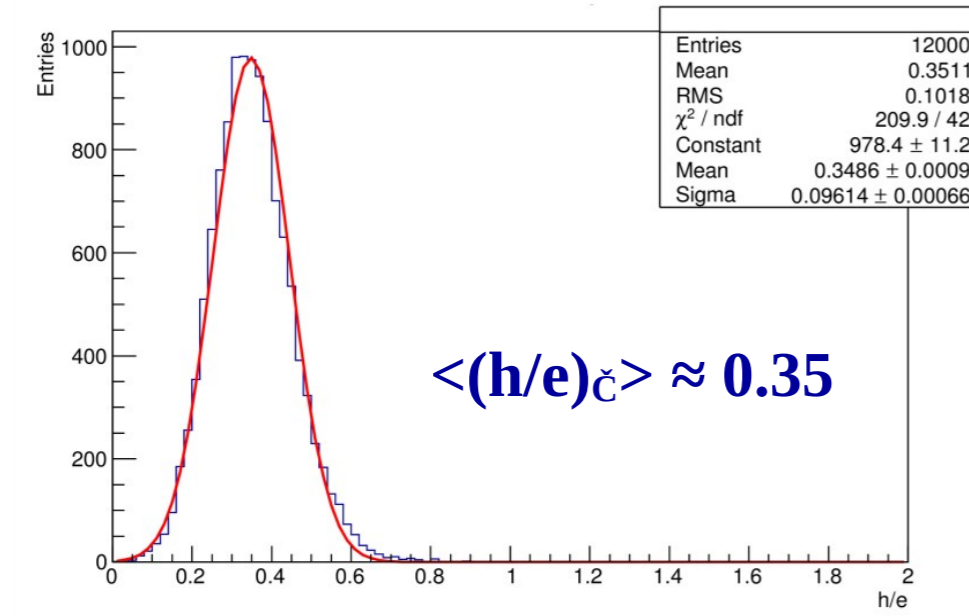
$$\text{if } \left(\frac{h}{e}\right)_s > \left(\frac{h}{e}\right)_c \Rightarrow \chi < 1$$

$\chi$  measurable if E known

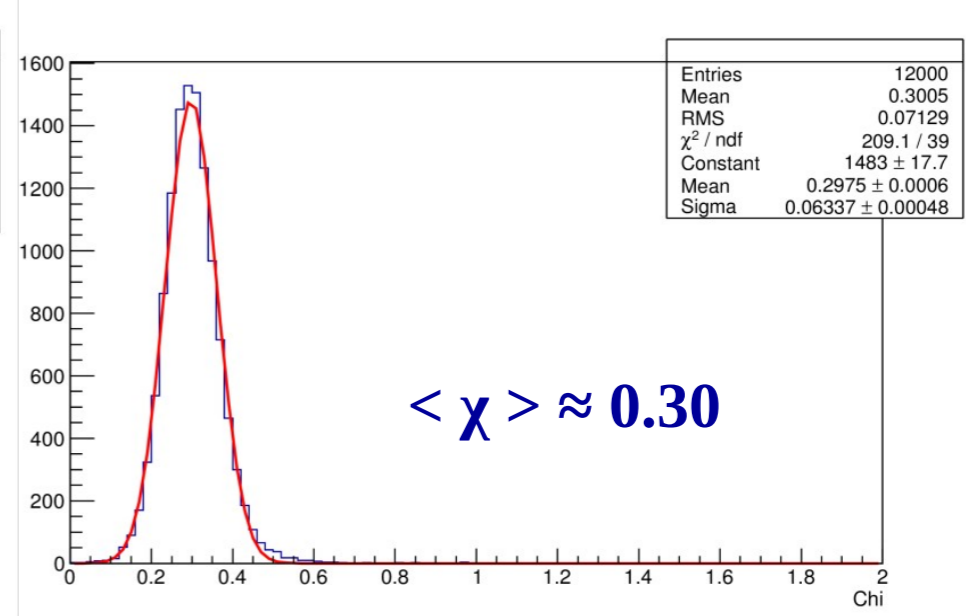
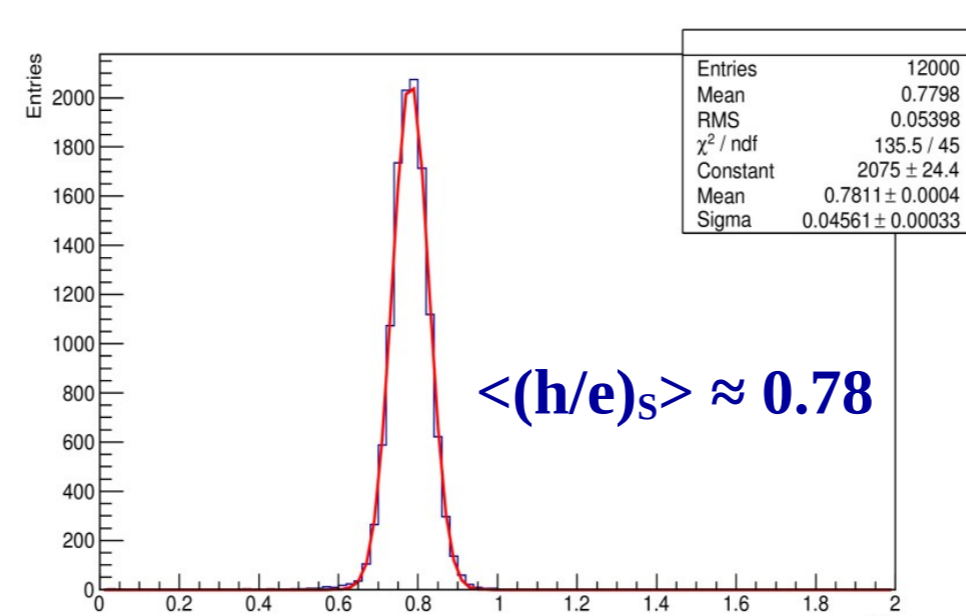
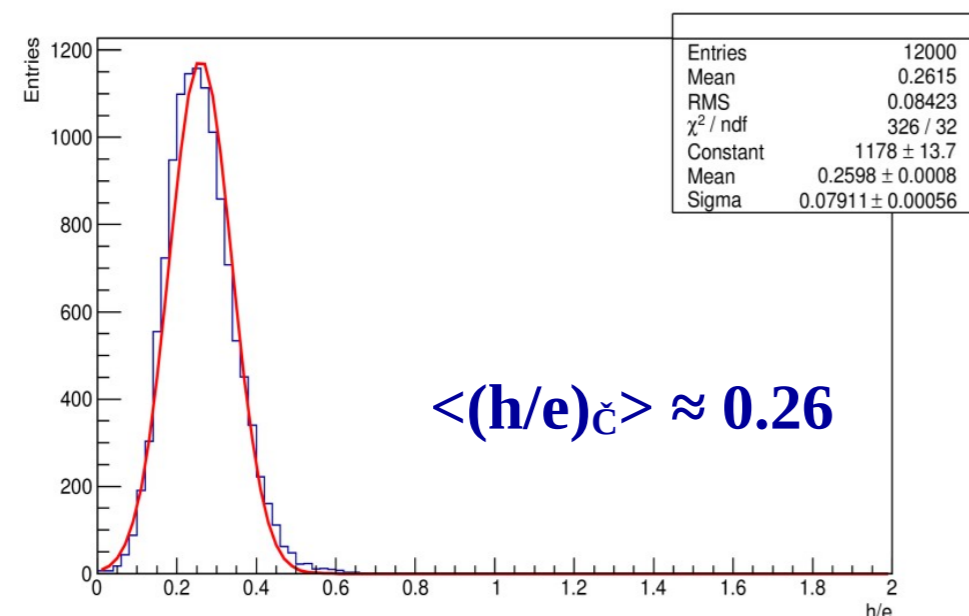
$\chi$  can be extracted from testbeam data



# Geant4 simulations – (h/e) and $\chi$ factors



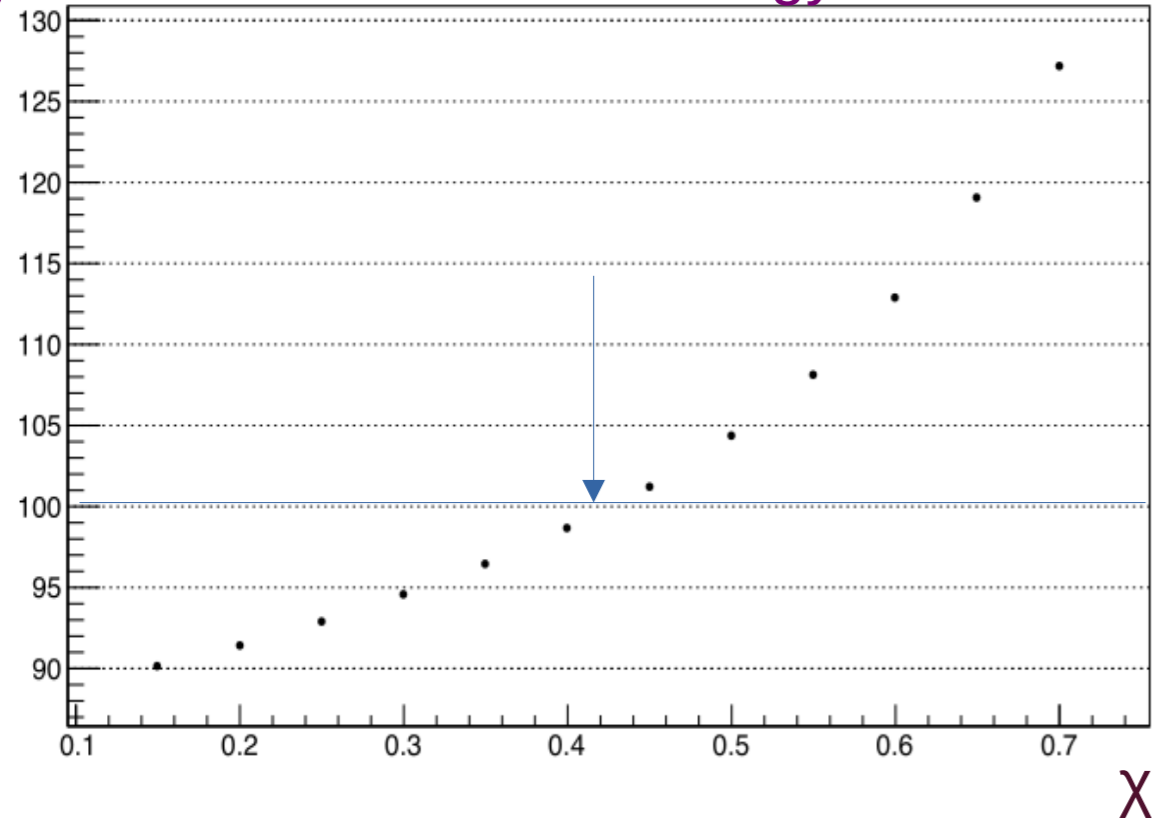
80 GeV protons in Copper  $\uparrow$  & Lead  $\downarrow$



# Geant4 simulations – $\chi$ scan

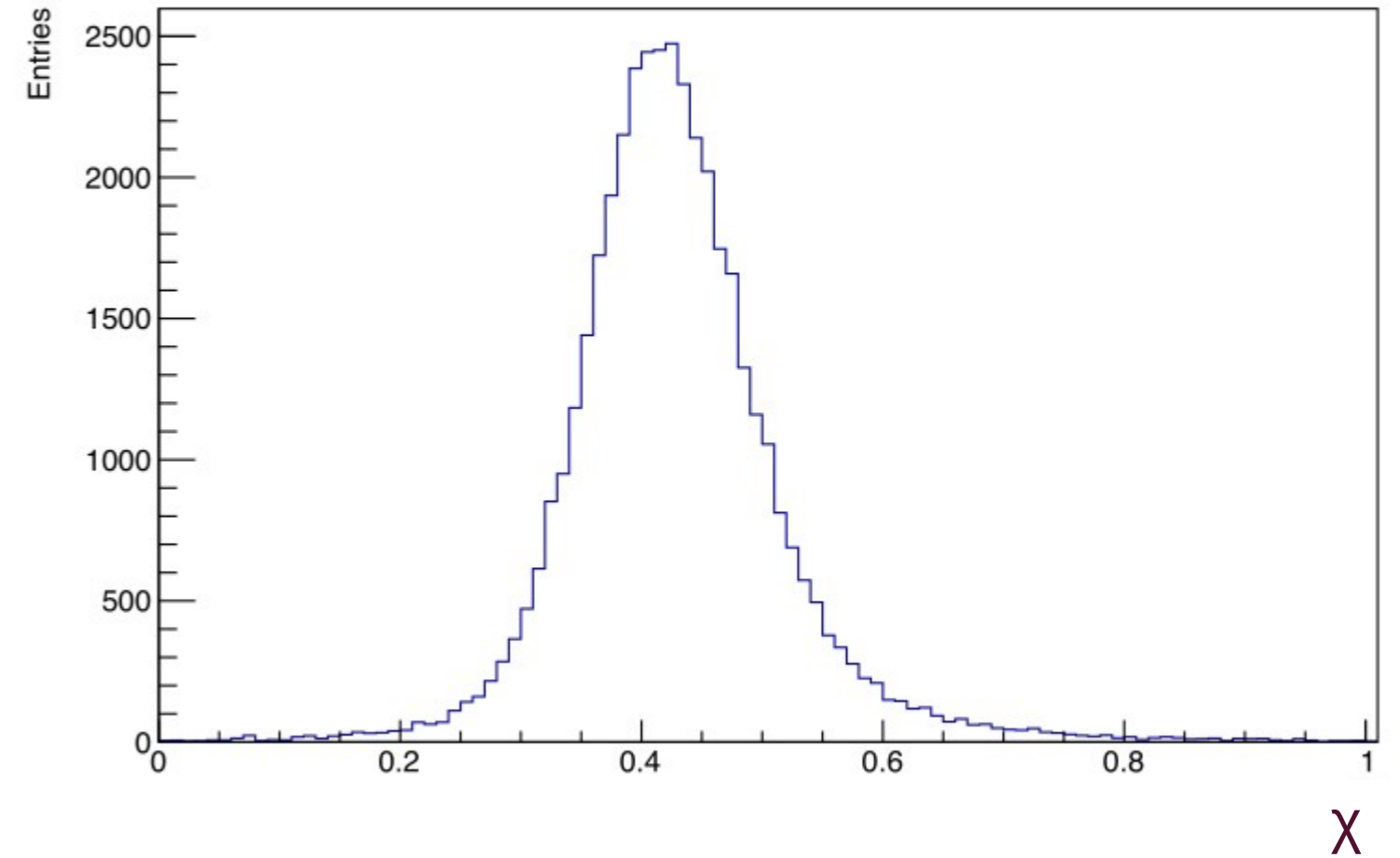
GeV

Reconstructed energy



100 GeV  $\pi^-$

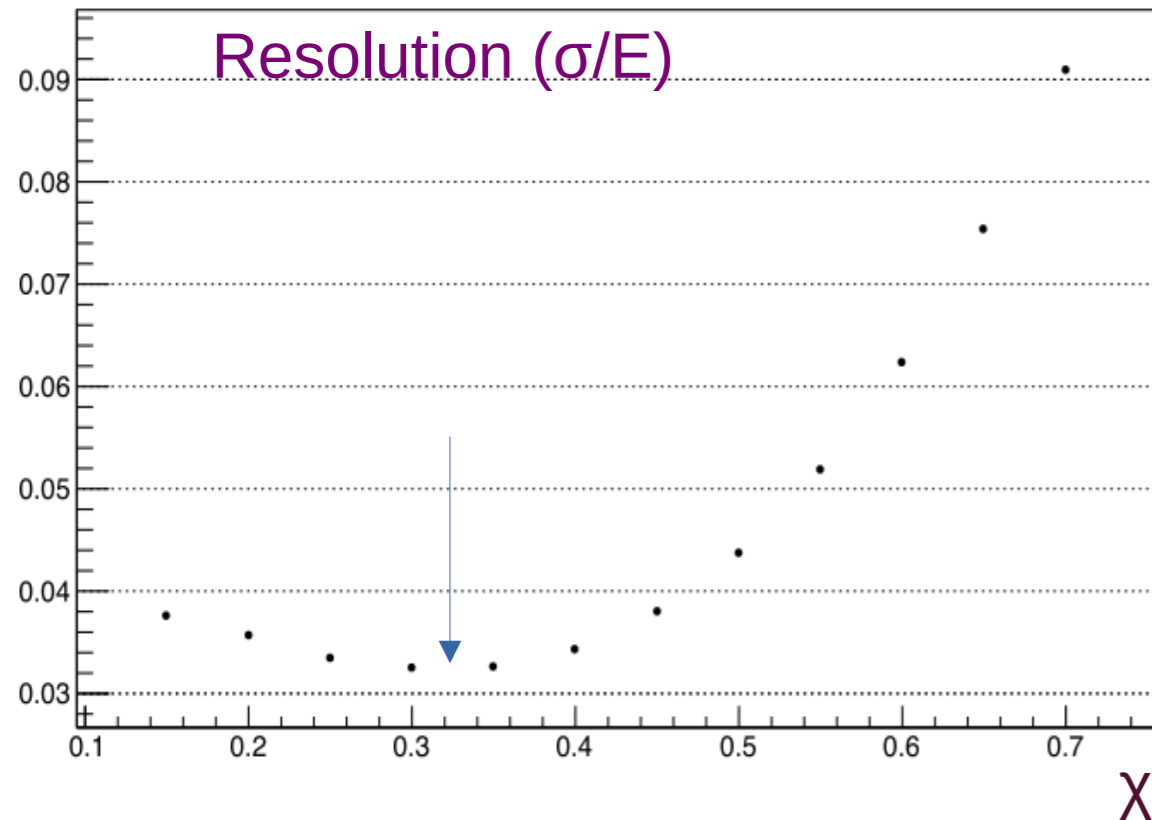
$\chi$  for optimal linearity



Can't optimise both !

Target should be linearity

Resolution ( $\sigma/E$ )



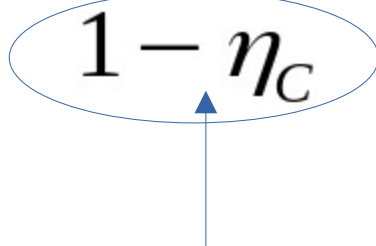


# $f_{em}$ (really $f_h$ ) estimation

---

Independently for S and C signals, you can easily get:

$$\eta_x \equiv (h/e)_x$$

$$f_h \stackrel{\text{def}}{=} (1 - f_{em}) = \frac{1 - S/E}{1 - \eta_S} = \frac{1 - S/E}{\chi \cdot (1 - \eta_C)} = \frac{1 - C/E}{1 - \eta_C}$$


$f_h$  can be estimated event-by-event within scale factor  $\approx 1$   
(since  $\eta_C \ll 1$ )

# (h/e) estimation (?)

Up to few hundreds GeV,  $\langle f_h \rangle$  as function of  $E$ , should be fairly well described by:

$$\langle f_h(E) \rangle \approx (E/E_0)^{m-1} \quad \text{for } E > E_0$$

where mainly (?)  $m$  should depend on absorber,  $E_0$  on particle type

Two-parameter fit to:

$$1 - \langle C/E \rangle \approx (1 - \eta_C) \times (E/E_0)^{m-1} = \lambda \times E^{m-1}$$

$$\lambda \equiv (1 - \eta_C) \times E_0^{1-m}$$

Some more input/assumptions (?):

$$m \in [0.80, 0.87] \Rightarrow 1 - m \in [0.13, 0.20] \ll 1$$

$$E_0(\pi) \ [ \ E_0(p) \ ] \approx 1 \text{ GeV} \ [ \ 2.6 \text{ GeV} \ ]$$

with pion data, since  $E_0^{1-m}(\pi) \approx 1 \Rightarrow \lambda(\pi) \approx 1 - \eta_C$

then with proton [ kaon, ... ] data  $\Rightarrow E_0(p) \ [ \ E_0(K), \dots \ ]$

to be checked with M.C.  
and (hopefully) validated  
with some TB data ...

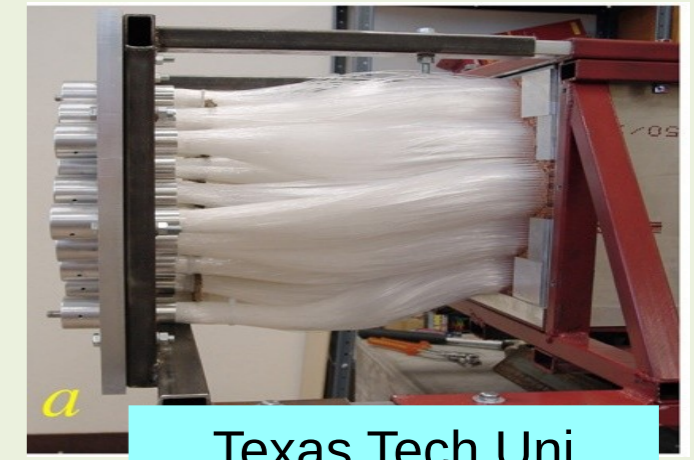
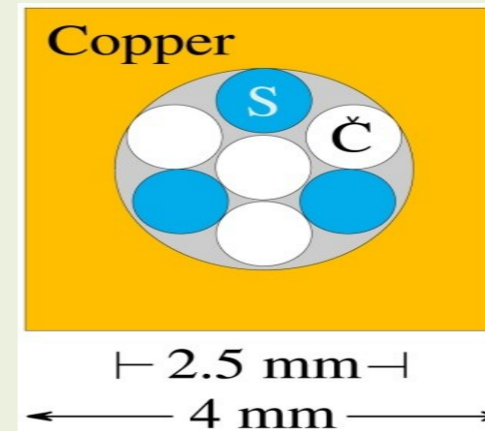
---

## 3. Few DREAM/RD52 results

# DREAM/RD52 dual-readout spaghetti prototypes

2003  
DREAM

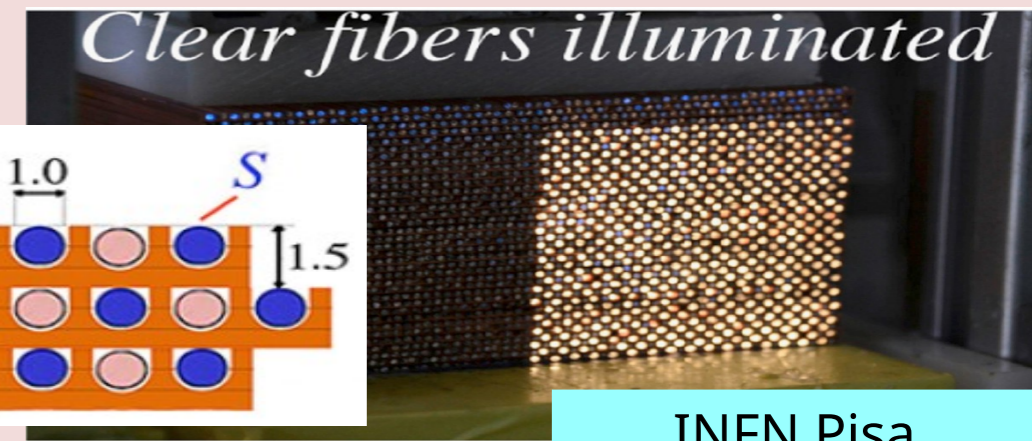
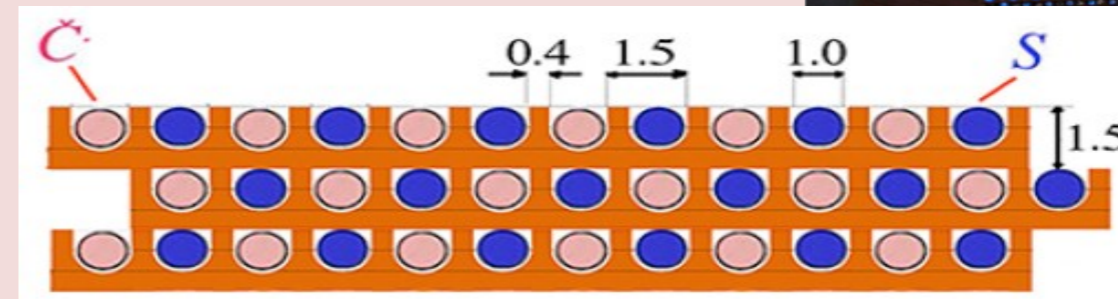
Cu: 19 towers, 2 PMT each  
2 m long, 16.2 cm radius  
Sampling fraction: 2%  
Depth:  $\sim 10 \lambda_{\text{int}}$



Texas Tech Uni

2012  
RD52

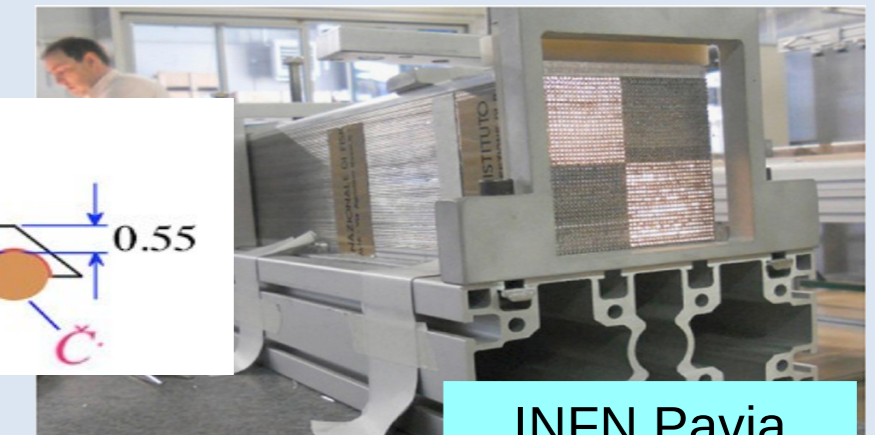
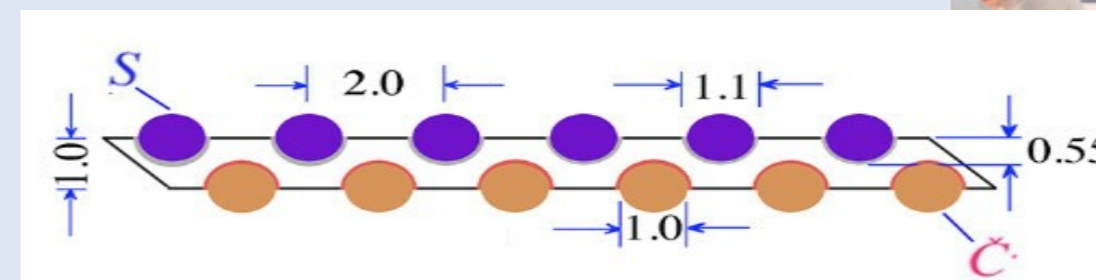
Cu, 2 modules  
Each module:  $9.2 \times 9.2 \times 250 \text{ cm}^3$   
Fibers: 1024 S + 1024 C, 8 PMT  
Sampling fraction:  $\sim 4.6\%$   
Depth:  $\sim 10 \lambda_{\text{int}}$



INFN Pisa

2012  
RD52

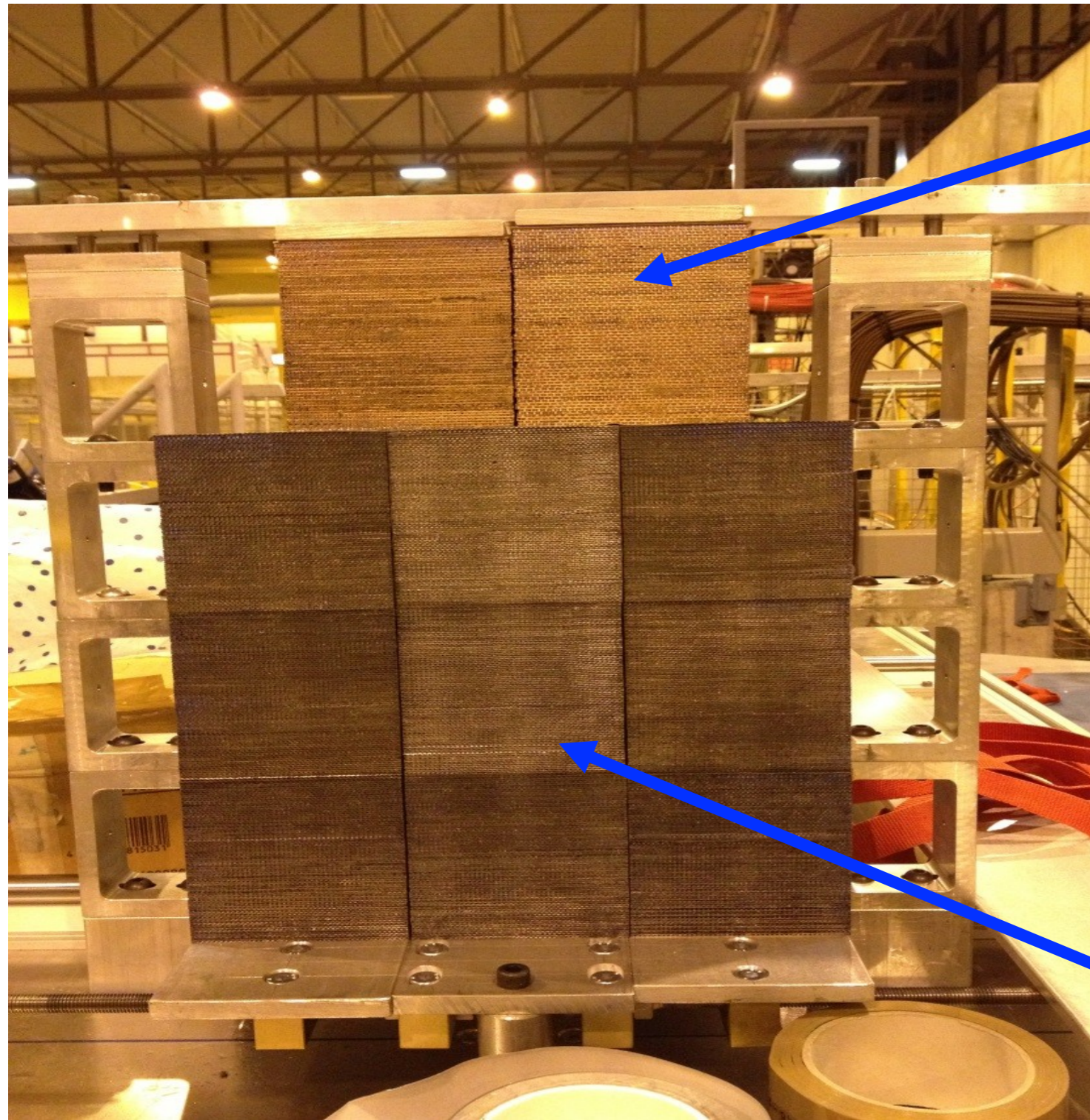
Pb, 9 modules  
Each module:  $9.2 \times 9.2 \times 250 \text{ cm}^3$   
Fibers: 1024 S + 1024 C, 8 PMT  
Sampling fraction:  $\sim 5.3\%$   
Depth:  $\sim 10 \lambda_{\text{int}}$



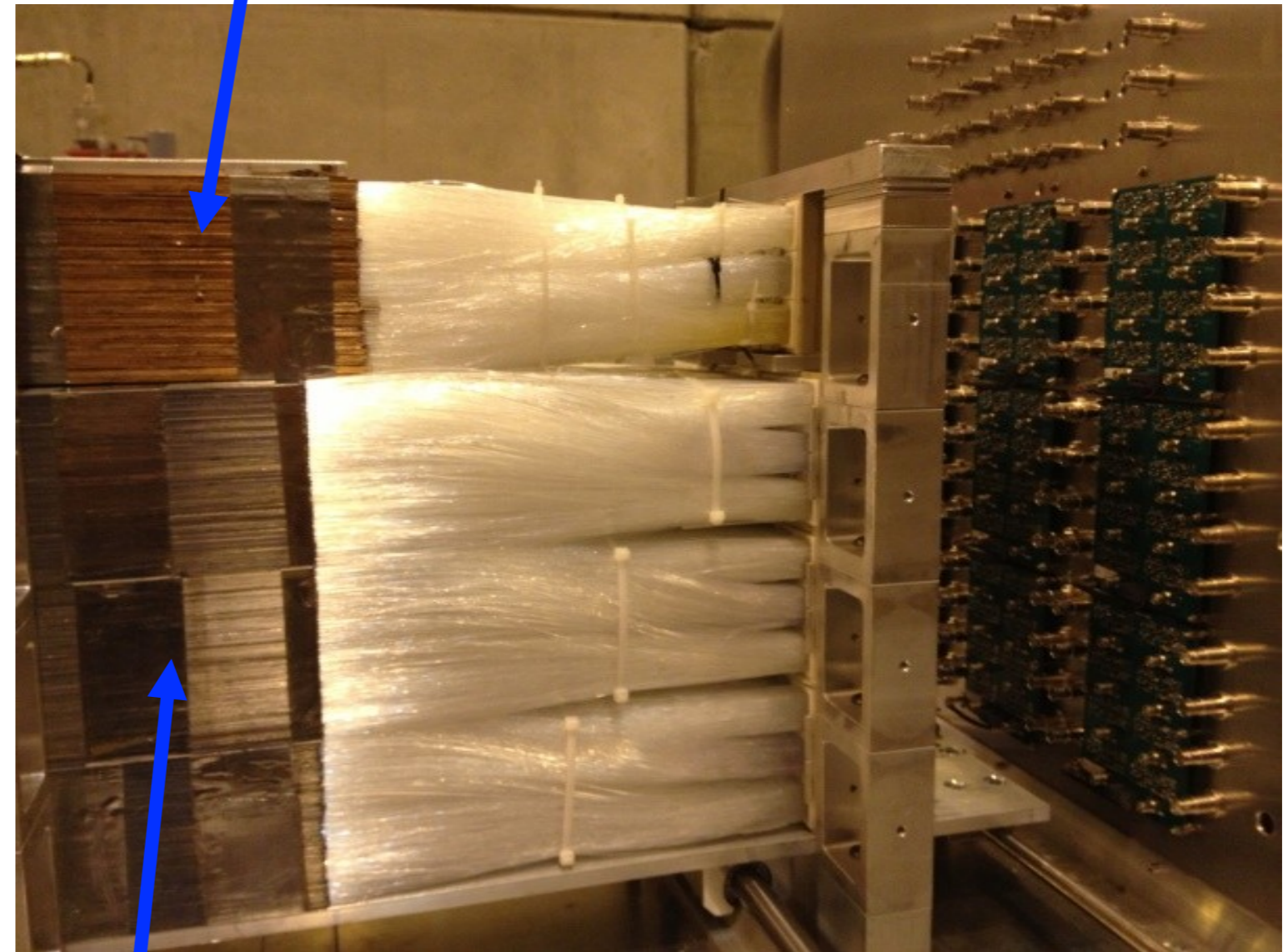
INFN Pavia



# RD52 dual-readout spaghetti prototypes



2 Cu modules



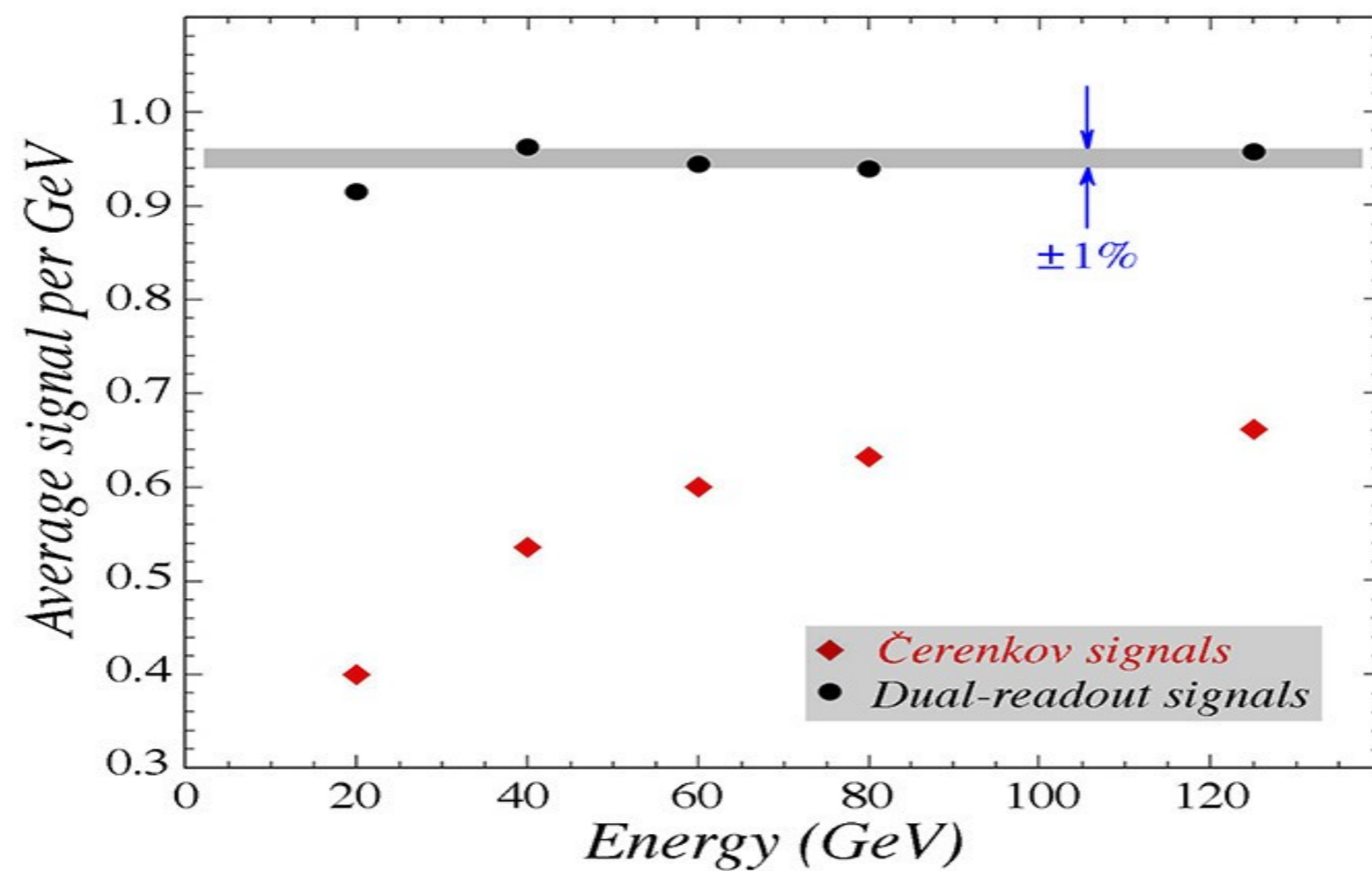
3x3 lead matrix



# dual-readout at work (1)

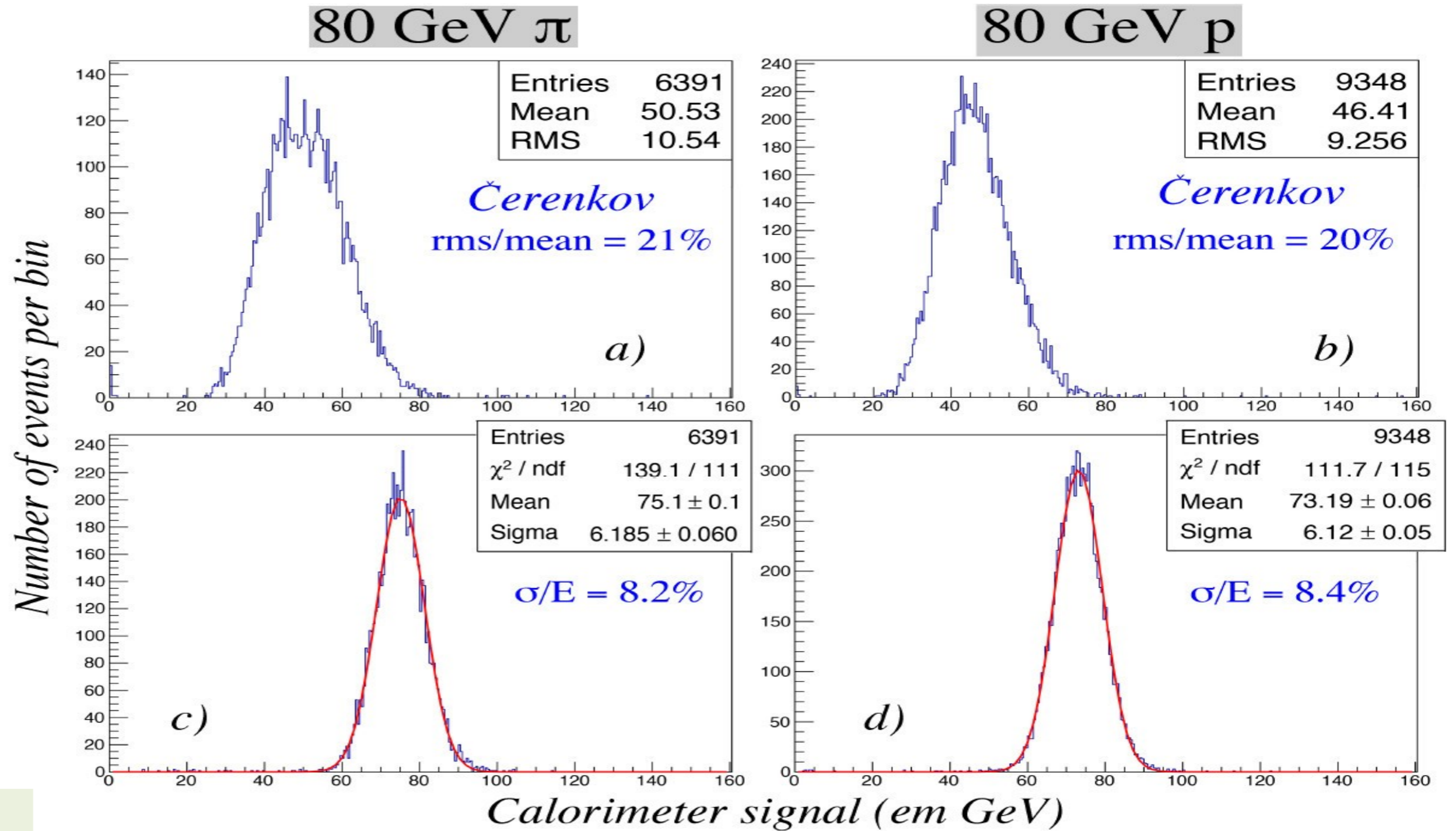
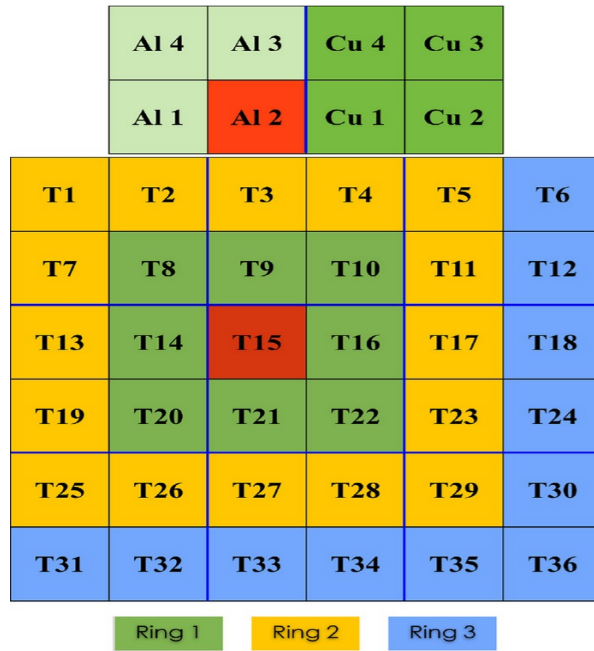
## *Effects of the dual-readout method*

### Signal linearity



NIM A 866 (2017) 76

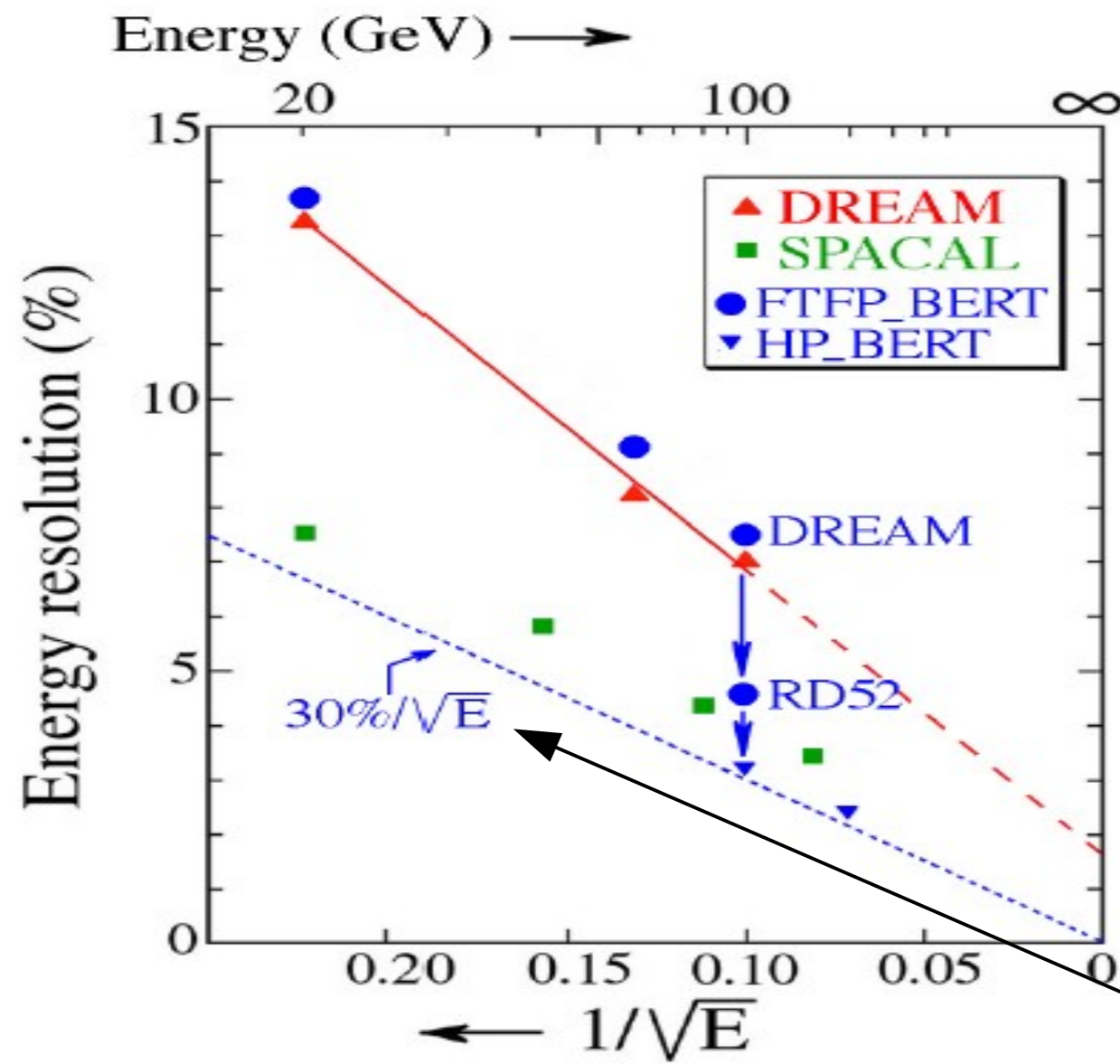
# dual-readout at work (2)



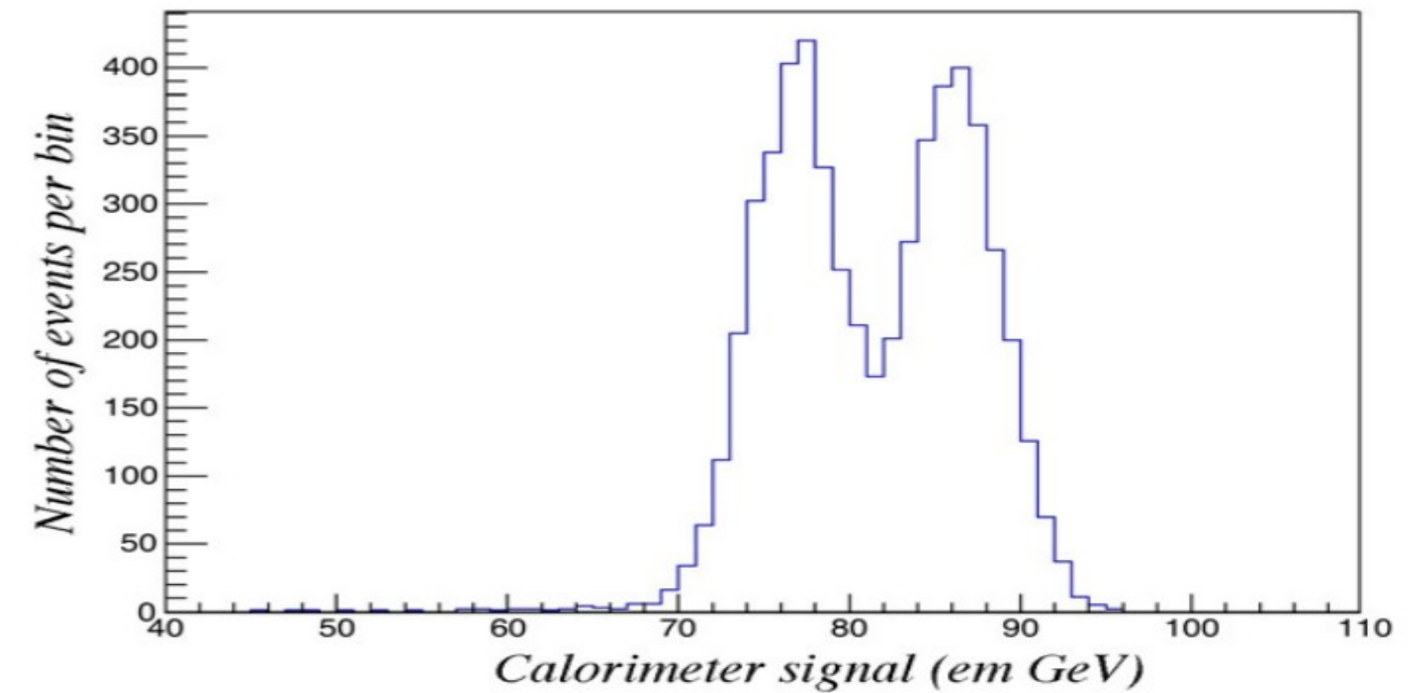
NIM A 866 (2017) 76

# RD52 expected hadronic performance

## Hadronic Resolution



## W/Z separation



Geant4 simulations

NIM A 824 (2016) 721



# particle ID (electron/hadron discrimination)

RD52 lead calorimeter

(60 GeV)  $e^-$  vs.  $\pi^-$

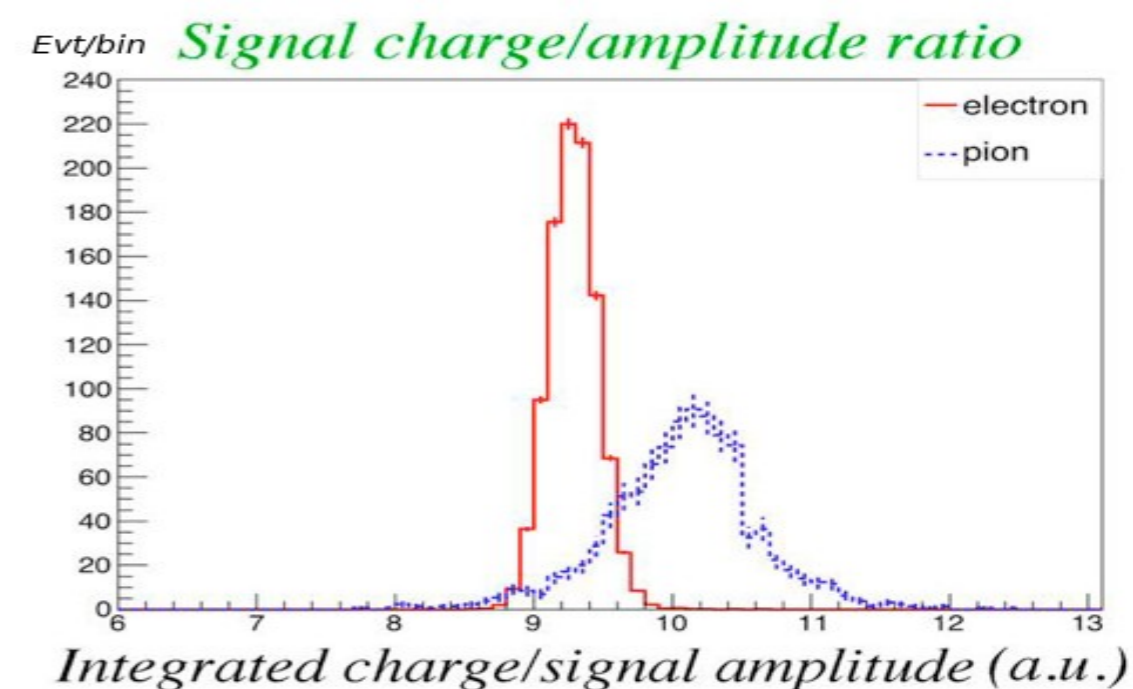
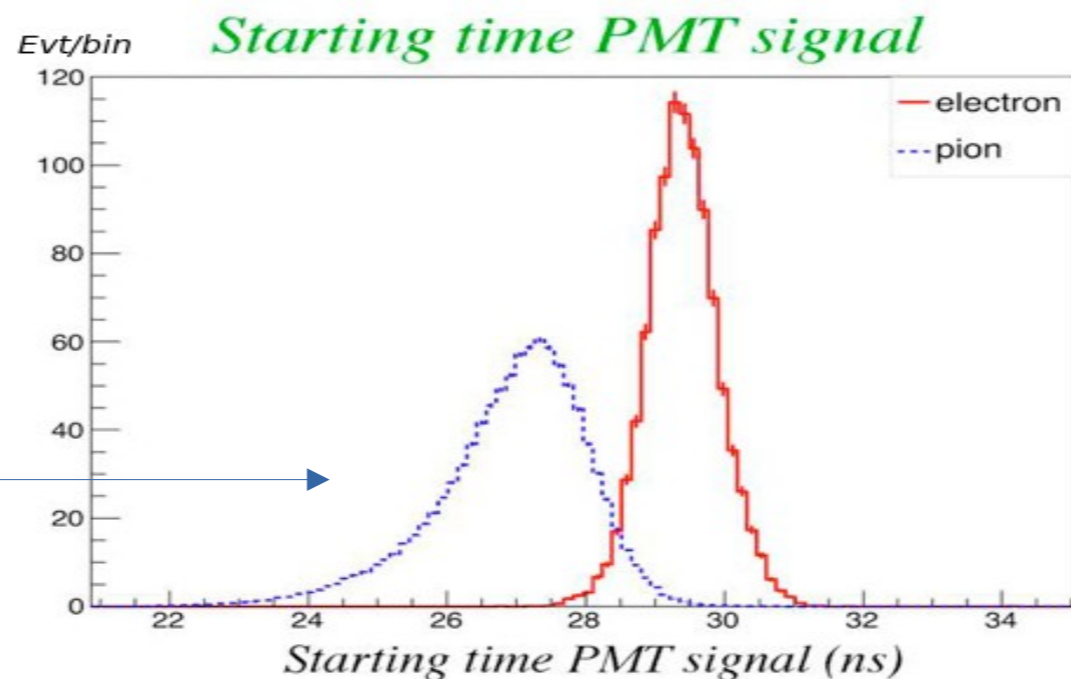
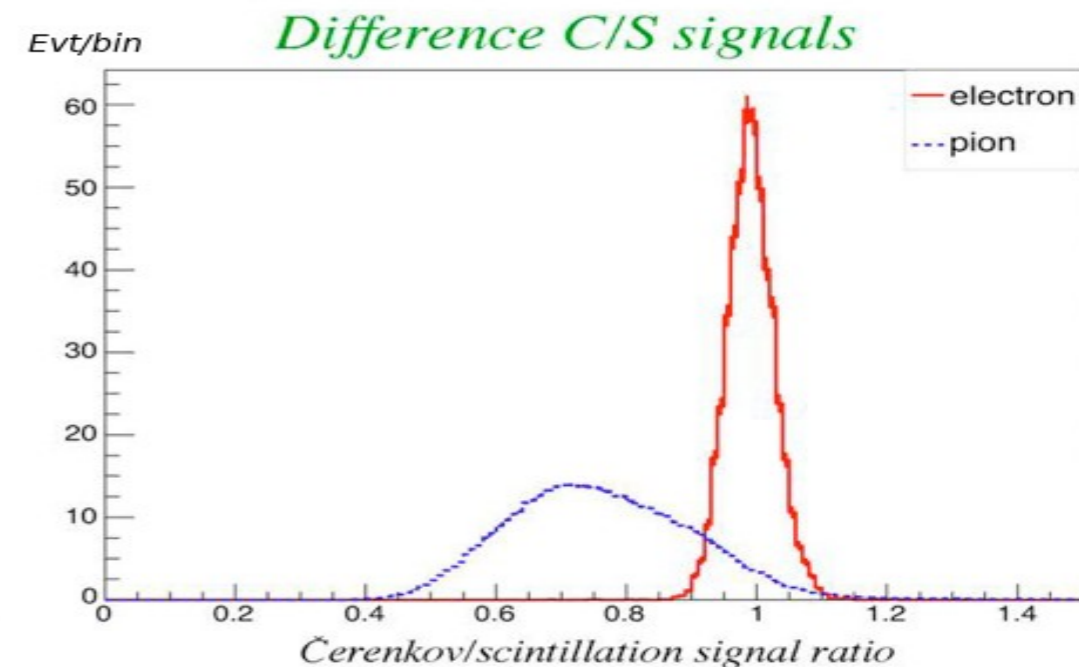
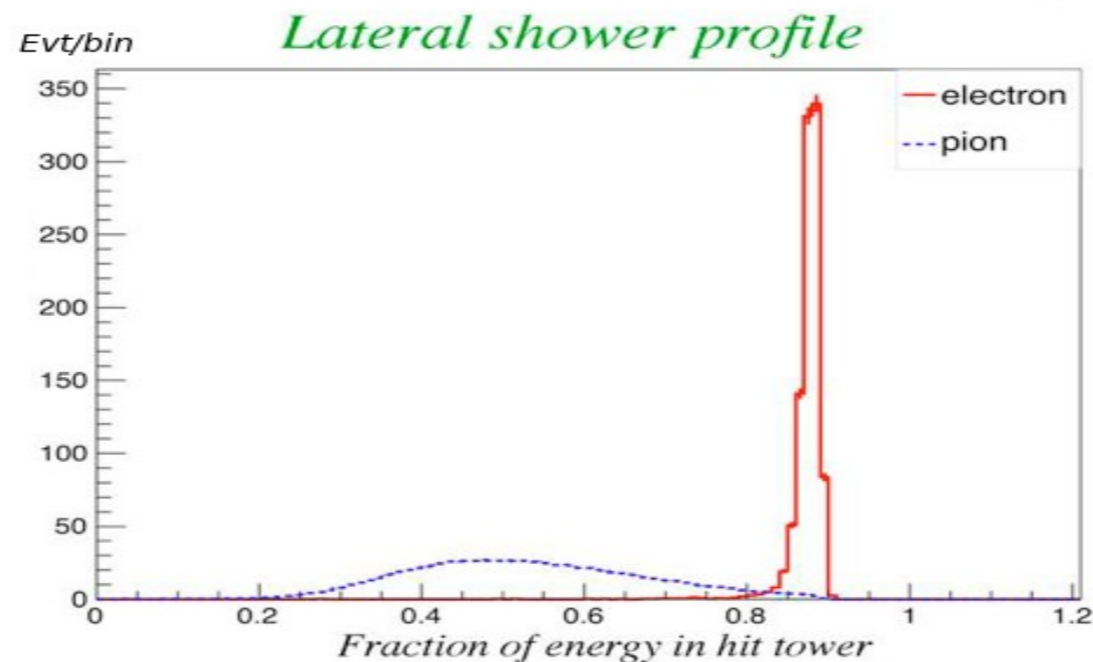
$\epsilon(e^-) > 99\%$

$R(\pi^-) \sim 500$

NIM A 735 (2014) 120

time-of-arrival distribution  
measured w/ TDC

*Methods to distinguish  $e/\pi$  in longitudinally unsegmented calorimeter*



*Combination of cuts:  $>99\%$  electron efficiency,  $<0.2\%$  pion mis-ID*

---

## 4. Dual readout goes granular ( IDEA fibre calorimeter )

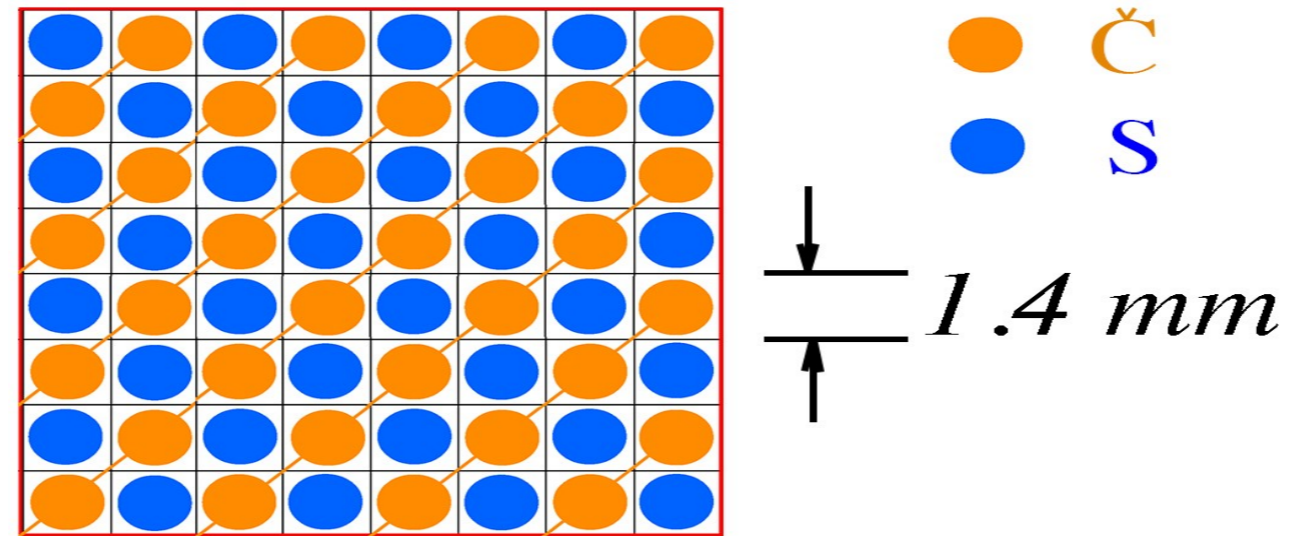
# RD52 SiPM module

Brass module, dimensions: ~ 112 cm long, 12 x 12 mm<sup>2</sup>

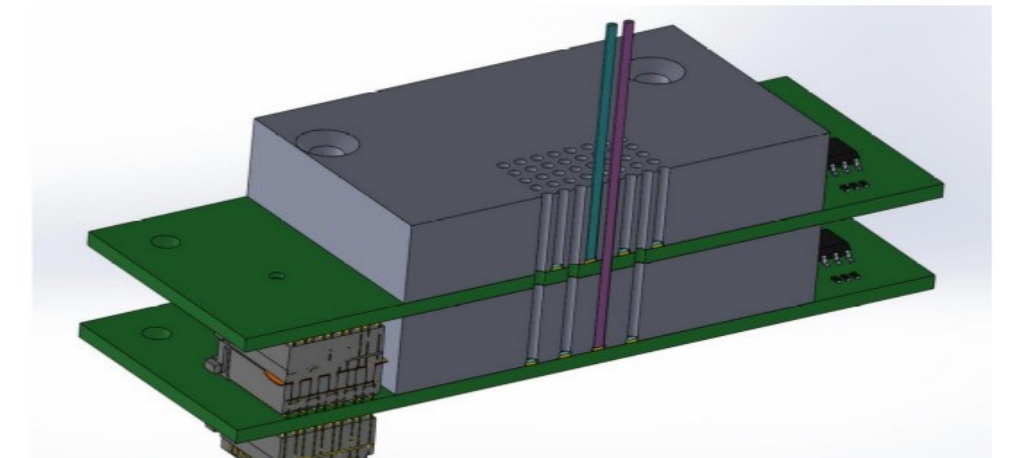
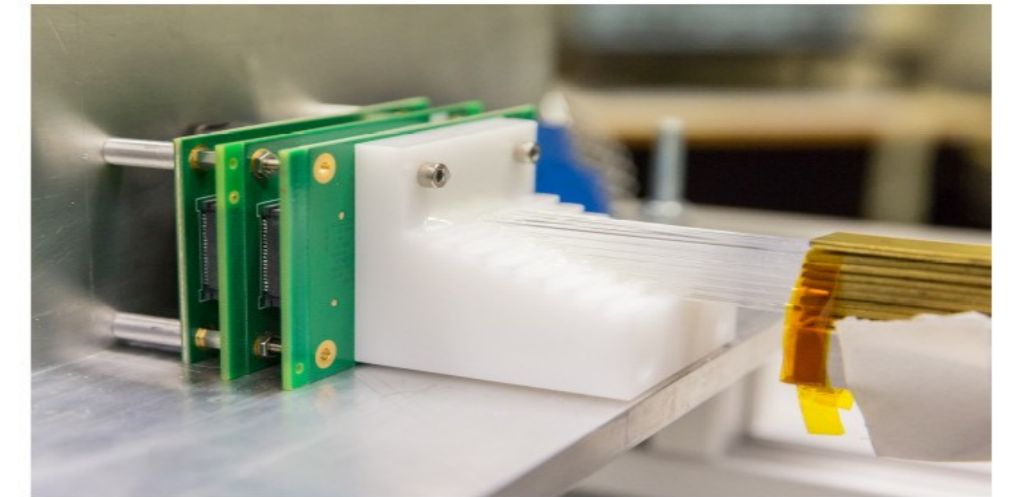
32 (S) + 32 (Č) fibres  
 $X_0 \sim 29$  mm  
 $R_M \sim 31$  mm

$\sim (0.4 R_M)^2 \times 39 X_0$

shower cont.  $\sim 45\%$   
 $f_{\text{sampl}} \sim 5-6\%$

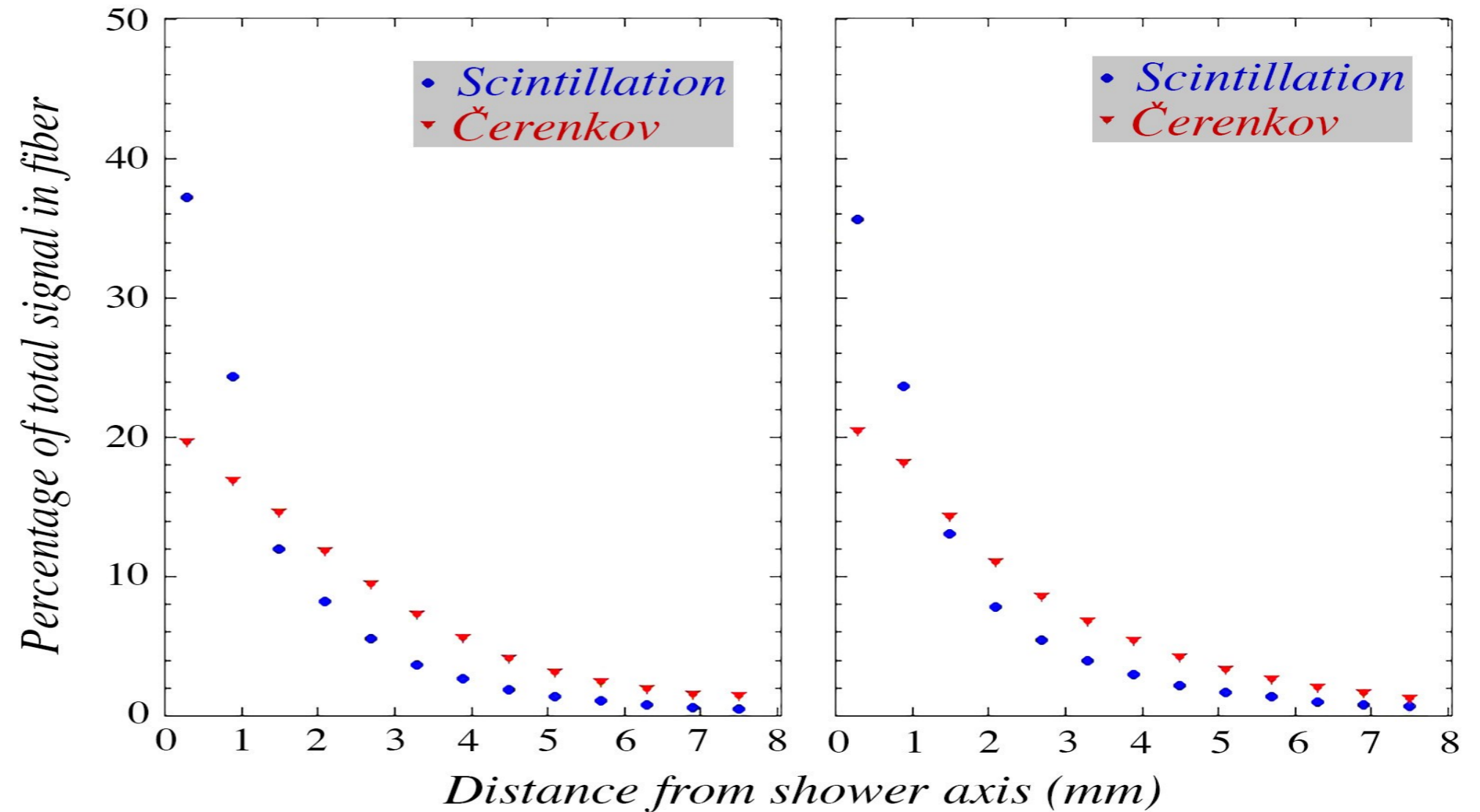


Light sensors (SiPM)



# lateral shower profile w/ SiPMs

10 / 40 GeV  $e^-$   
 $\theta, \Phi = 0^\circ$



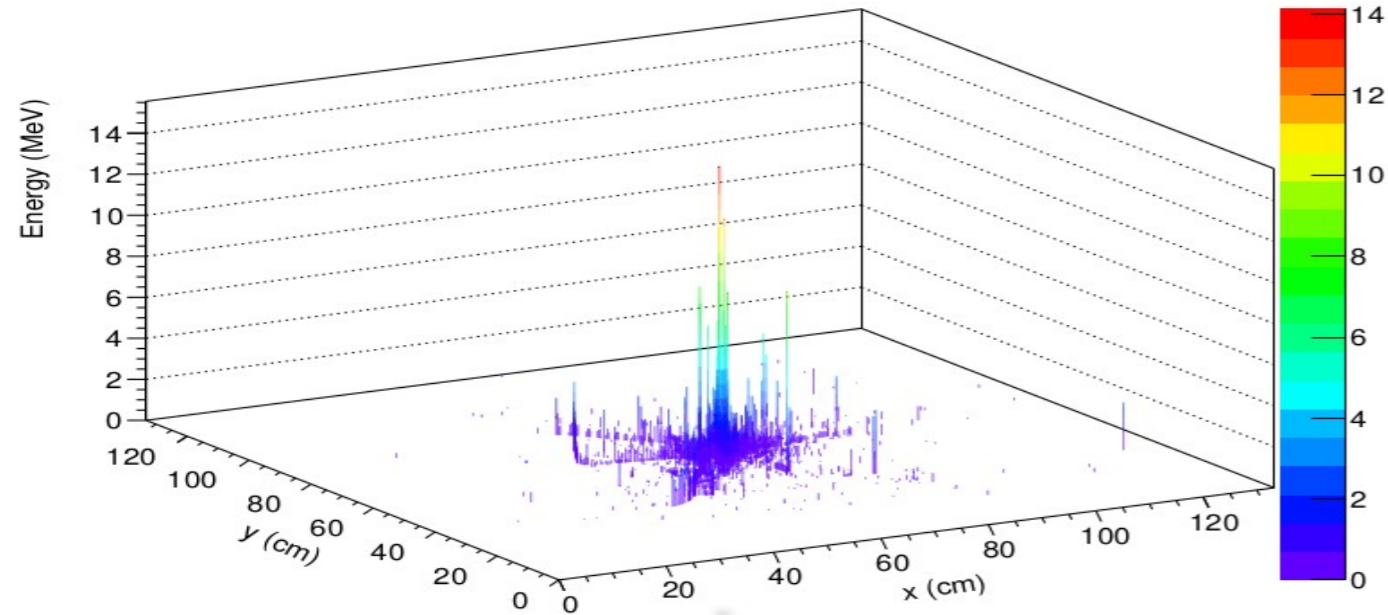
em shower very narrow:

- ~10% (~50%) within ~1 (~10) mm from shower axis
- fibre readout can easily provide (powerful) input to PFA



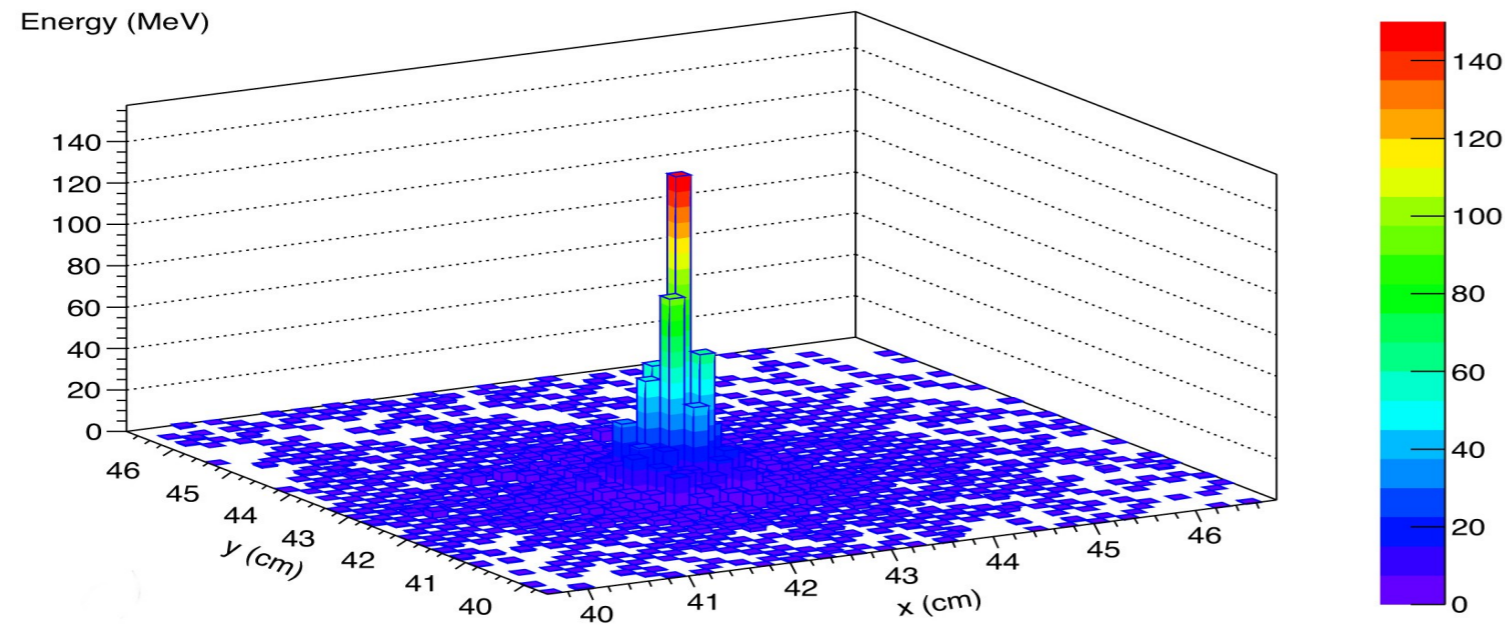
# 2D fibre imaging

## 80 GeV $\pi^-$

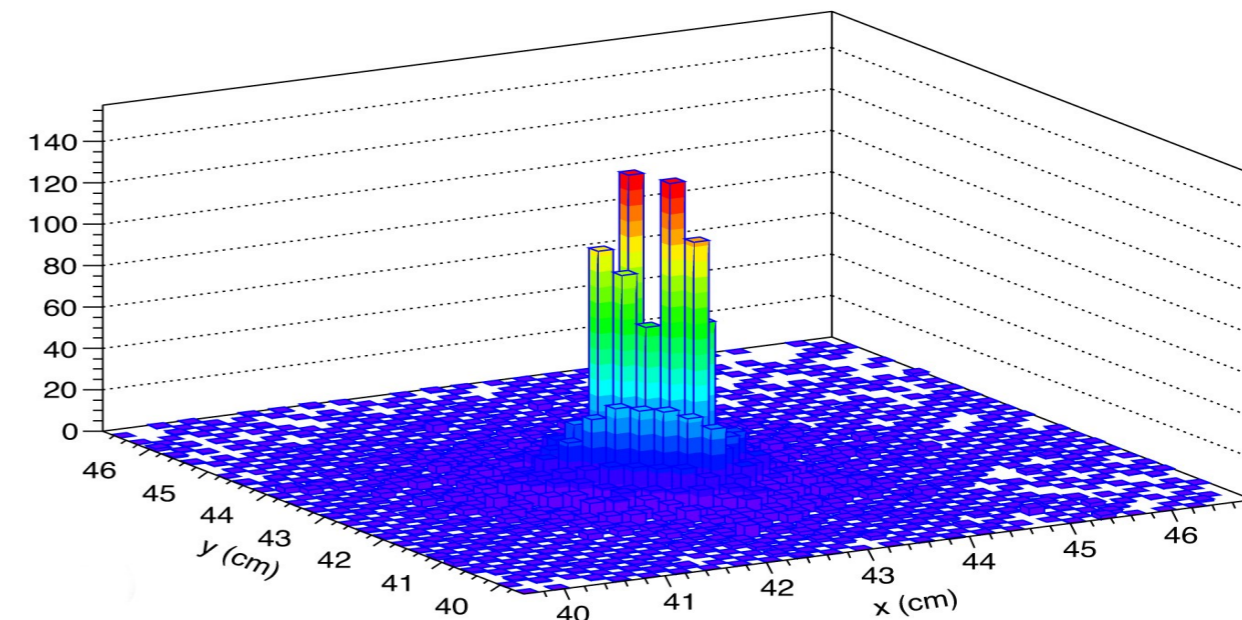


## Geant4 single-particle simulations

## 50 GeV $e^-$



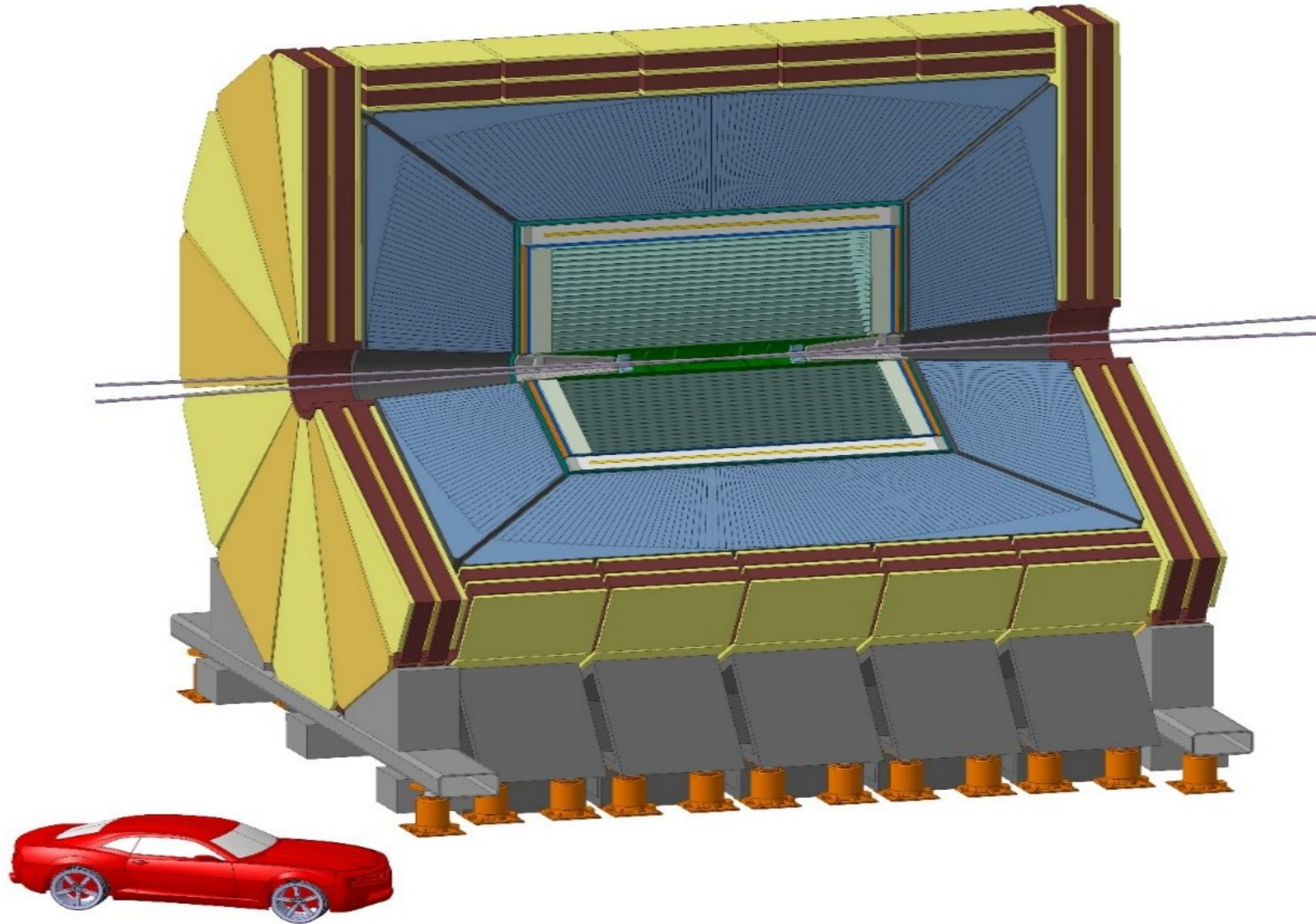
## 100 GeV $\pi^0$





# IDEA: Innovative Detector for e<sup>+</sup>e<sup>-</sup> Accelerators

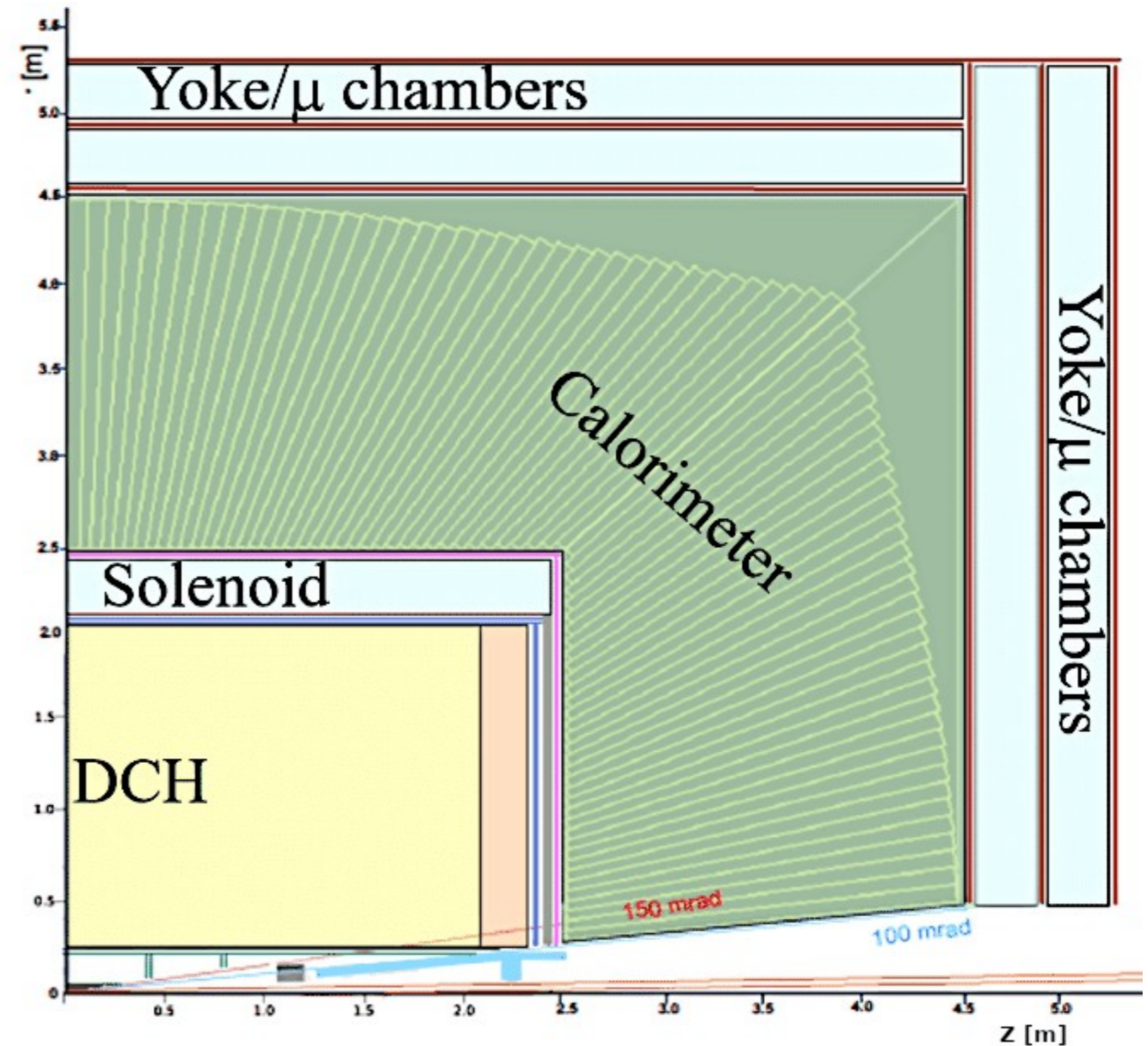
---





# IDEA baseline concept

- ◆ Muon chambers
  - ◆  $\mu$ -RWELL in return yoke
- ◆ Dual-readout calorimetry 2 m /  $7 \lambda_{\text{int}}$ 
  - ◆  $\mu$ -RWELL preshower
- ◆ Thin superconducting solenoid
  - ◆ 2 T, 30 cm,  $\sim 0.7 X_0$ ,  $0.16 \lambda_{\text{int}}$  @  $90^\circ$
- ◆ Highly transparent for tracking
  - ◆ Si pixel vertex detector
  - ◆ Drift Chamber
  - ◆ Si wrappers (strips)
- ◆ Beam pipe:  $r \sim 1.5$  cm



# IDEA dual-readout calorimetry group

---

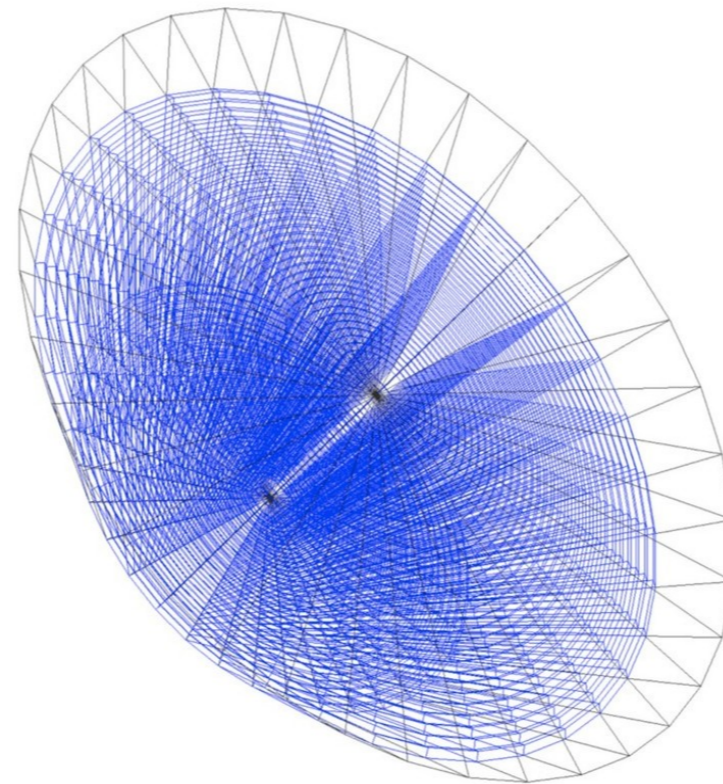
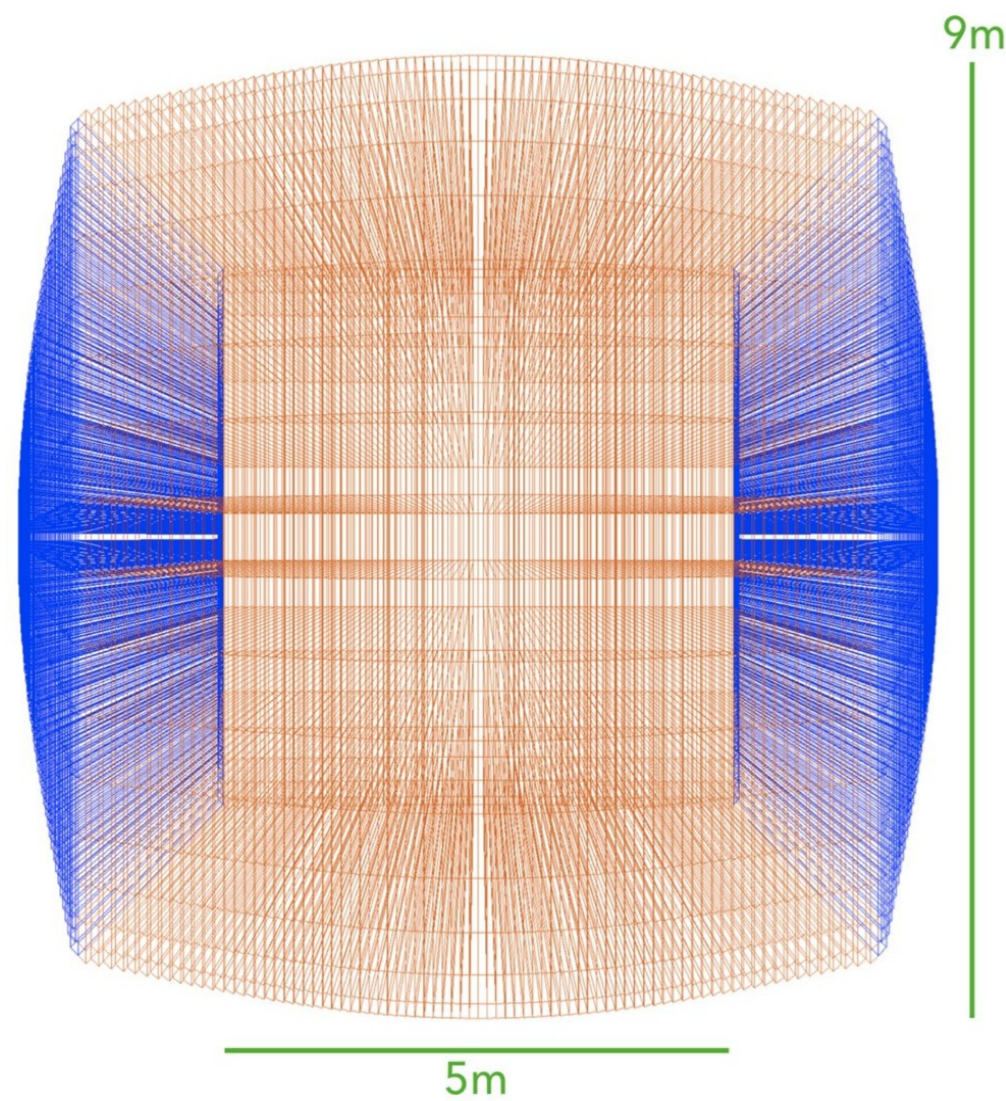
Three main activity pillars:

1. Europa: INFN, Sussex University → mainly (but not only) fibre-sampling calorimetry
2. Korea → projective fibre-sampling calorimetry
3. U.S. (Calvision project) → mainly (but not only) crystal em calorimetry

keywords: dual readout, high granularity & timing



# IDEA all-fibre DR calorimeter option

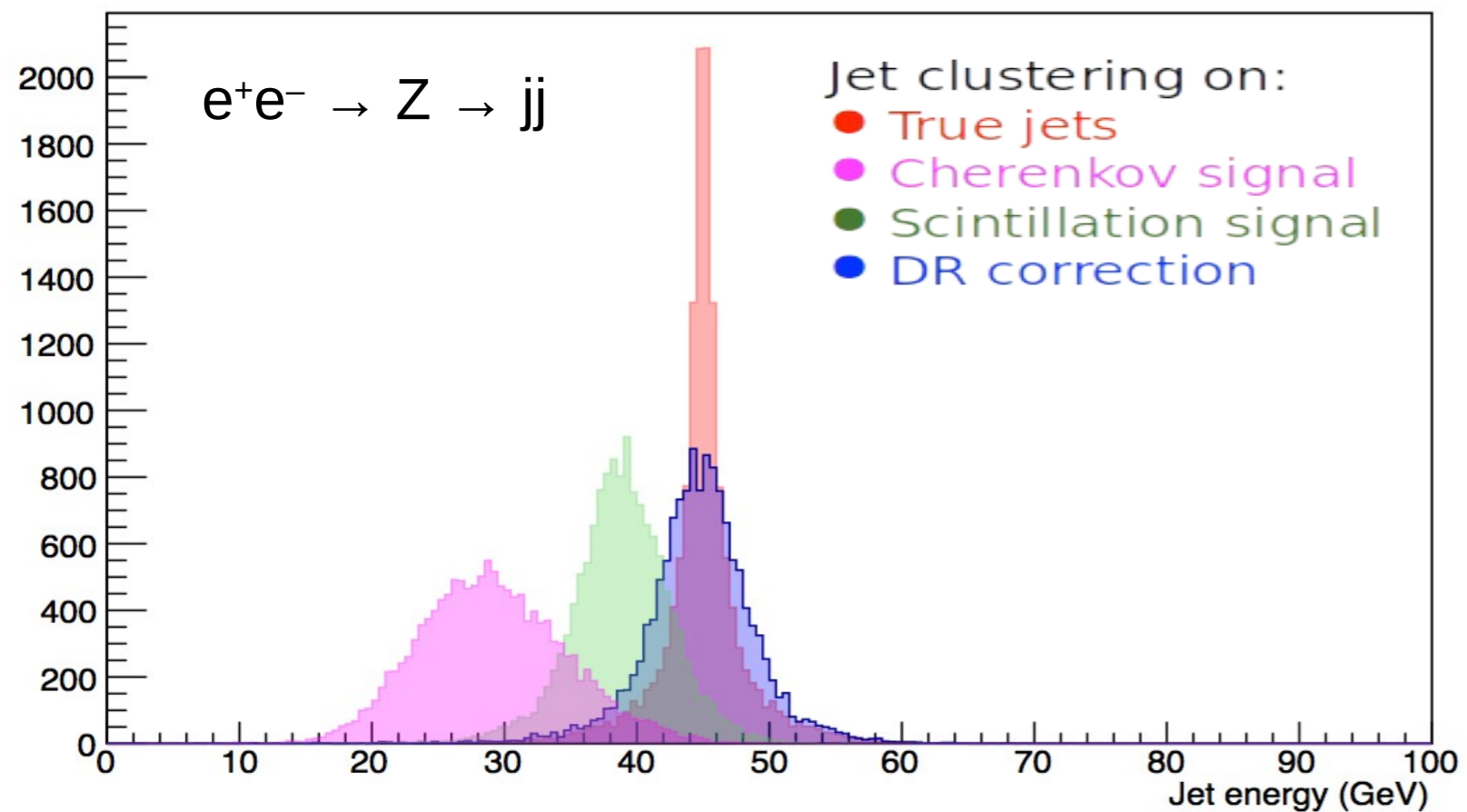


- ◆ DR fibre calorimeter
  - ◆ O(100 M) fibres
    - ◆ 1 mm  $\varnothing$ , 1.5 mm pitch
  - ◆ copper absorber
  - ◆ 75 projective towers  $\times$  36 slices
    - ◆  $\Delta\vartheta = 1.125^\circ$ ,  $\Delta\phi = 10.0^\circ$
    - ◆  $\vartheta$  coverage:  $|\vartheta| > 100$  mrad
- ◆ G4 simulation available
  - ◆ tuned to RD52 TB data

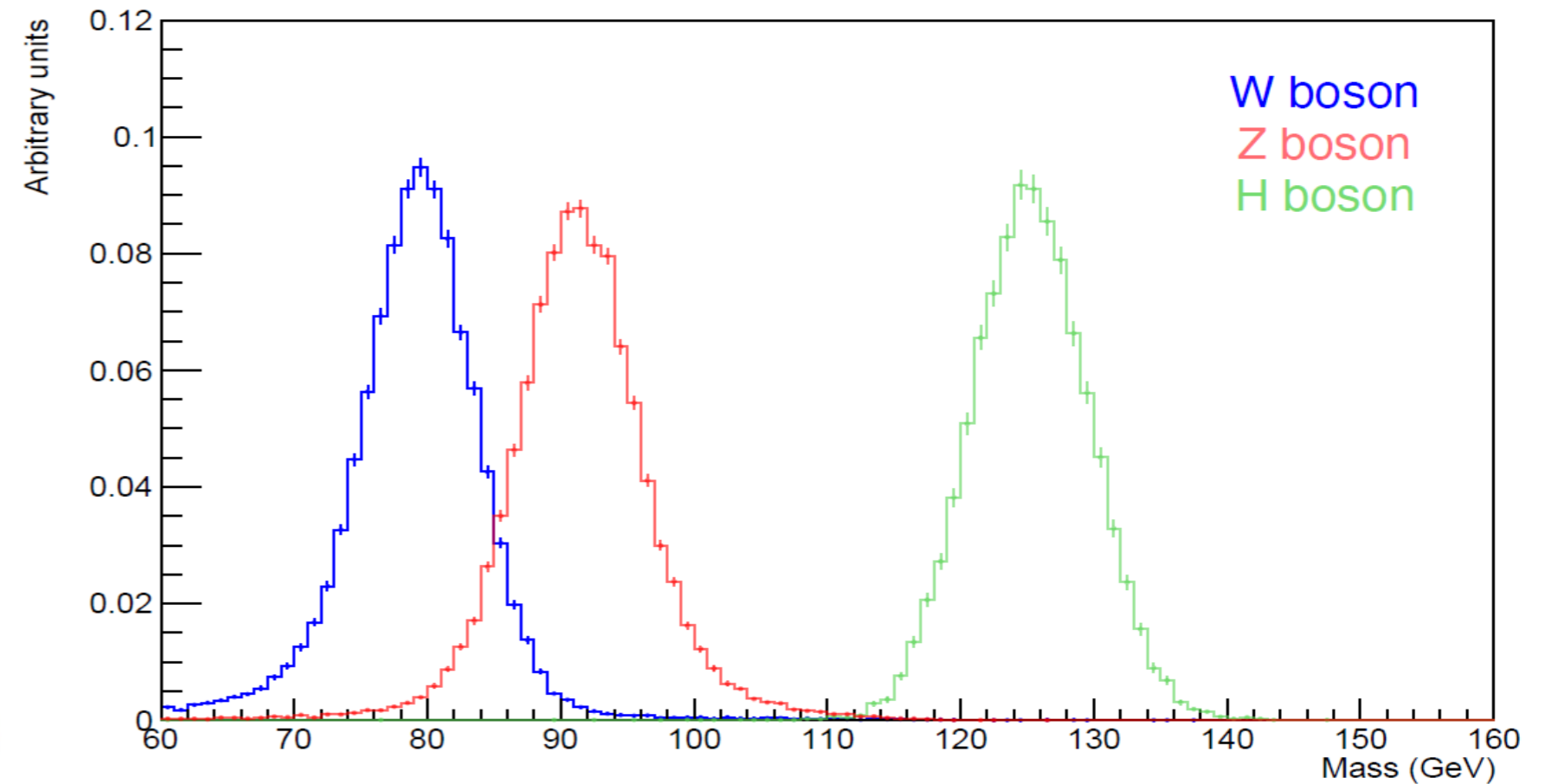
# Geant4 simulations

- ◆ Gaussian resolution
- ◆ Adequate separation of W / Z / H

Single jet resolution @ 45 GeV



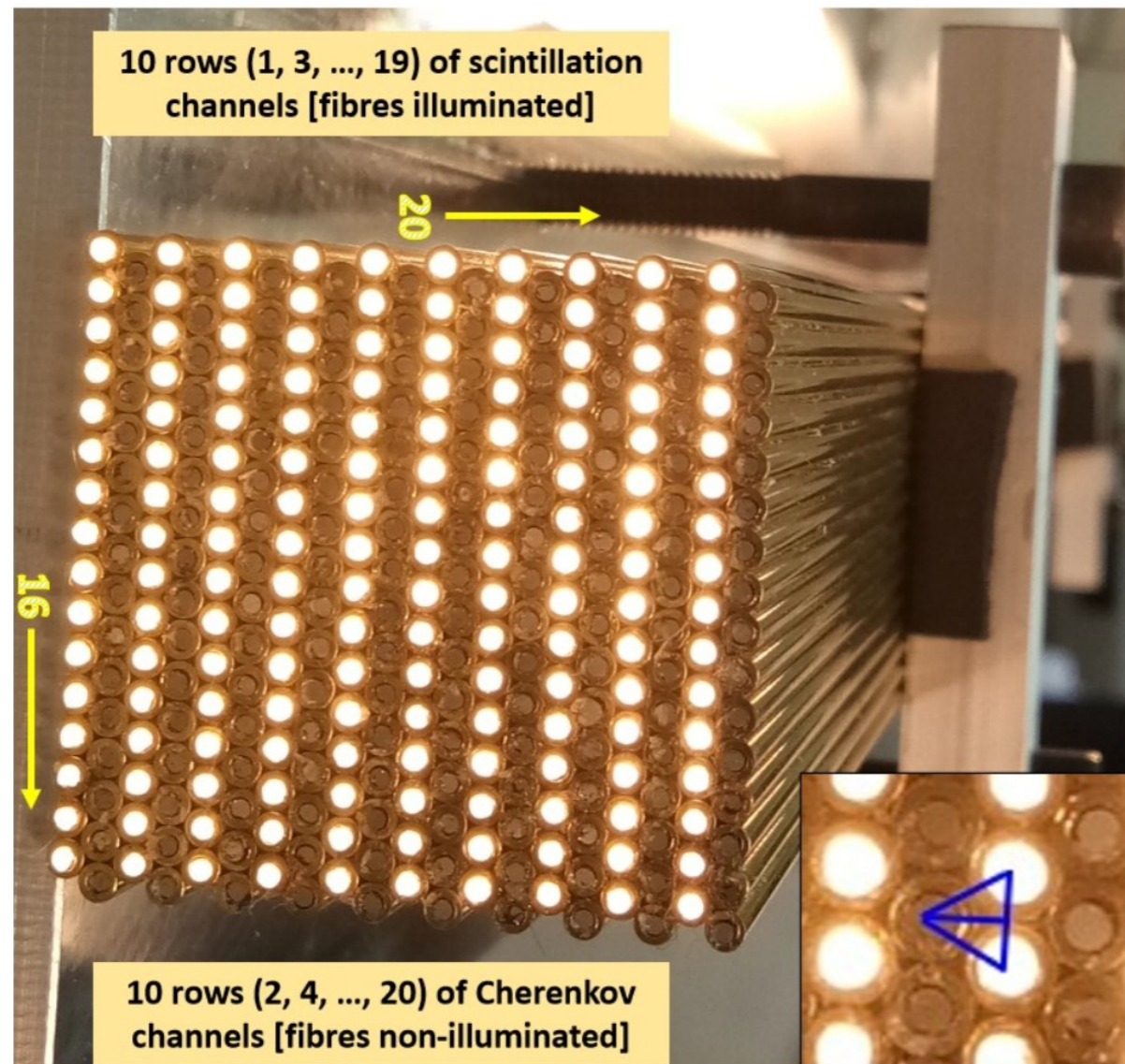
W/Z/H  $\rightarrow$  jj invariant mass



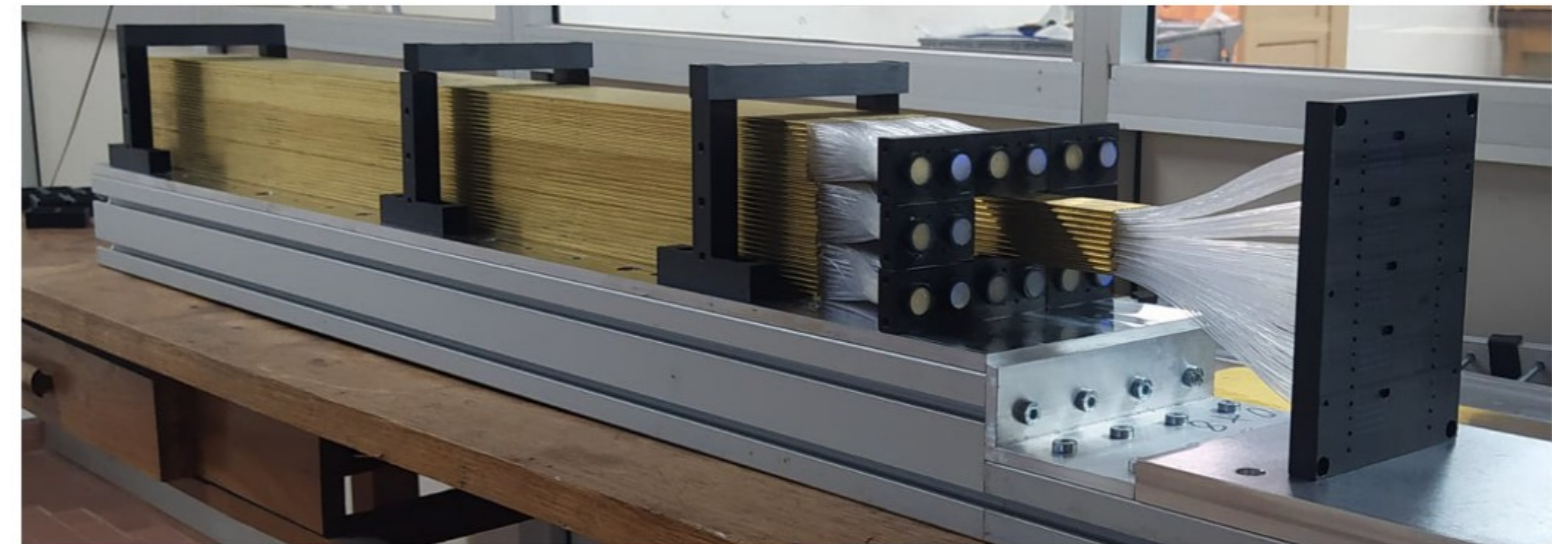


# IDEA 2020 em-size bucatini prototype (EU)

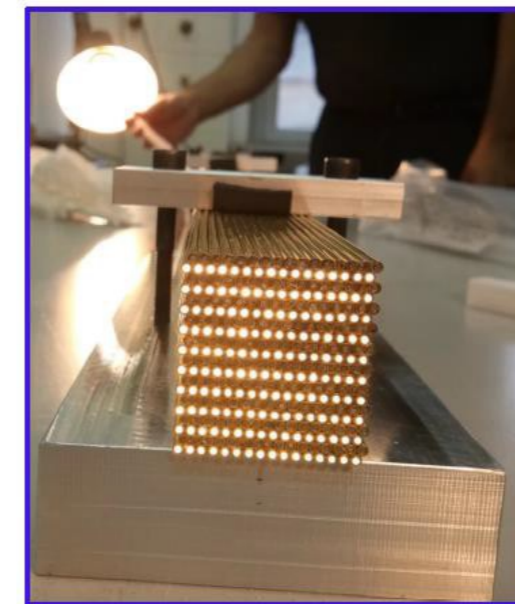
Nine  $\sim 3.5 \times 3.3$  cm<sup>2</sup> towers made of capillary brass tubes



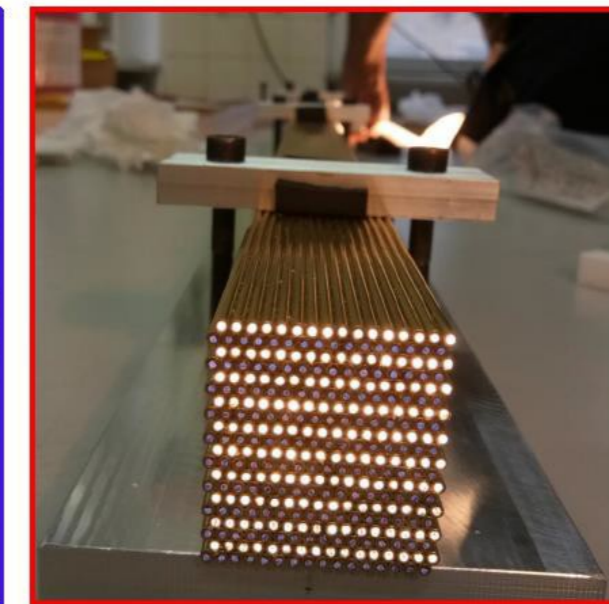
Central tower (360 fibres) w/ highly granular SiPM readout



Eight (surrounding) towers read out with PMTs



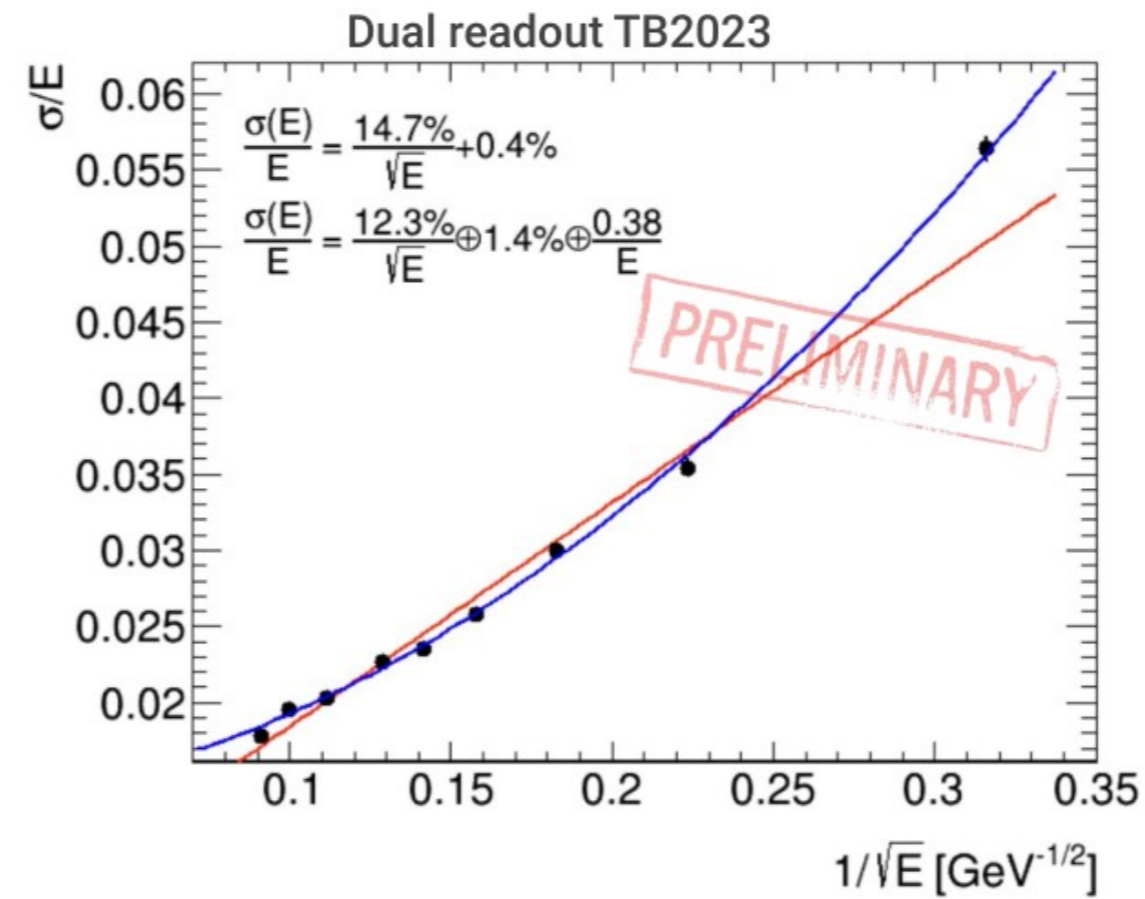
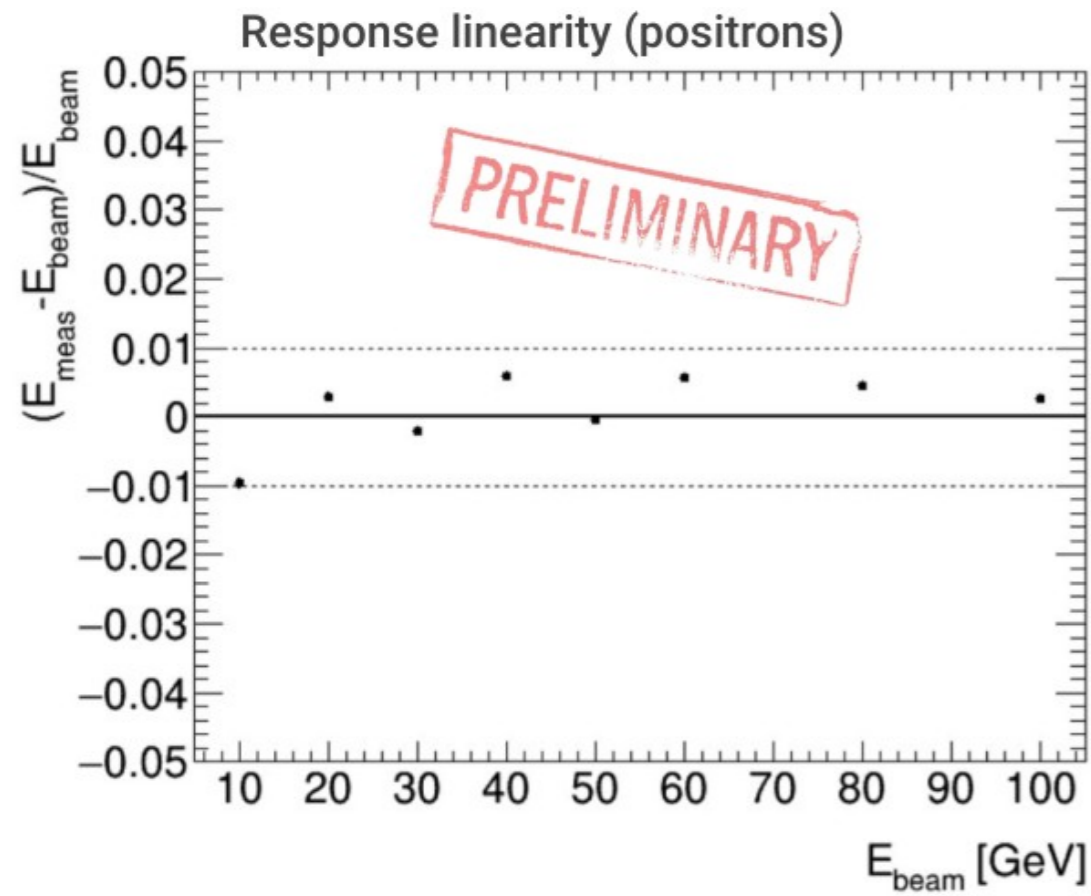
Scintillation fibers



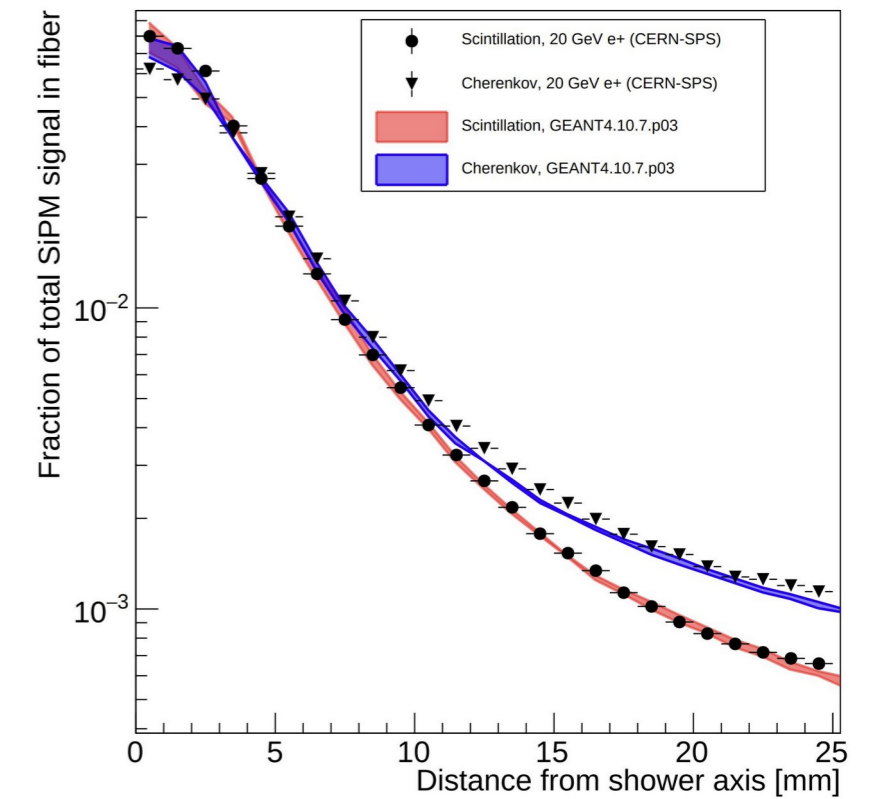
Cherenkov fibers



# Few testbeam results



### Lateral shower profile (2021 TB)



---

## 5. Exploiting timing and DNNs

# $\tau$ -decay tagging w/ DNNs

---

Testbeam module (brass absorber): dimensions:  $133.2 \times 133.2 \times 250 \text{ cm}^3$

Reduced granularity ( $1.2 \times 1.2 \text{ cm}^2$ , 32 S & 32 C fibres):  $111 \times 111$  modules

Simulation of both detector and SiPM response

Feature extraction: E(Q), Pk, ToP, ToA, ToT

→ each event represented by  $111 \times 111 \times 5 \times 2$  tensor

# NN implementation

Two DNN architecture variants studied:

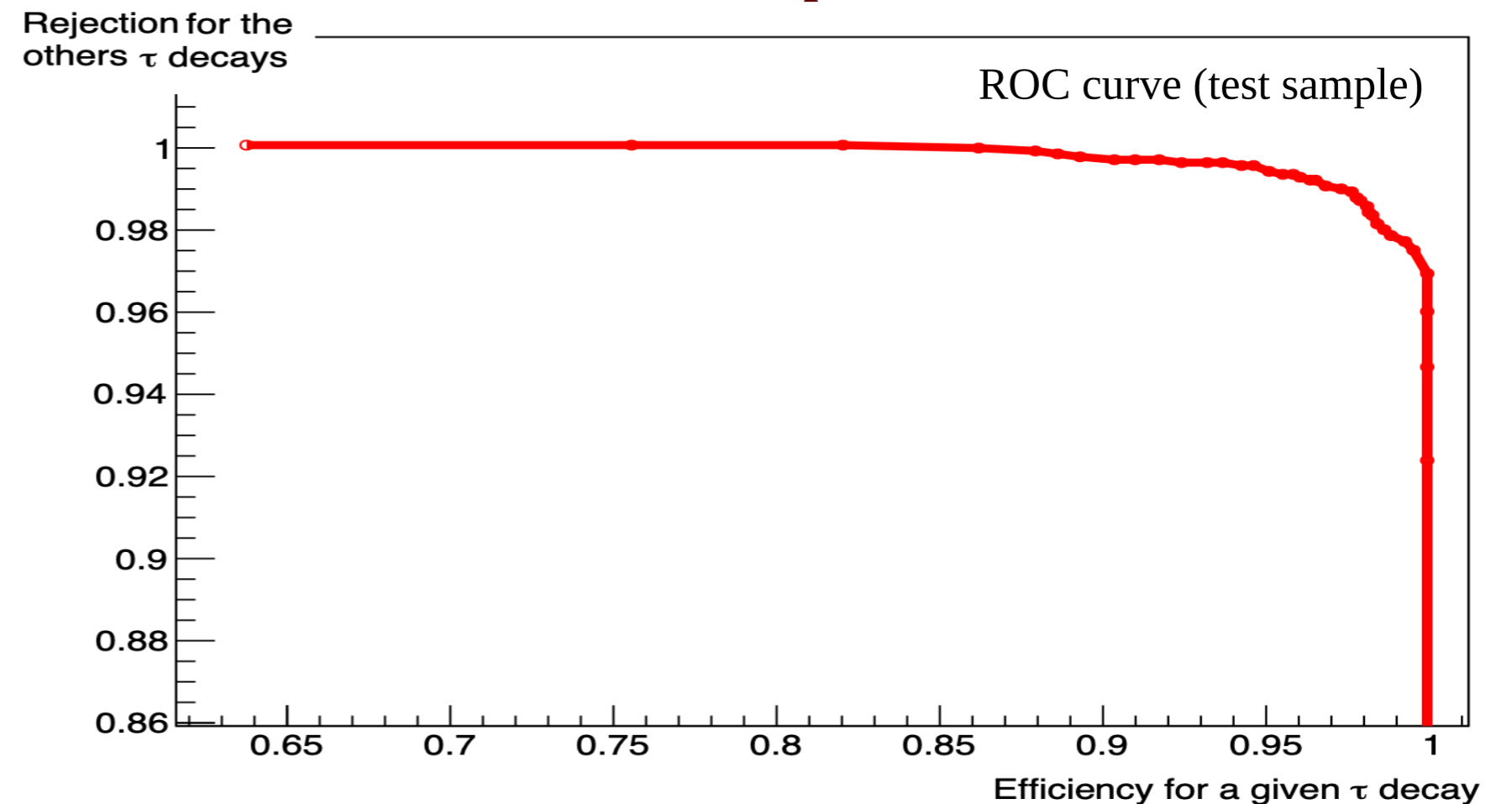
- VGG-11 like (VGG = Visual Geometry Group, Oxford Un.)
- Dynamic Graph CNN (DGCNN)

6 event classes (covering  $\sim 90\%$  of  $\tau$  decays)

Training set: 6 BR  $\times$  2000 evts

$\tau \rightarrow \pi\pi^0\nu$
$\tau \rightarrow \mu\nu\nu$
$\tau \rightarrow e\nu\nu$
$\tau \rightarrow \pi\nu$
$\tau \rightarrow \pi\pi\pi\nu$
$\tau \rightarrow \pi\pi^0\pi^0\nu$

VGG example

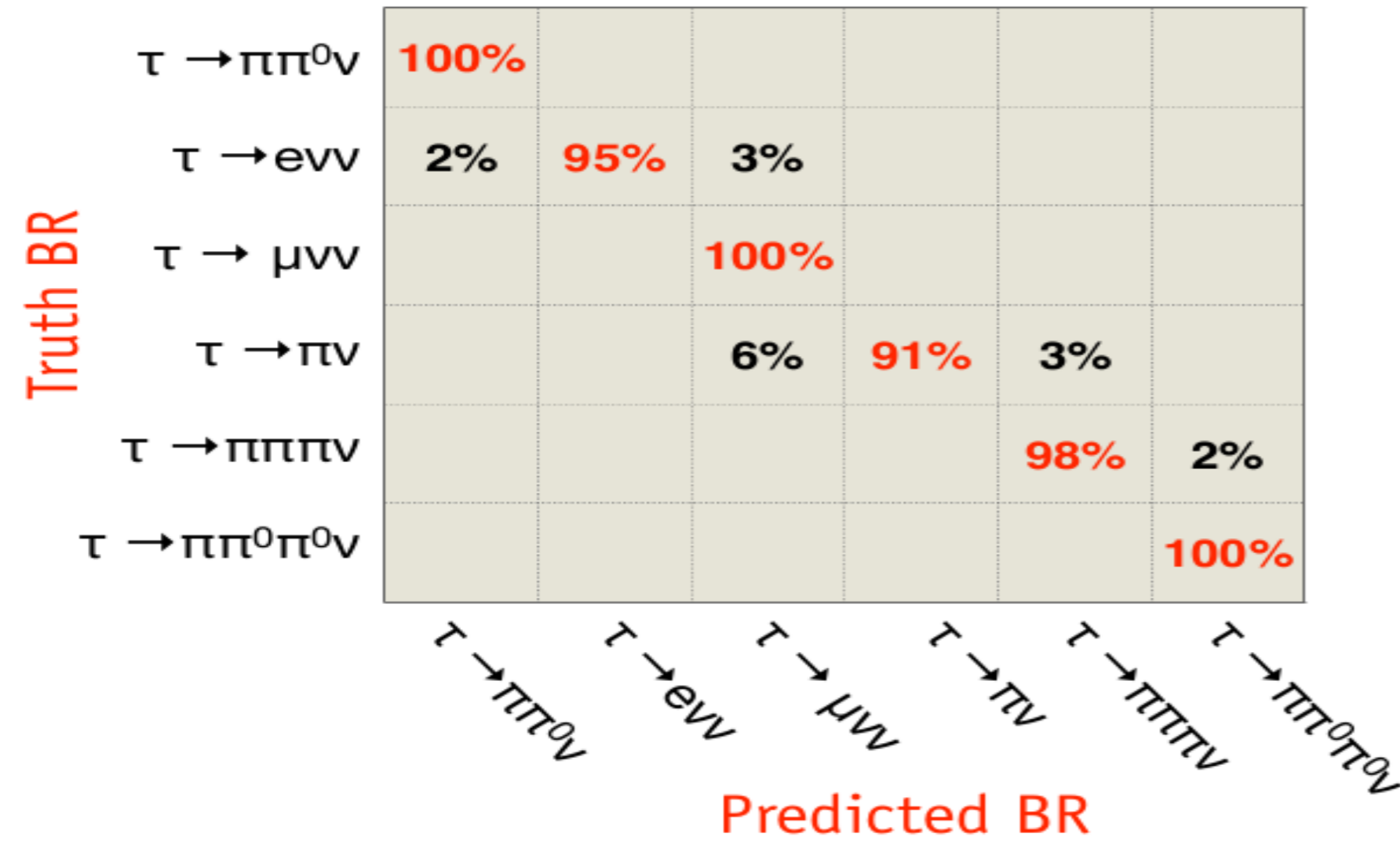




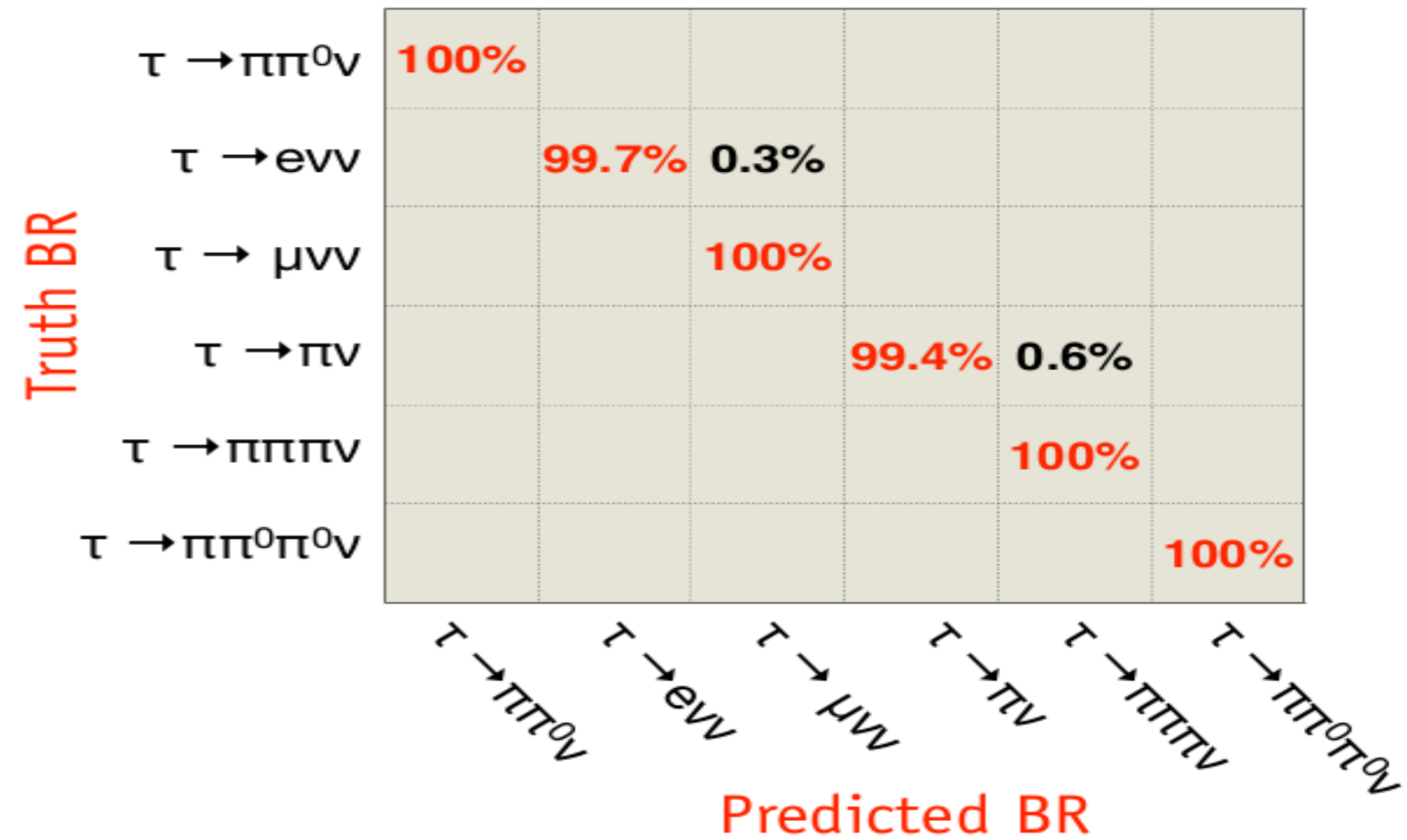
# NN performance

## Confusion matrix on test set

VGG-11  
average accuracy: 97.3%



DGCNN  
average accuracy: 99.9%



# DNN w/ IDEA layout (but no time info)

No SiPM response simulation

→ information: fibre signal output (# p.e.)

3-class classification:

$\tau_{lep}$ ,  $\tau_{had}$ , QCD jet

8-class classification:

$\tau_0$ ,  $\tau_1$ ,  $\tau_2$ ,  $\tau_3$ ,  $\tau_4$ ,  $\tau_5$ ,  $\tau_6$ , QCD jet

[  $\tau$  from  $Z \rightarrow \tau\tau$  decays ]

3-class label	8-class label	
0	0	$\tau \rightarrow \mu\nu\nu$
0	1	$\tau \rightarrow e\nu\nu$
1	2	$\tau \rightarrow \pi\nu$
1	3	$\tau \rightarrow \pi\pi^0\nu$
1	4	$\tau \rightarrow \pi\pi^0\pi^0\nu$
1	5	$\tau \rightarrow \pi\pi\pi\nu$
1	6	$\tau \rightarrow \pi\pi\pi^0\nu$
2	7	$Z \rightarrow qq$ jets

# DGCNN w/ geometrical information only

DGCNN optimised but w/o #pe as input feature  
B field and material in

Truth BR	$\tau \rightarrow e\nu\nu$	90.36	4.07	2.21	0.03	0.00	0.00	3.34	0.00
	$\tau \rightarrow \pi\nu$	2.57	86.24	5.39	0.25	3.59	0.17	1.57	0.22
	$\tau \rightarrow \pi\pi^0\nu$	2.10	18.92	72.67	2.76	1.97	1.01	0.27	0.30
	$\tau \rightarrow \pi\pi^0\pi^0\nu$	0.74	3.54	58.43	33.04	0.84	2.81	0.05	0.54
	$\tau \rightarrow \pi\pi\pi\nu$	0.11	9.88	6.22	0.46	75.32	6.49	0.00	1.52
	$\tau \rightarrow \pi\pi\pi\pi^0\nu$	0.11	1.49	9.30	2.90	38.28	43.75	0.05	4.12
	$\tau \rightarrow \mu\nu\nu$	2.50	0.70	0.17	0.00	0.03	0.00	96.60	0.00
	$Z \rightarrow qq \text{ jets}$	0.08	0.33	0.63	0.94	2.92	3.09	0.08	91.92
		$\tau \rightarrow e\nu\nu$	$\tau \rightarrow \pi\nu$	$\tau \rightarrow \pi\pi^0\nu$	$\tau \rightarrow \pi\pi^0\pi^0\nu$	$\tau \rightarrow \pi\pi\pi\nu$	$\tau \rightarrow \pi\pi\pi\pi^0\nu$	$\tau \rightarrow \mu\nu\nu$	$Z \rightarrow qq \text{ jets}$
		Predicted BR							

input: fibre coordinates only  
avg accuracy: 73.7%

Truth BR	$\tau \rightarrow e\nu\nu$	96.95	0.79	0.62	0.03	0.00	0.00	1.58	0.03
	$\tau \rightarrow \pi\nu$	3.09	89.03	3.48	0.41	2.02	0.39	1.44	0.14
	$\tau \rightarrow \pi\pi^0\nu$	1.77	4.83	80.45	9.25	1.61	1.67	0.16	0.25
	$\tau \rightarrow \pi\pi^0\pi^0\nu$	0.30	0.38	10.43	84.55	0.16	3.87	0.05	0.25
	$\tau \rightarrow \pi\pi\pi\nu$	0.16	3.52	1.38	0.35	84.82	8.79	0.03	0.95
	$\tau \rightarrow \pi\pi\pi\pi^0\nu$	0.11	0.24	1.98	2.60	10.19	82.60	0.08	2.20
	$\tau \rightarrow \mu\nu\nu$	2.53	0.48	0.11	0.00	0.03	0.00	96.82	0.03
	$Z \rightarrow qq \text{ jets}$	0.08	0.25	0.19	1.05	2.54	4.08	0.06	91.75
		$\tau \rightarrow e\nu\nu$	$\tau \rightarrow \pi\nu$	$\tau \rightarrow \pi\pi^0\nu$	$\tau \rightarrow \pi\pi^0\pi^0\nu$	$\tau \rightarrow \pi\pi\pi\nu$	$\tau \rightarrow \pi\pi\pi\pi^0\nu$	$\tau \rightarrow \mu\nu\nu$	$Z \rightarrow qq \text{ jets}$
		Predicted BR							

input: fibre coordinates + type  
avg accuracy: 88.3% (w/ #p.e. 90.8%)

# longitudinal segmentation w/ timing (U.S.)

Dual-readout fibre calorimeter → signal sampled at 20 GHz

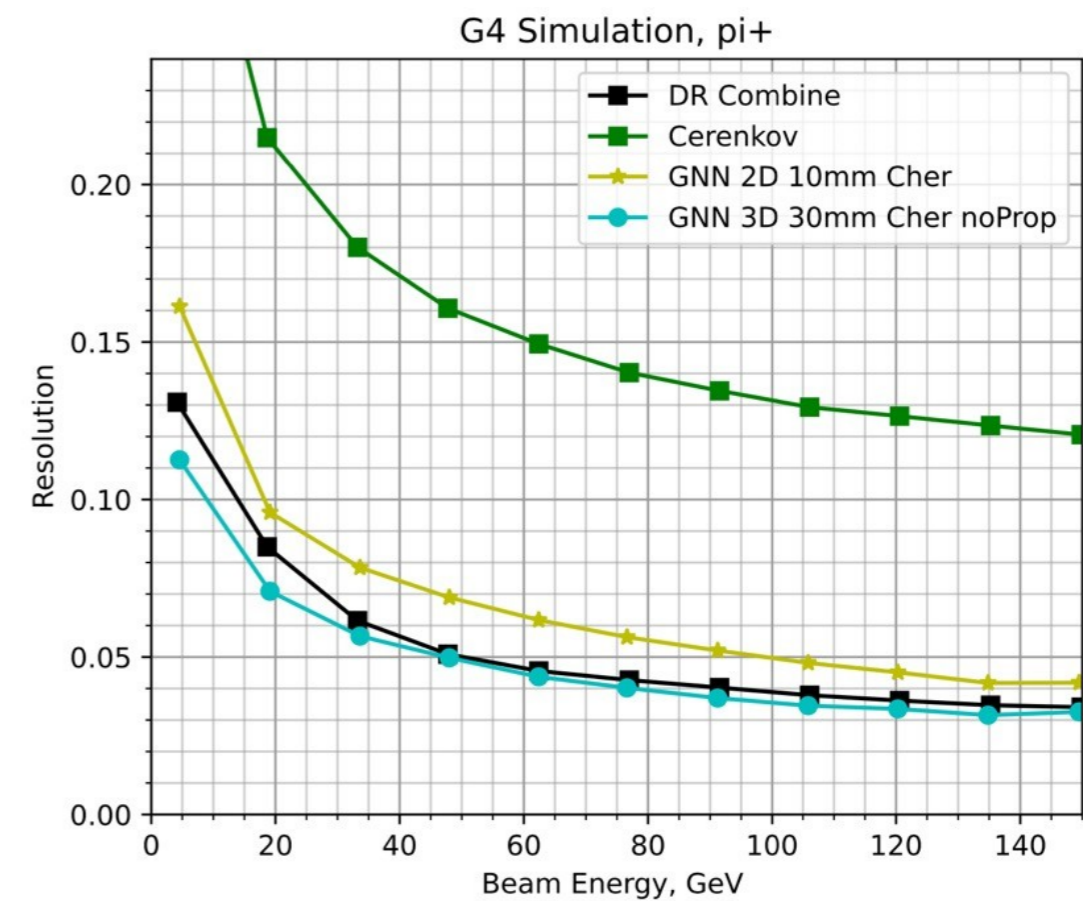
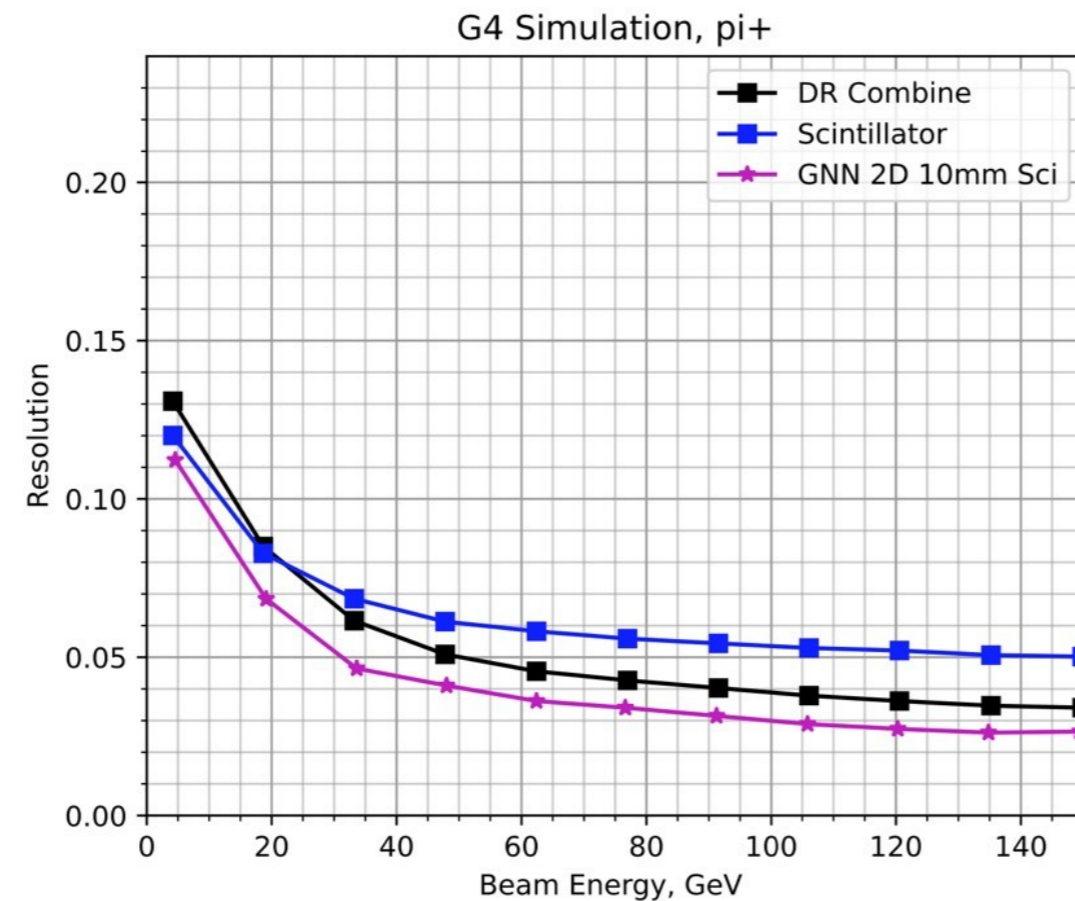
Cu absorber (2 m deep)

Preliminary results  
No optimisation

Fibre axis aligned w/ beam direction: 1 mm  $\Phi$  fibres, 1.5 mm spacing

Transverse segmentation: 1×1 cm<sup>2</sup> for 2D analysis, 3×3 cm<sup>2</sup> for 3D analysis

## 3D imaging fibre DR calorimeter coupled to Graph DNN





# longitudinal segmentation w/ timing (U.S.)

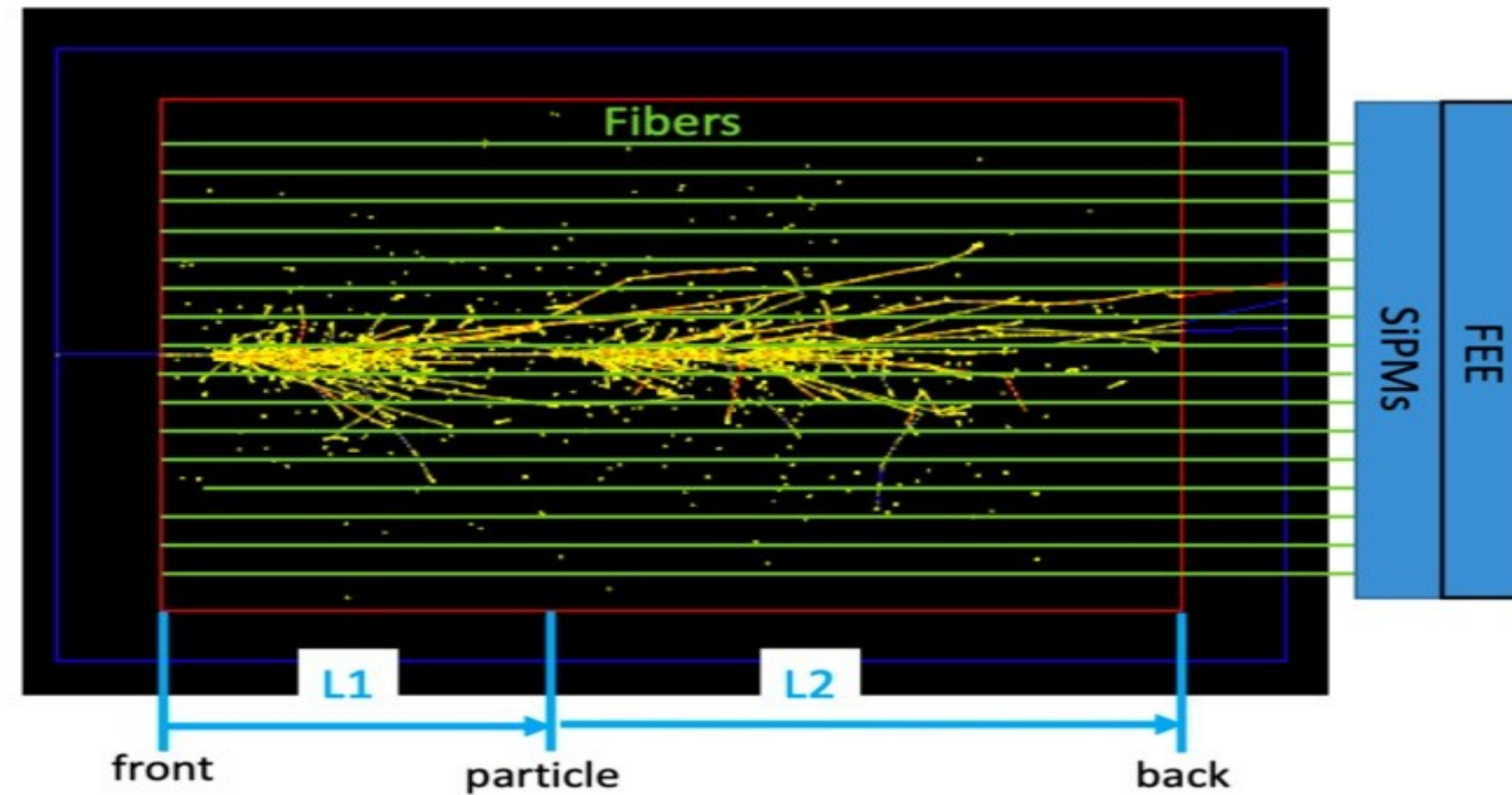


**Table 1.** The energy resolution of the 3D GNN reconstruction with various timing resolutions for longitudinal segmentation.

Timing Resolution $\Delta(t), \text{ps}$	Position Resolution $\Delta(z), \text{cm}$	Energy Resolution $\sigma/E, \%$	@ 100 GeV
0	0.0	3.6	
100	5.0	3.9	
150	7.5	4.0	
200	10.0	4.2	

only Cherenkov fibres

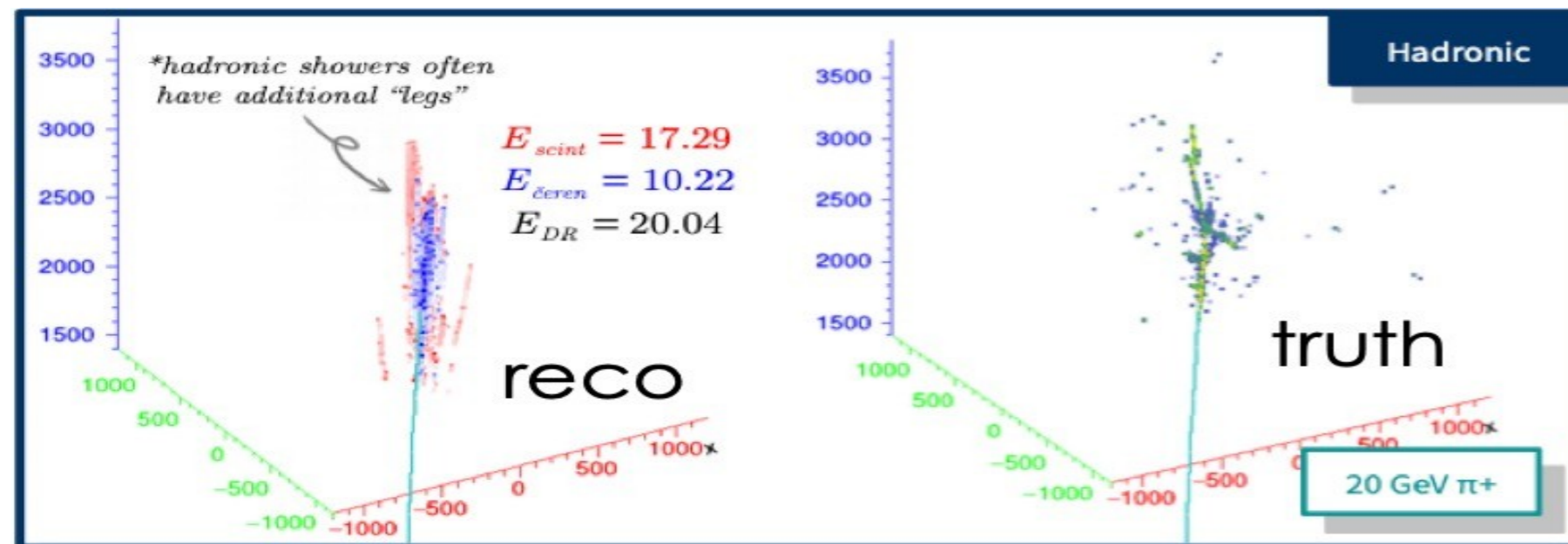
# longitudinal segmentation w/ timing (Korea)

Full SiPM signal sampled at 10 GHz

FFT used to mitigate exponential tail

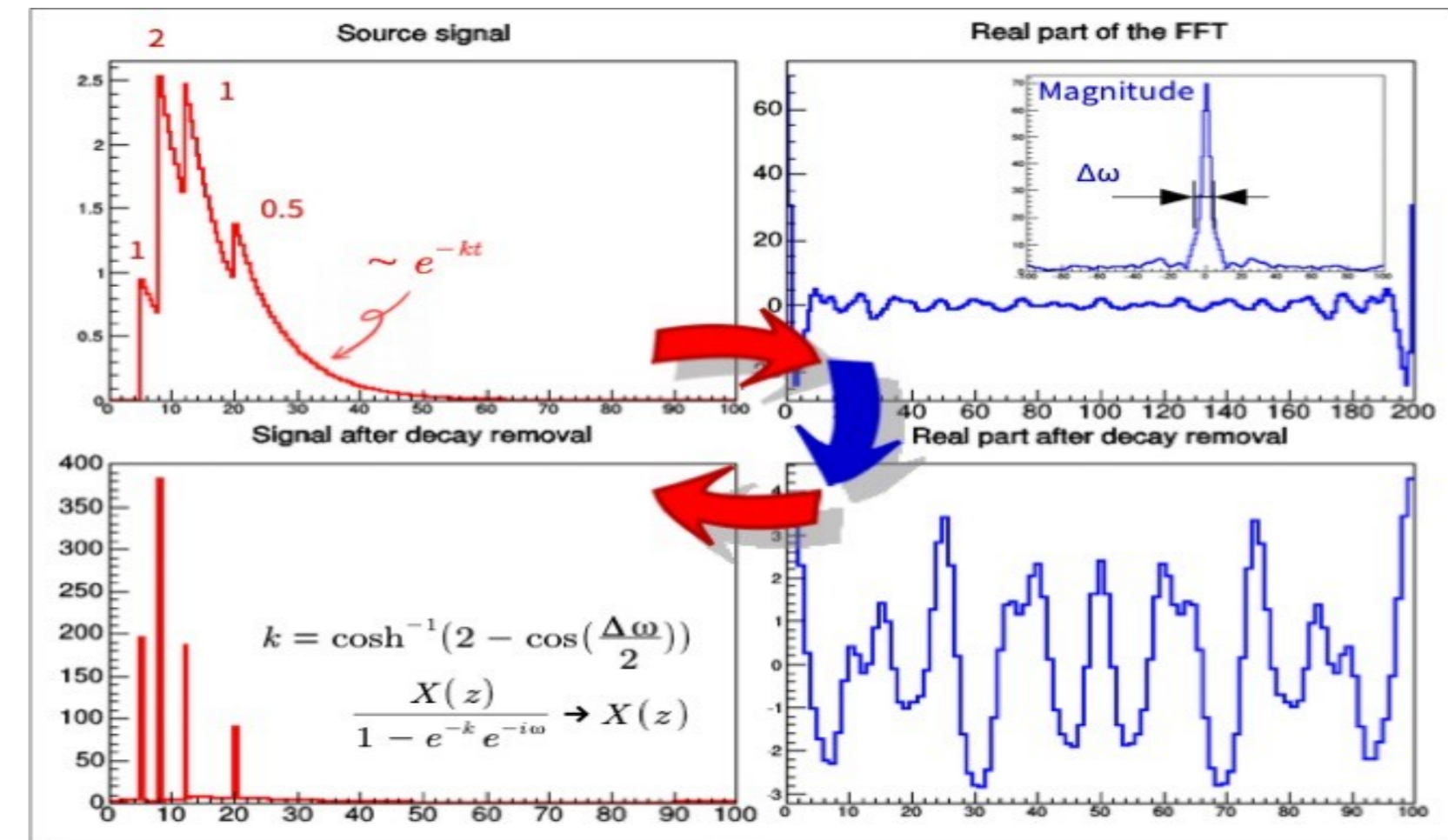
Unlocks full longitudinal information about energy deposit

Combined with DR information allows in-shower cluster identification



Time domain

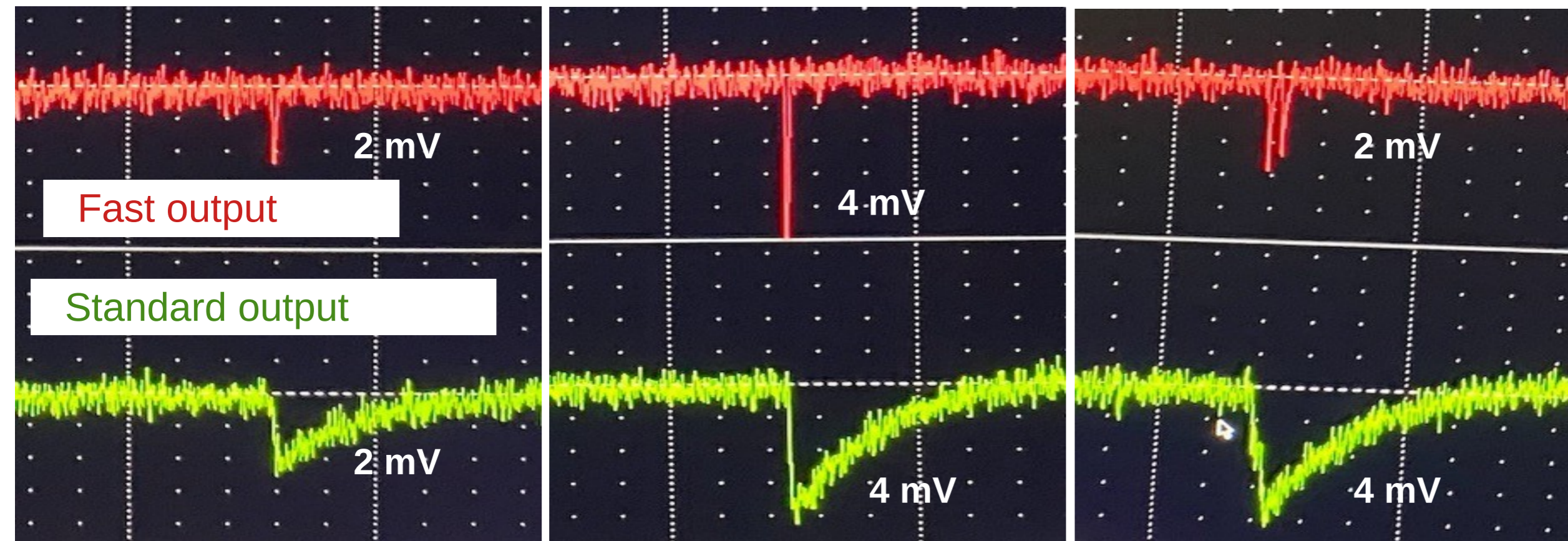
Frequency domain





# waveform digitisation (U.S.)

Results with SensL (MicroFC-30020SMT):  
SiPM with both fast and standard outputs



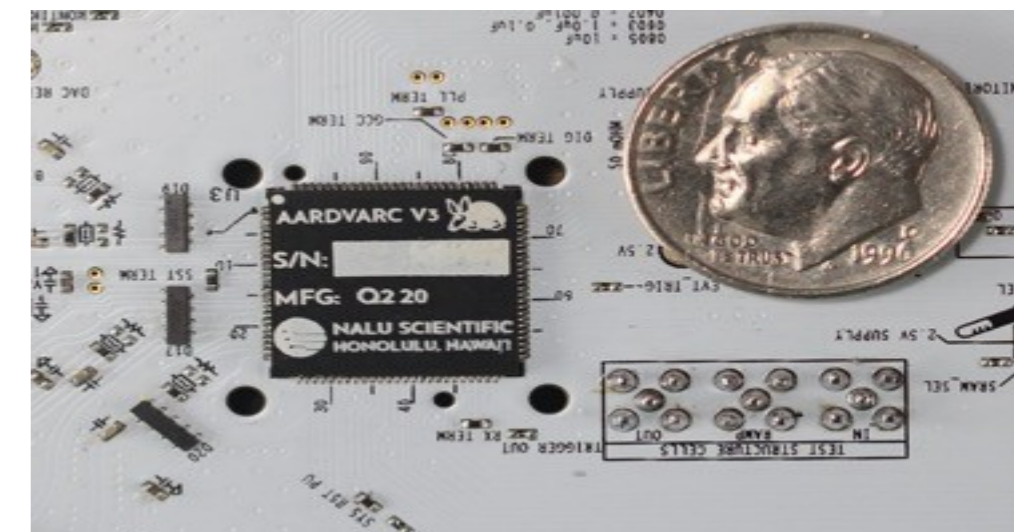
One-photon event

Two-photon event  
(simultaneous)

Two-photon event  
(5 ns apart)

NALU Scientific  
AARDVARC v3

- Sampling rate 10-14 GS/s
- 12 bits ADC
- 4-8 ps timing resolution
- 32 k sampling buffer
- 2 GHz bandwidth
- System-on-Chip (CPU)



---

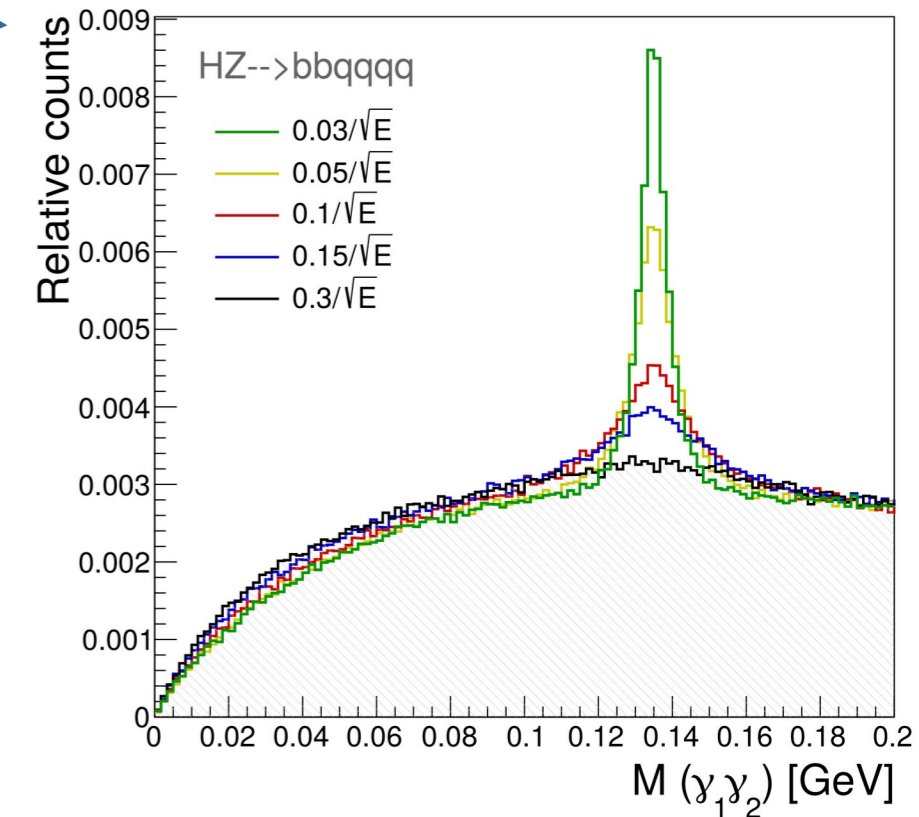
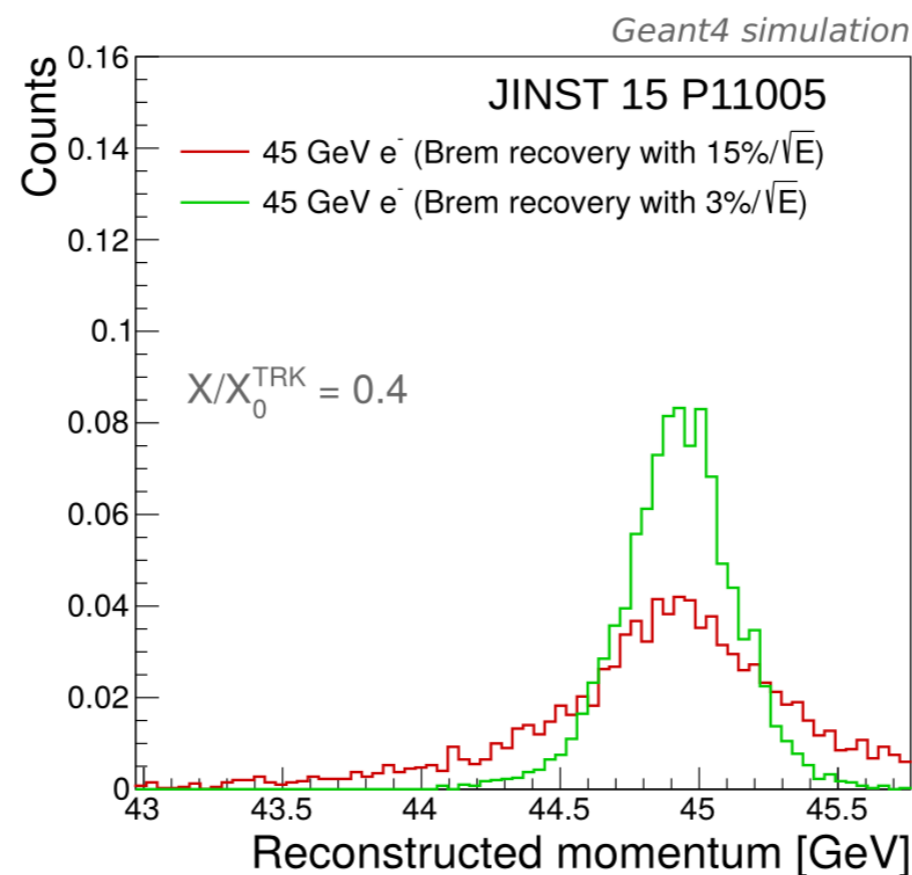
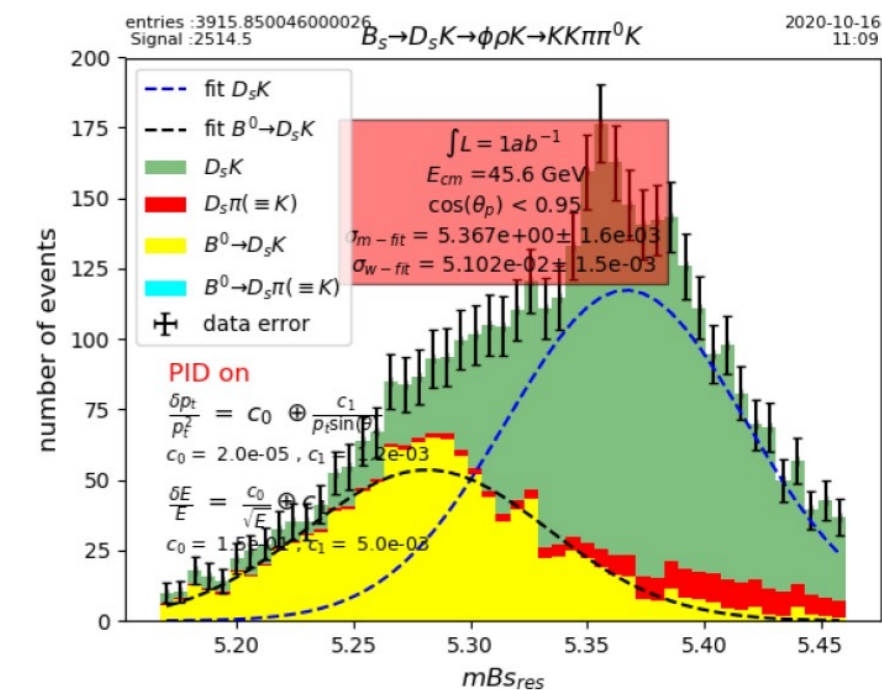
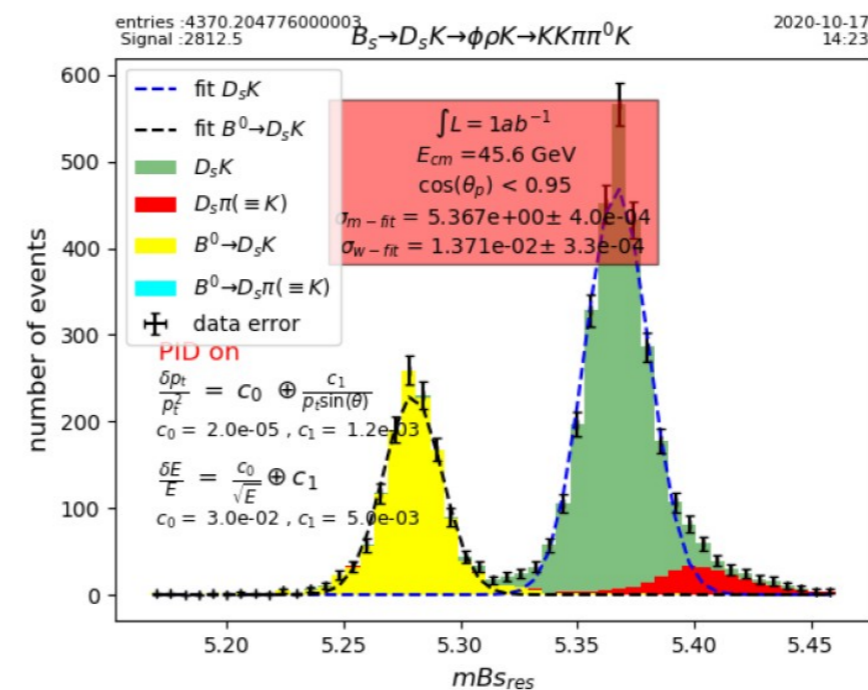
## 6. Crystal option (IDEA++) and pPFA



# high EM energy resolution @ FCC-ee

3%/√E EM energy resolution → improve event reconstruction and **expand landscape for physics studies @ e<sup>+</sup>e<sup>-</sup> colliders**

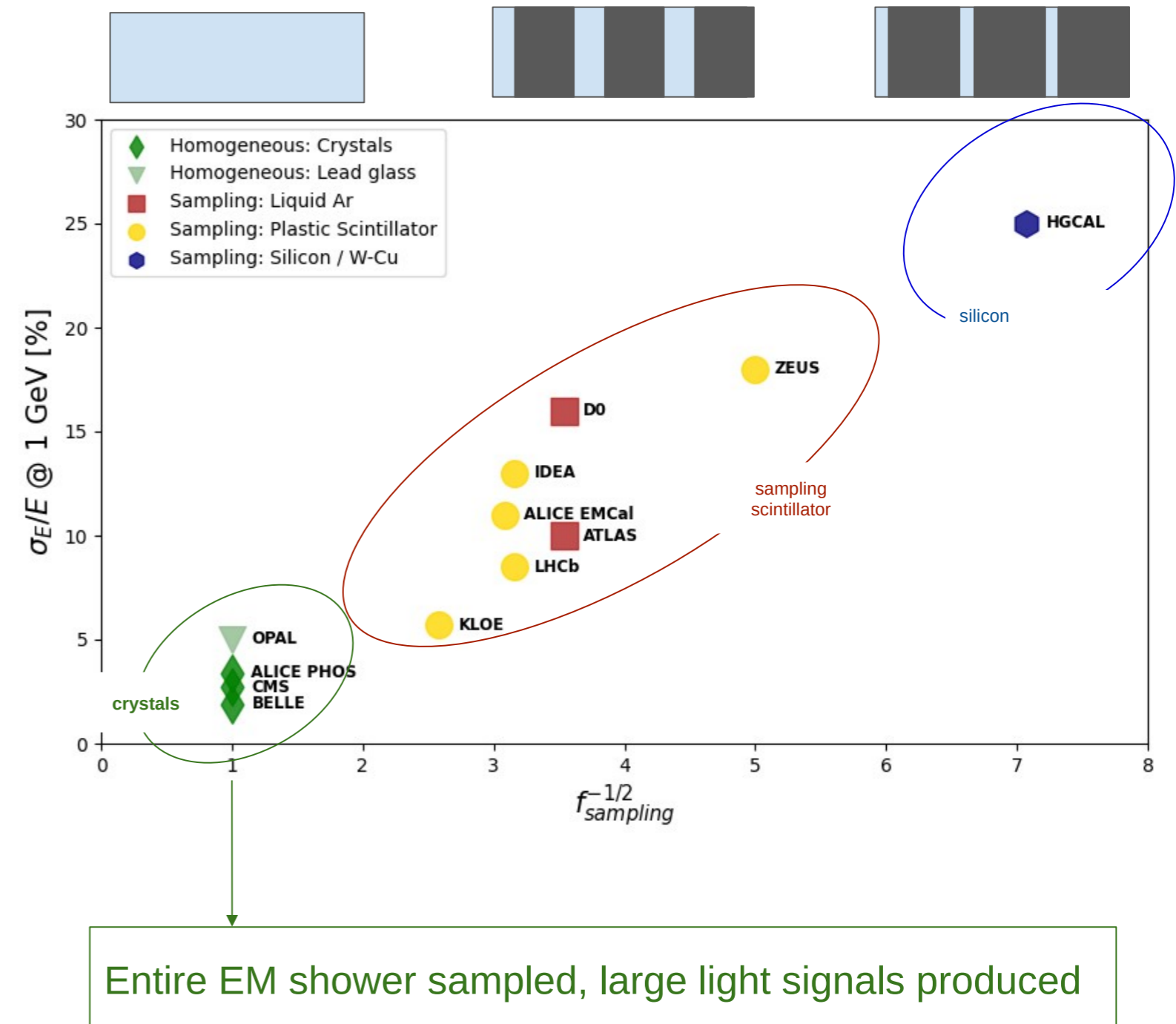
- CP violation studies with B<sub>s</sub> decay to final states with low energy photons
- Clustering of π<sup>0</sup>'s photons to improve performance of jet clustering algorithms
- Improve resolution of recoil-mass signal from Z → ee decays (recovering brems photons)



# homogeneous crystal calorimetry

- Long history in pushing frontier of high EM resolution
- Only way to get  $1-3\%/\sqrt{E}$  energy resolution for photons (and thus  $\pi^0$ 's)
- No stringent requirements on radiation tolerance and pileup @ future  $e^+e^-$  Higgs factorier → can exploit best possible precision of event reconstruction

A sample of existing and future calorimeters



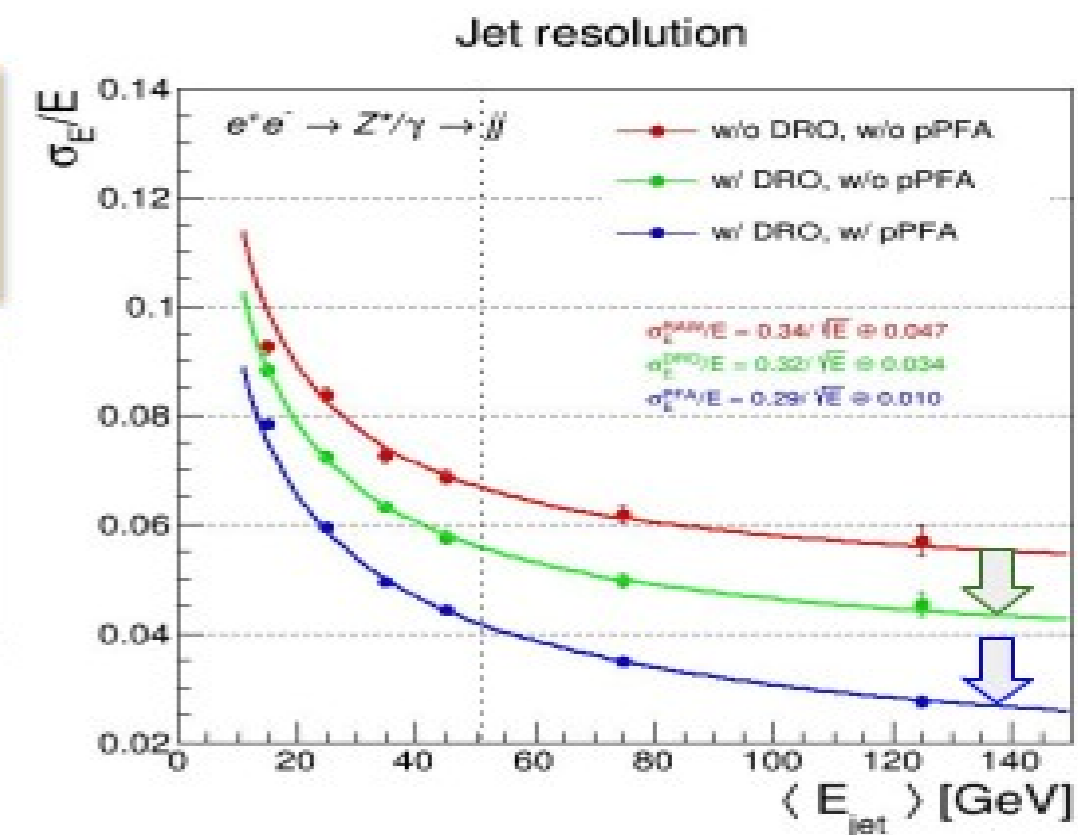
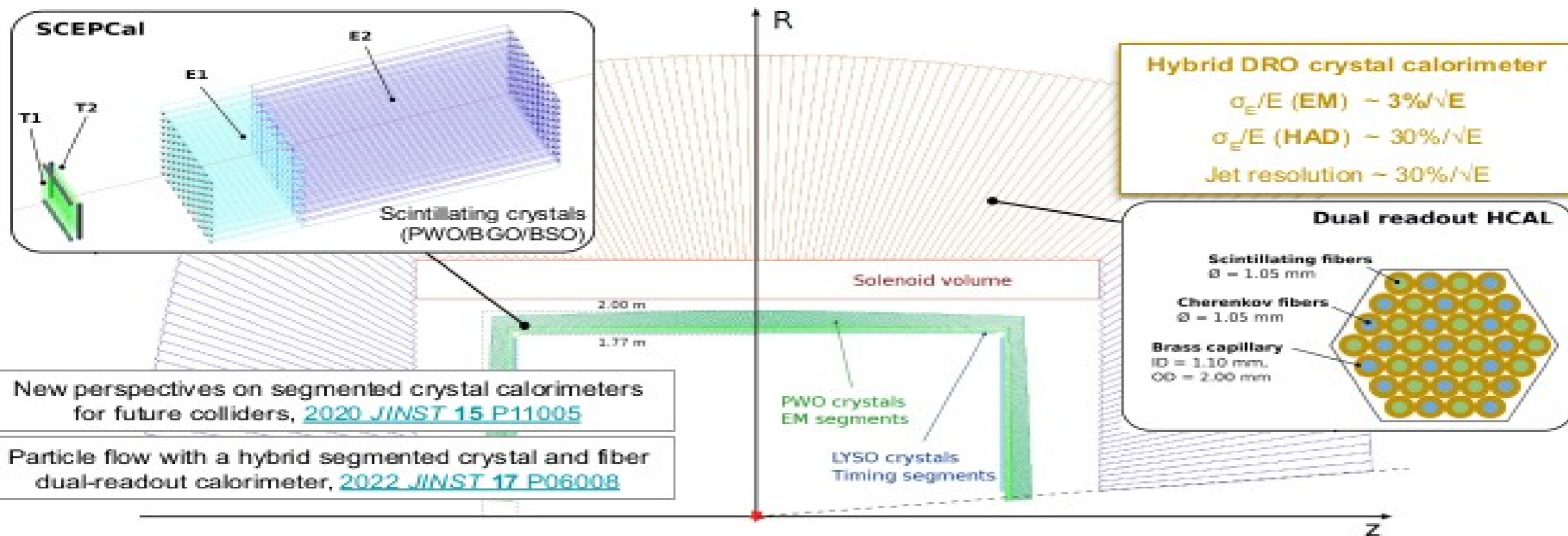
# dual-readout crystal option (IDEA++)

## Segmented Crystal EM Precision Calorimeter

ongoing joint efforts within US Calvision, IDEA and Crystal Clear collaborations

proof-of-concept with lab measurements and prototypes (PWO, BGO, BSO, ... with SiPM readout)

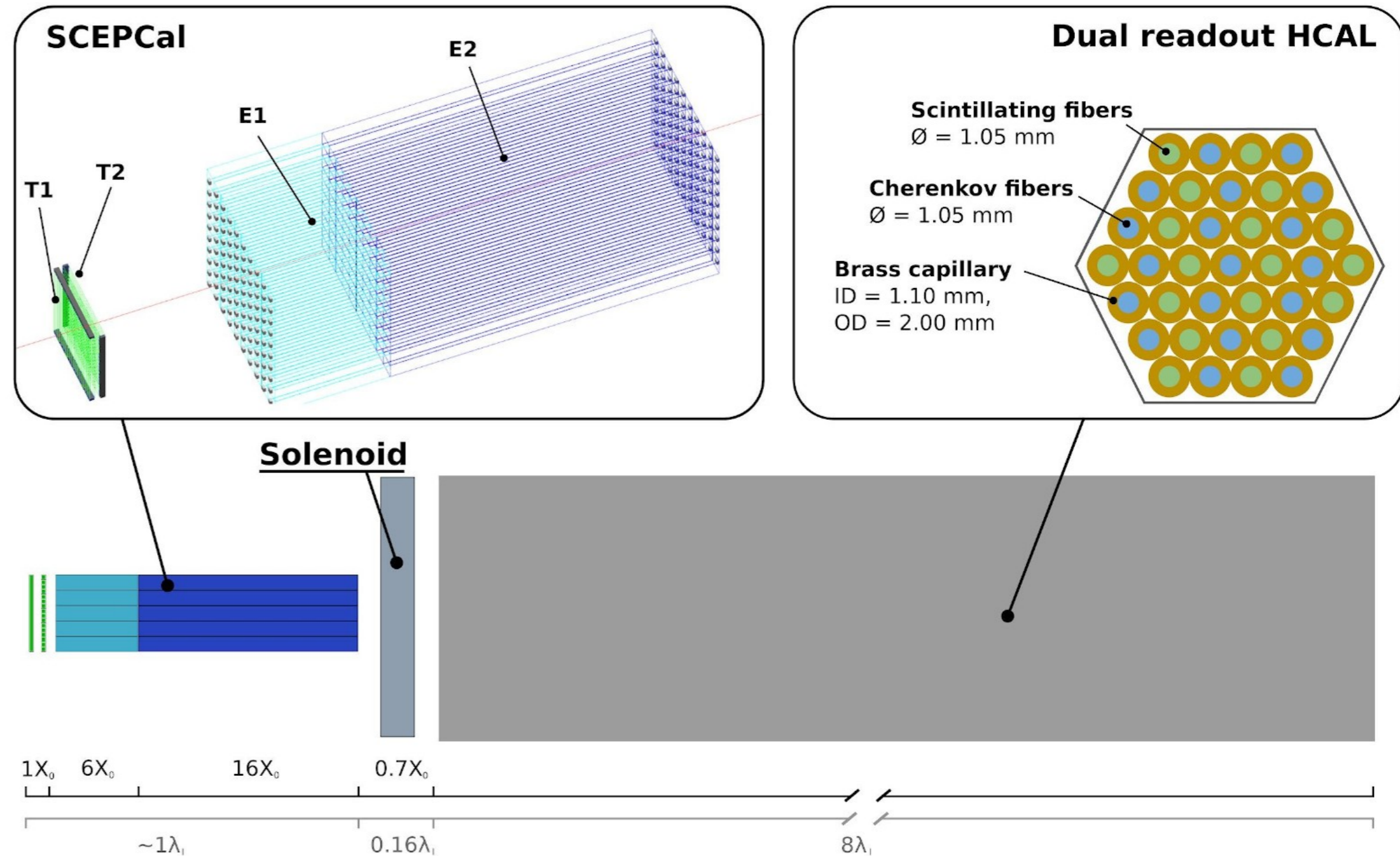
ongoing simulation effort in DD4HEP and FCC software + DR-pPFA developments





# dual-readout crystal option (IDEA++)

- ◆ **ECAL** ~20 cm  $\text{PbWO}_4$ 
  - ◆ 2 layers: 6+16  $X_0$
  - ◆ DR with filters
  - ◆  $\sigma_{\text{EM}} \approx 3\% / \sqrt{E}$
- ◆ **timing layer**
  - ◆ LYSO:Ce crystals
  - ◆  $\sigma_t \sim 20$  ps
- ◆ **HCAL layer**
  - ◆  $\sigma_{\text{HAD}}/E \sim 26\% / \sqrt{E}$

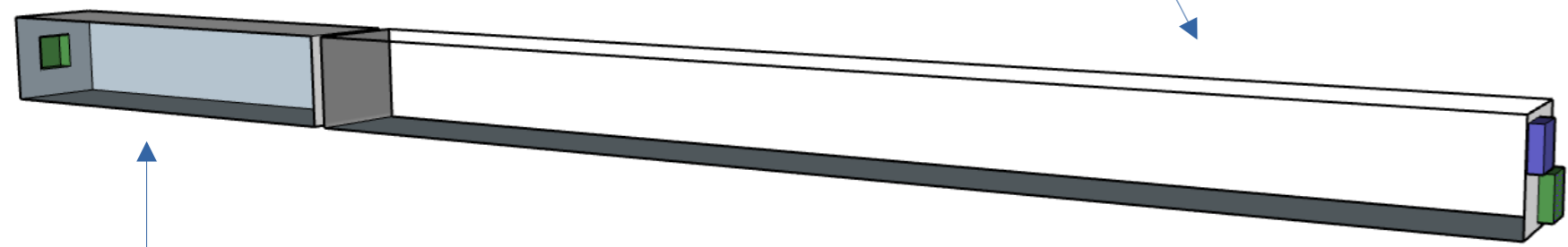




# dual-readout in crystals

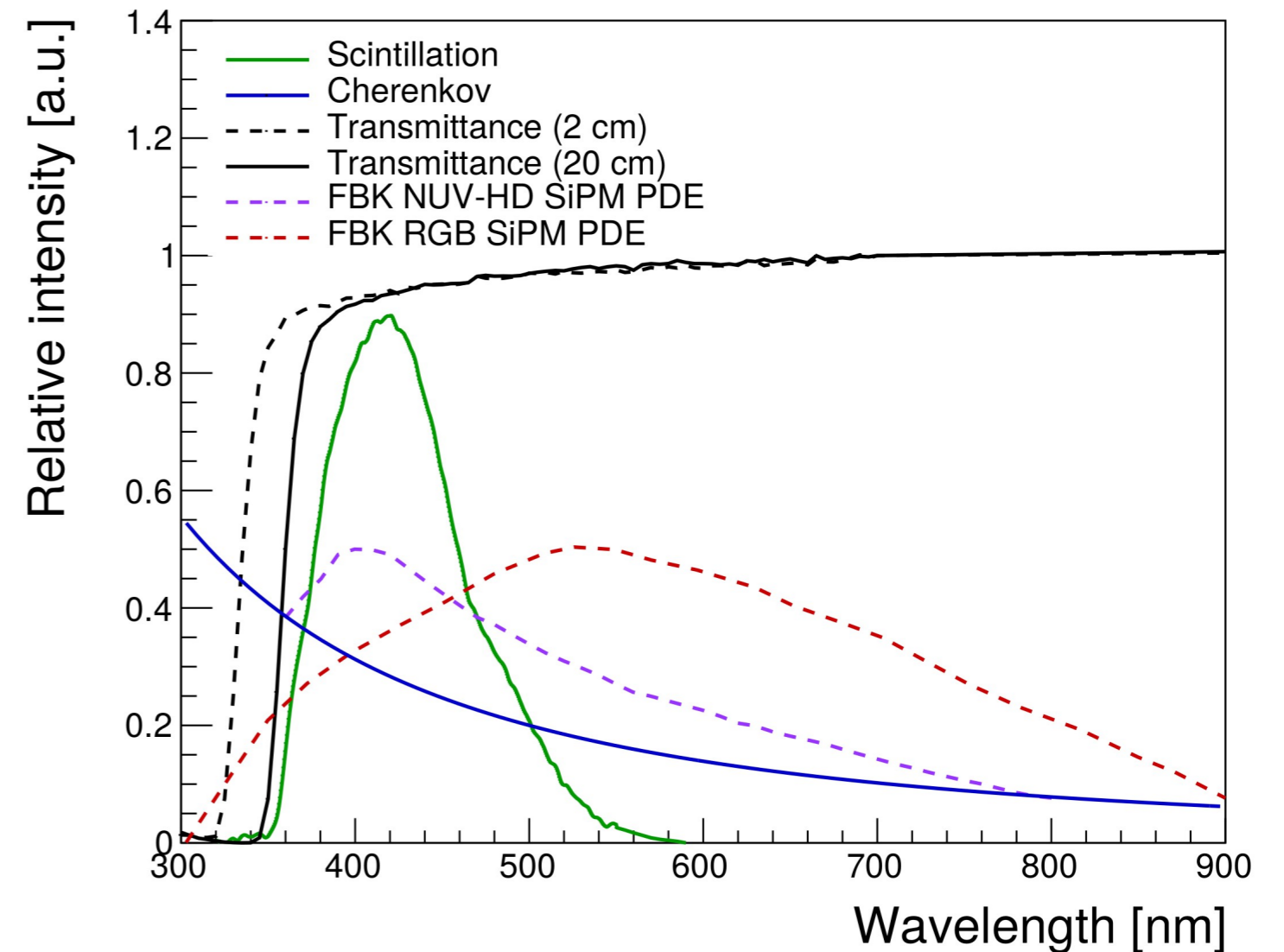
- Simultaneous readout of scintillation and Cherenkov light from same active element with dedicated SiPMs and wavelength filters

Rear crystal ECAL segment: two  $4 \times 4 \text{ mm}^2$  SiPMs with optical filters optimised for scintillation and Cherenkov detection



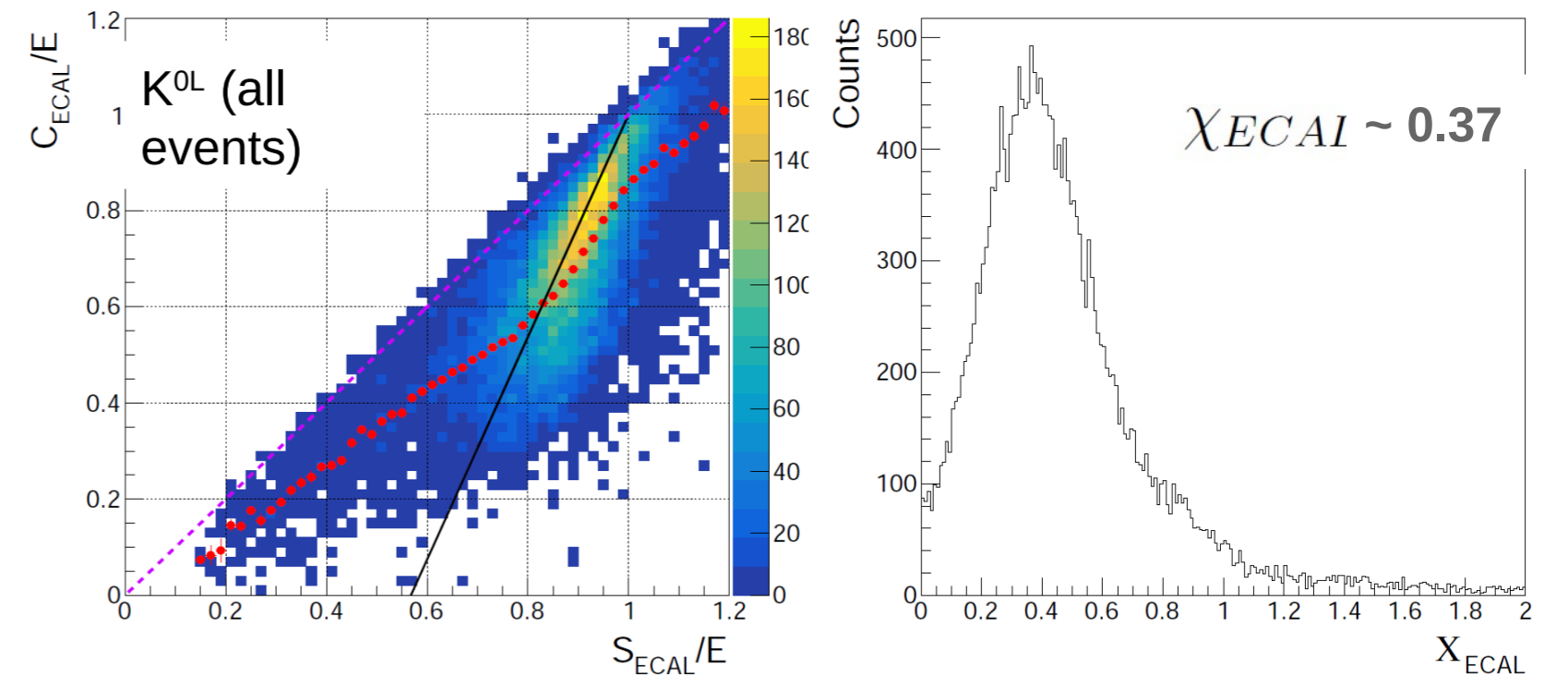
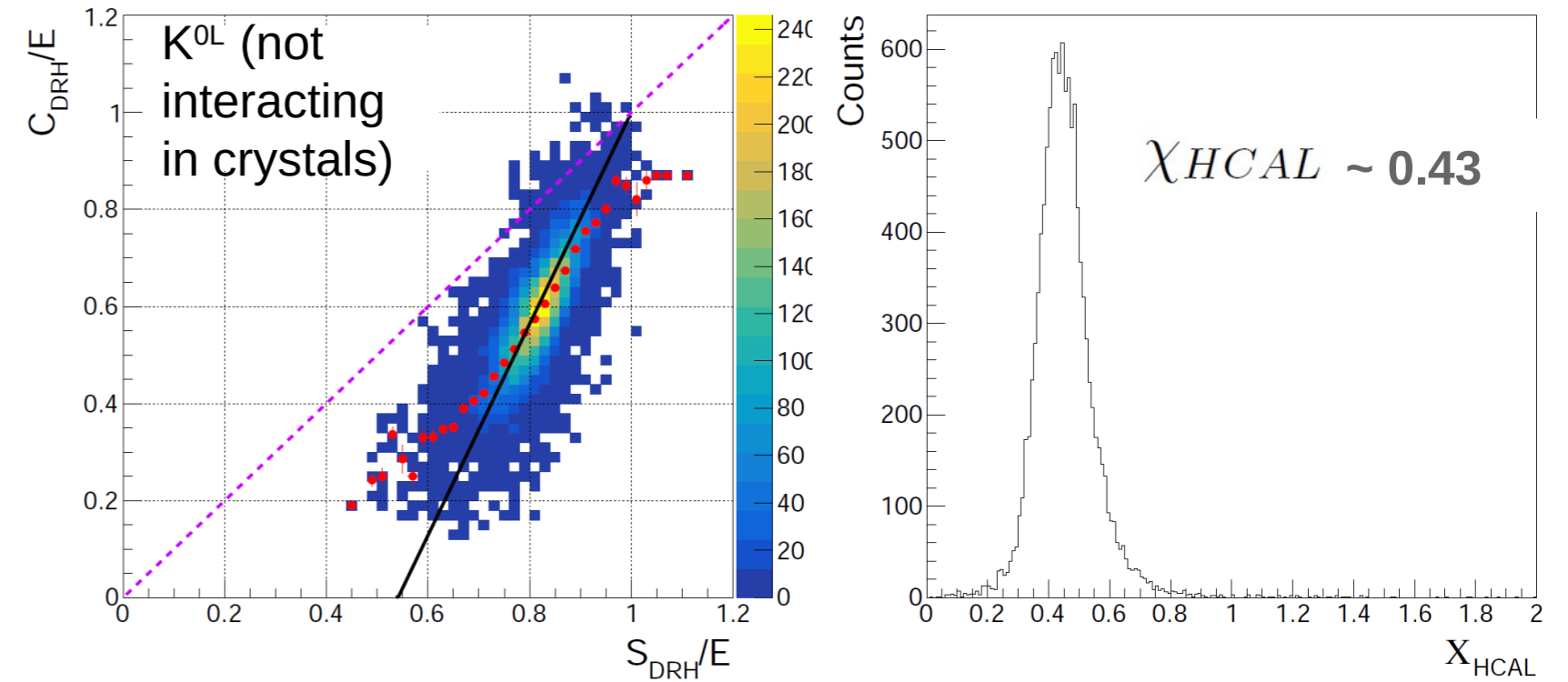
Front crystal ECAL segment: single  $5 \times 5 \text{ mm}^2$  SiPM per crystal optimised for scintillation light detection

PWO



# dual-readout method in hybrid system

1. Independently evaluate  $\chi$ -factors for crystal and fibre sections
2. Independently apply DRO correction on energy deposits for crystal and fibre sections
3. Add up corrected energy from both sections



$$\chi_{HCAL} = \frac{1 - (h/e)_s^{HCAL}}{1 - (h/e)_c^{HCAL}}$$

$$\chi_{ECAL} = \frac{1 - (h/e)_s^{ECAL}}{1 - (h/e)_c^{ECAL}}$$

$$E_{HCAL} = \frac{S_{HCAL} - \chi_{HCAL} C_{HCAL}}{1 - \chi_{HCAL}}$$

$$E_{ECAL} = \frac{S_{ECAL} - \chi_{ECAL} C_{ECAL}}{1 - \chi_{ECAL}}$$

$$E_{total} = E_{HCAL} + E_{ECAL}$$

# light yields (assumptions)

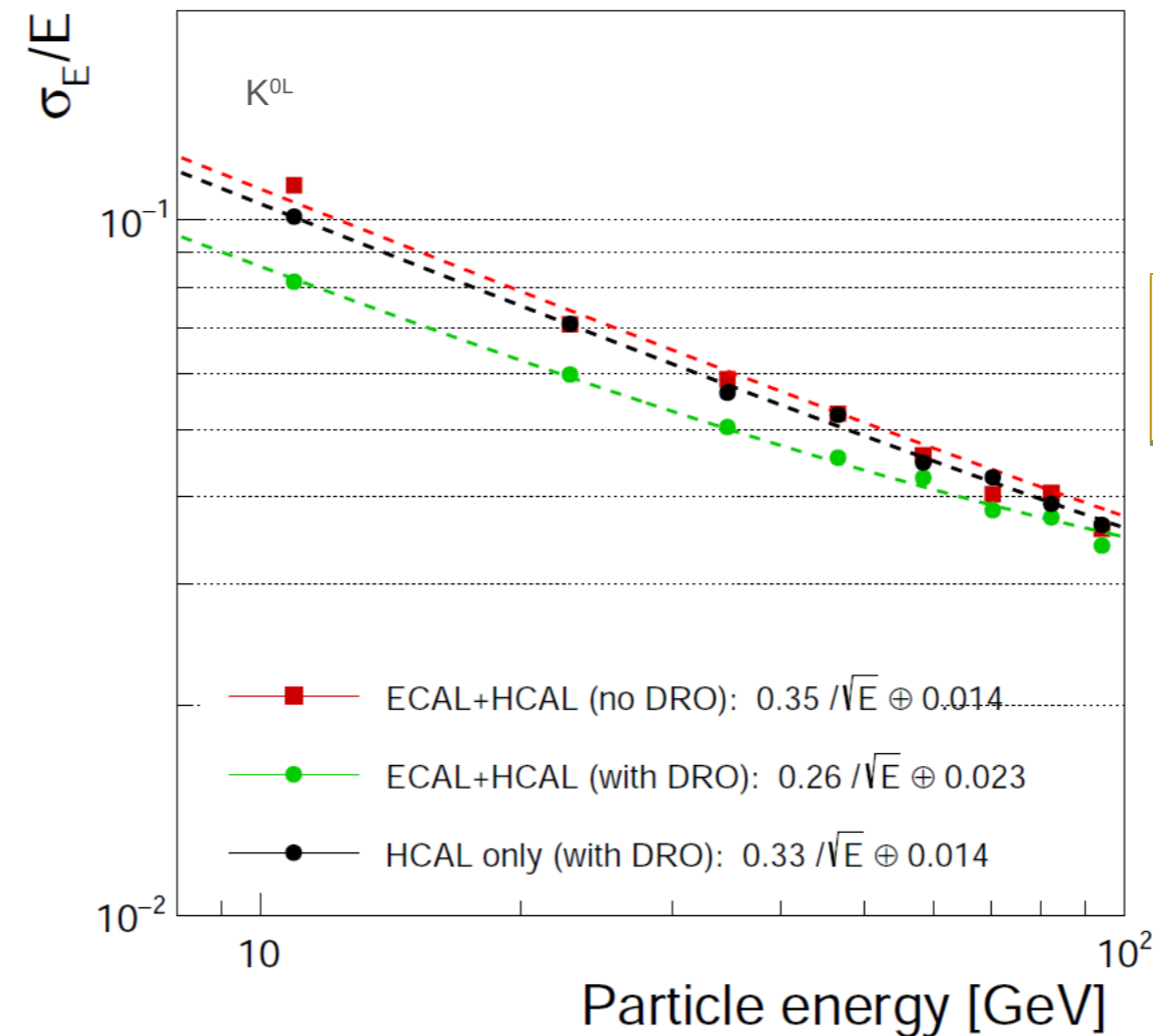
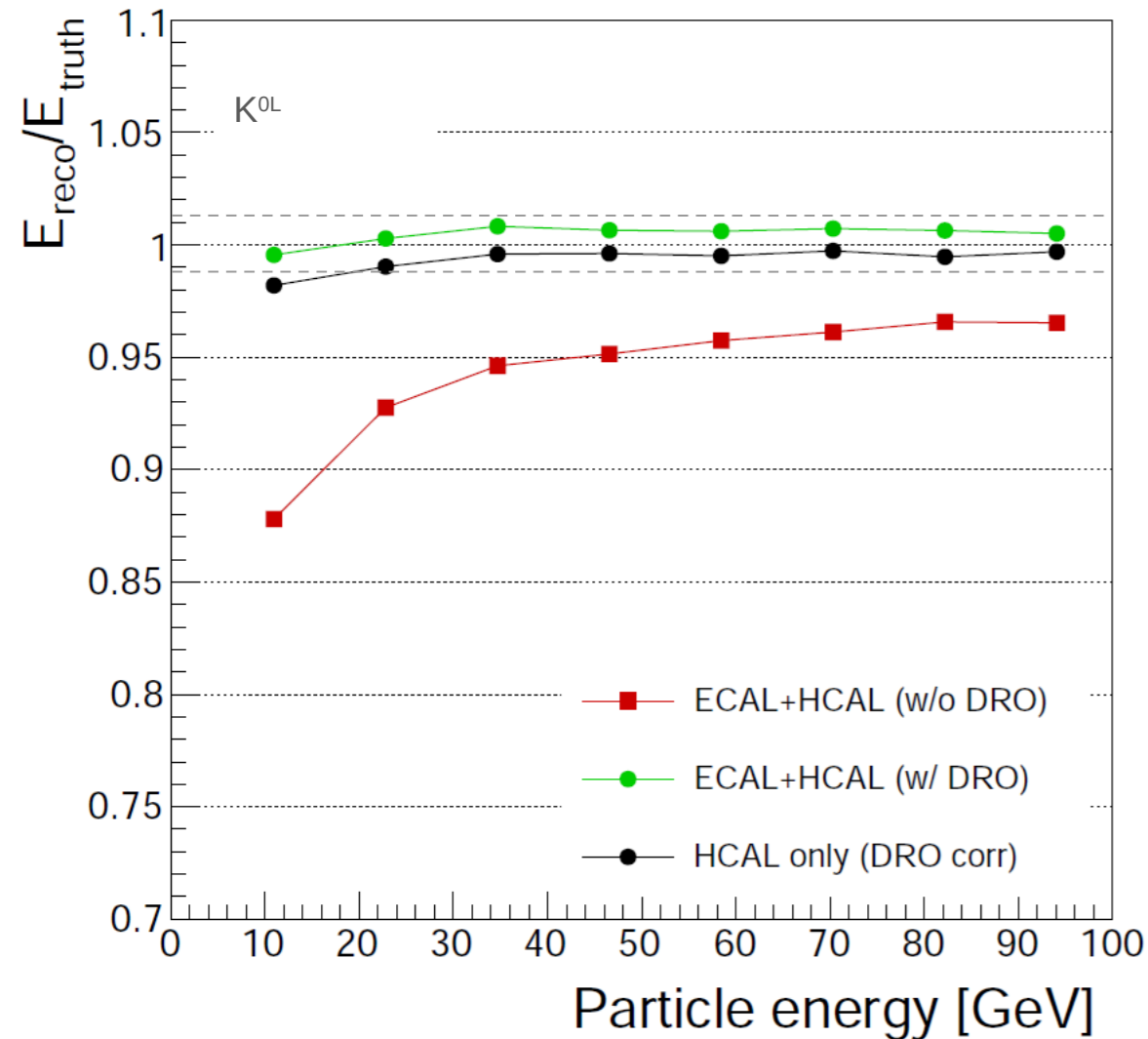
---

- ECAL (crystal section): 2000 (scintillation) and 160 (Cherenkov) p.e./GeV
- HCAL (fibre section): 400 (S) and 100 (C ) p.e./GeV

# Energy resolution for neutral hadrons

- **Dual-readout method confirms applicability to hybrid calorimeter system**

- Response linearity to hadrons restored within  $\pm 1\%$
- Hadron energy resolution comparable to fibre-only IDEEA calorimeter



$$\sigma_E/E_{\text{HAD}} \sim 27\%/\sqrt{E} \oplus 2\%$$



# DR-oriented PF approach (DR-pPFA)

- Different optimisation of PF algorithm required for coarsely segmented calorimeter
- Q: Could better energy linearity and resolution offset coarser longitudinal segmentation?

	High granularity Si/W ECAL and scintillator based HCAL	Fiber-based dual-readout calorimeter	Hybrid crystal and dual-readout calorimeter	
N. of longitudinal layers	> 40	1	5	Moderate longitudinal segmentation (helpful to identify and measure $\pi^0$ jet component)
ECAL cell cross-section	25–100 mm <sup>2</sup>	2–144 mm <sup>2</sup>	100 mm <sup>2</sup>	
HCAL cell cross-section	100–900 mm <sup>2</sup>		400–2500 mm <sup>2</sup>	
EM energy resolution	15 – 25%/ $\sqrt{E}$	10 – 15%/ $\sqrt{E}$	$\approx 3\%/\sqrt{E}$	Highest energy resolution and linearity
HAD energy resolution	45 – 55%/ $\sqrt{E}$	25 – 30%/ $\sqrt{E}$	$\approx 25 – 30\%/\sqrt{E}$	

Highest longitudinal segmentation

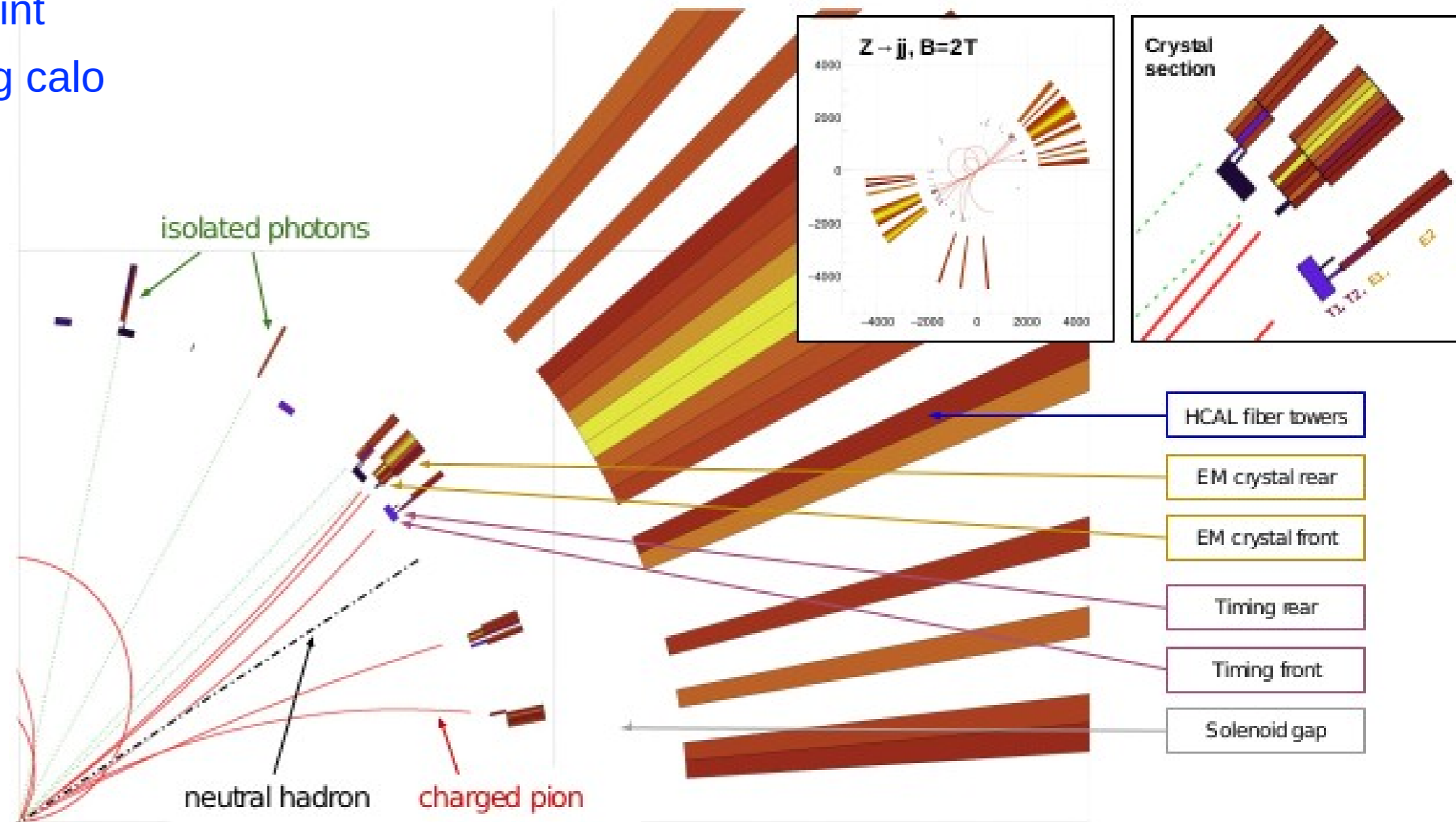
Highest transverse segmentation: full potential  
(e.g. using neural networks) yet to be explored

# jet reconstruction → IDEA++ DR-pPFA

<https://doi.org/10.1088/1748-0221/17/06/P06008>

Geant4 simulation of  $Z \rightarrow jj$  events:

- magnetic field ON but NO tracker
- Gaussian smearings of MC tracks according to expected IDEA tracker performance
- for each track, extrapolate impact point
- remove and store tracks not reaching calo



# jet reconstruction → IDEA++ DR-pPFA

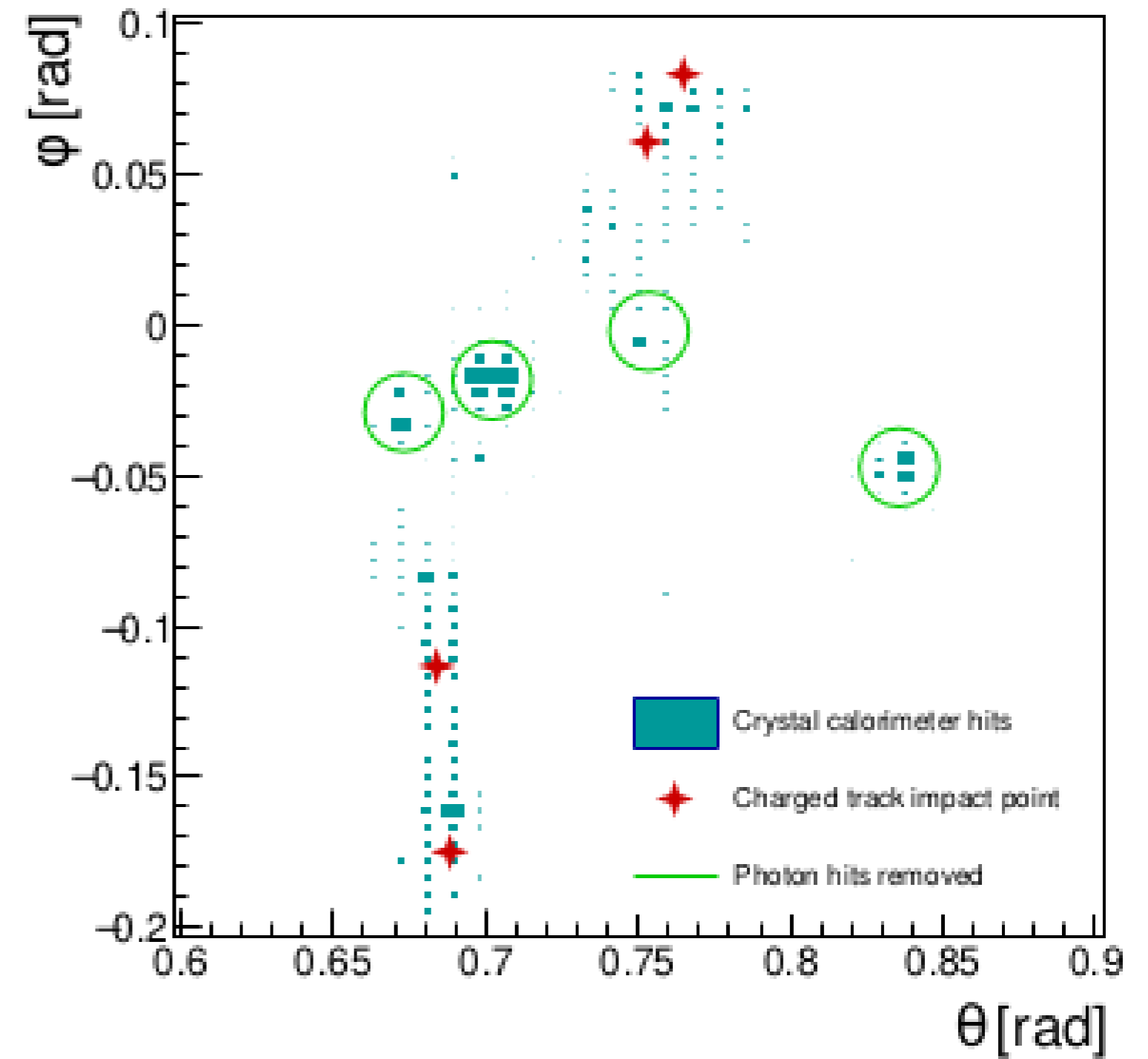
<https://doi.org/10.1088/1748-0221/17/06/P06008>

Geant4 simulation of  $Z \rightarrow jj$  events:

- magnetic field ON but NO tracker
- Gaussian smearings of MC tracks according to expected IDEA tracker performance
- for each track, extrapolate impact point
- remove and store tracks not reaching calo
- identify EM neutral clusters (photons) by cluster radius

$$R_{\text{transverse}} = \frac{E_{\text{seed}}}{\sum_i E_{\text{hit},i} (\Delta R_i < 0.013)}$$

- remove and store photons ( $R < 0.9$ )



# jet reconstruction → IDEA++ DR-pPFA

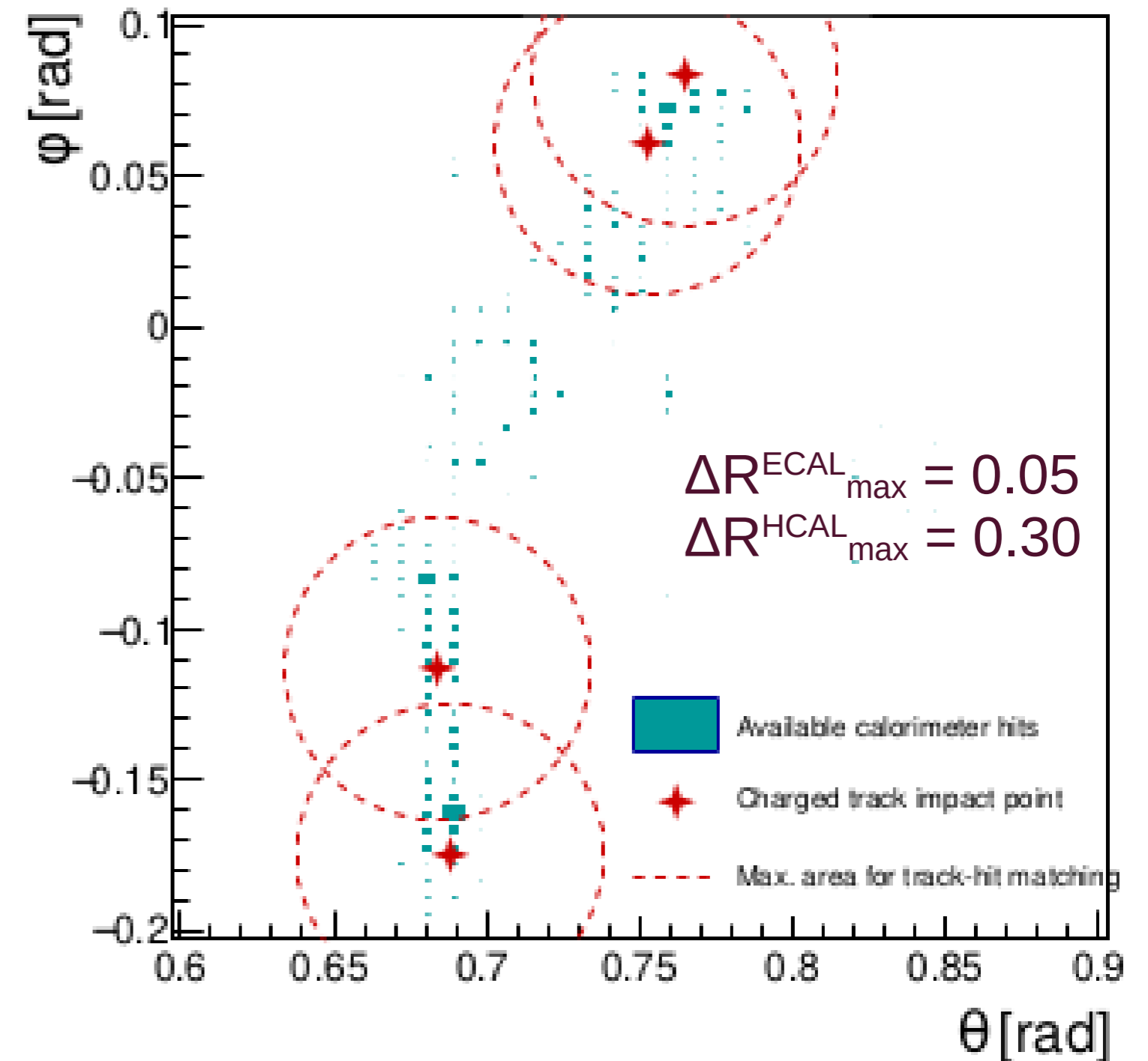
<https://doi.org/10.1088/1748-0221/17/06/P06008>

Geant4 simulation of  $Z \rightarrow jj$  events:

- magnetic field ON but NO tracker
- Gaussian smearings of MC tracks according to expected IDEA tracker performance
- for each track, extrapolate impact point
- remove and store tracks not reaching calo
- identify EM neutral clusters (photons) by cluster radius

$$R_{\text{transverse}} = \frac{E_{\text{seed}}}{\sum_i E_{\text{hit},i} (\Delta R_i < 0.013)}$$

- remove and store photons ( $R < 0.9$ )
- for each track, rank calo hits by distance





# jet reconstruction → IDEA++ DR-pPFA

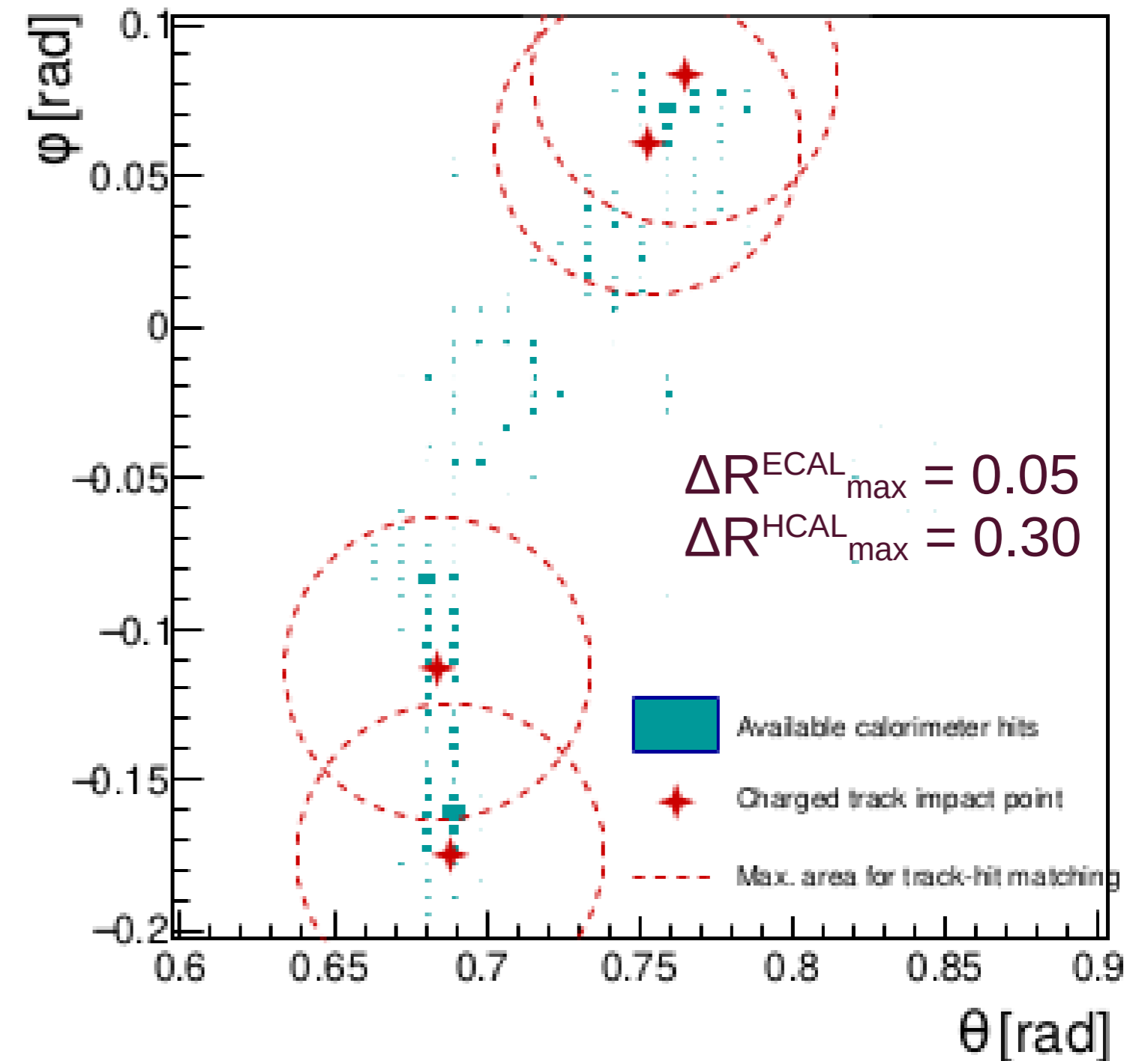
<https://doi.org/10.1088/1748-0221/17/06/P06008>

Geant4 simulation of  $Z \rightarrow jj$  events:

- magnetic field ON but NO tracker
- Gaussian smearings of MC tracks according to expected IDEA tracker performance
- for each track, extrapolate impact point
- remove and store tracks not reaching calo
- identify EM neutral clusters (photons) by cluster radius

$$R_{\text{transverse}} = \frac{E_{\text{seed}}}{\sum_i E_{\text{hit},i} (\Delta R_i < 0.013)}$$

- remove and store photons ( $R < 0.9$ )
- for each track, rank calo hits by distance
- collect hits in cone(s)



# jet reconstruction → IDEA++ DR-pPFA

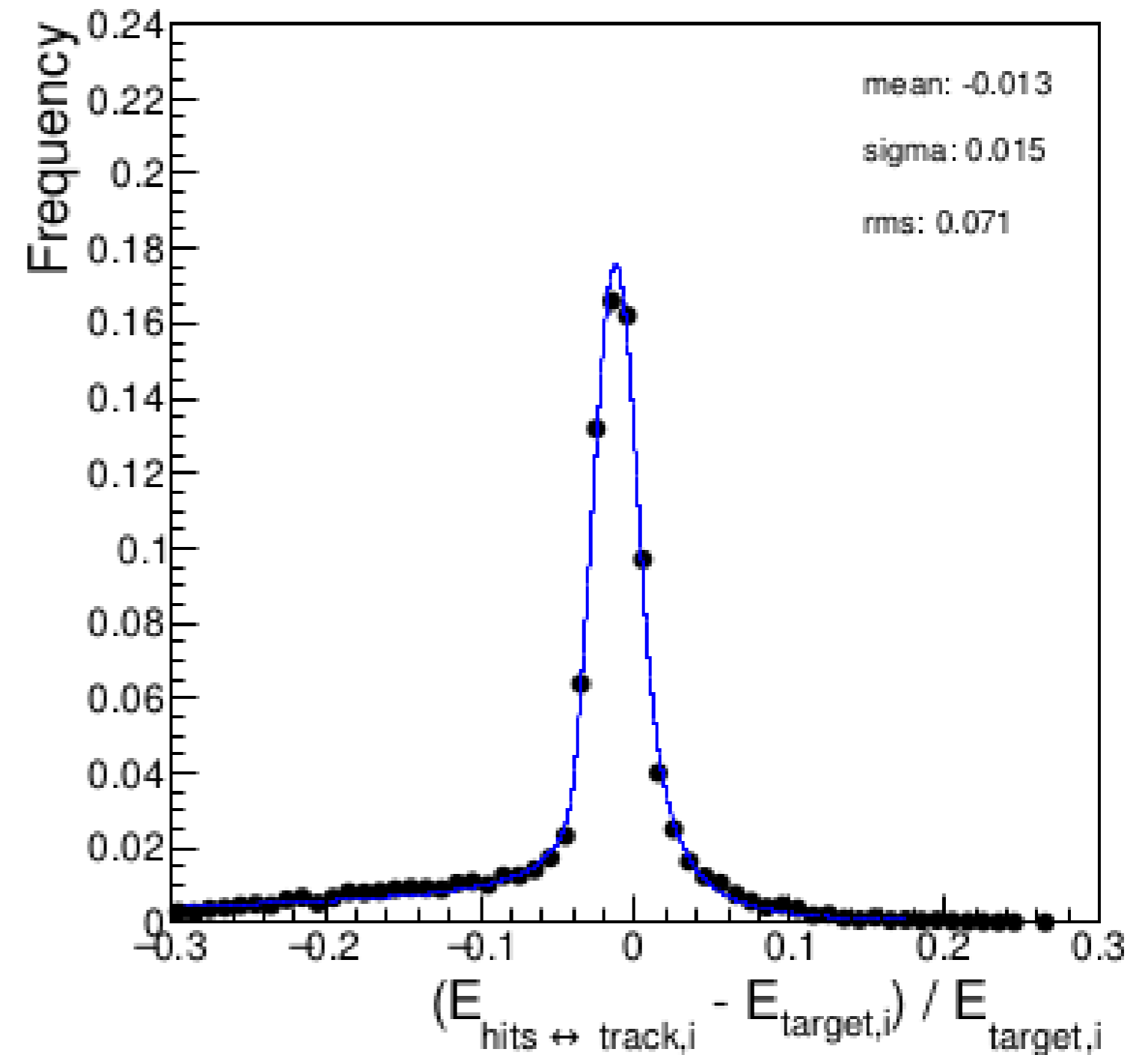
Geant4 simulation of  $Z \rightarrow jj$  events:

- magnetic field ON but NO tracker
- Gaussian smearings of MC tracks according to expected IDEA tracker performance
- for each track, extrapolate impact point
- remove and store tracks not reaching calo
- identify EM neutral clusters (photons) by cluster radius

$$R_{\text{transverse}} = \frac{E_{\text{seed}}}{\sum_i E_{\text{hit},i} (\Delta R_i < 0.013)}$$

- remove and store photons ( $R < 0.9$ )
- for each track, rank calo hits by distance
- collect hits in cone(s)
- compare with  $E_{\text{target}}(\text{track})$

<https://doi.org/10.1088/1748-0221/17/06/P06008>



# jet reconstruction → IDEA++ DR-pPFA

Geant4 simulation of  $Z \rightarrow jj$  events:

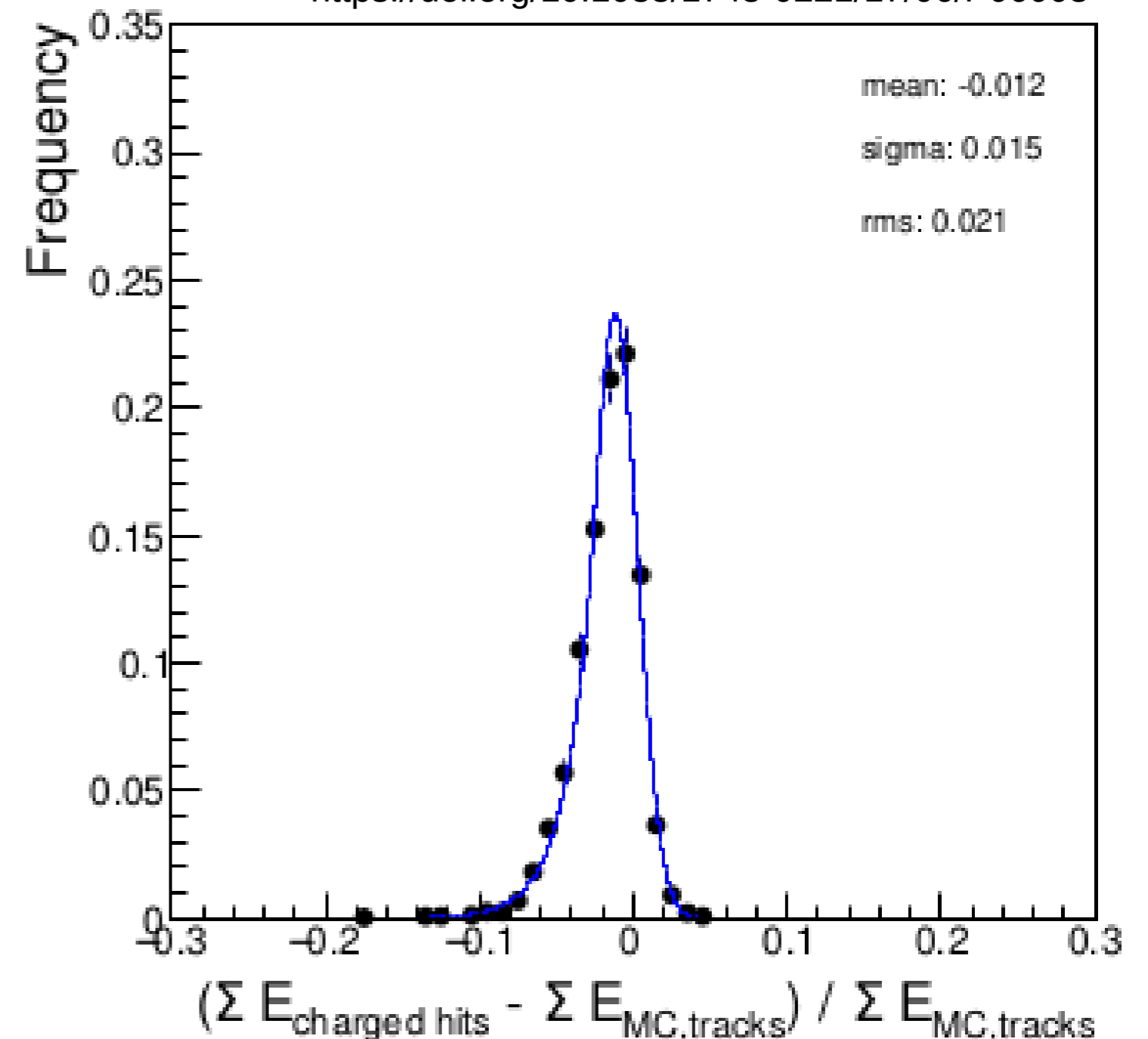
- magnetic field ON but NO tracker
- Gaussian smearings of MC tracks according to expected IDEA tracker performance
- for each track, extrapolate impact point
- remove and store tracks not reaching calo
- identify EM neutral clusters (photons) by cluster radius

$$R_{\text{transverse}} = \frac{E_{\text{seed}}}{\sum_i E_{\text{hit},i} (\Delta R_i < 0.013)}$$

- remove and store photons ( $R < 0.9$ )
- for each track, rank calo hits by distance
- collect hits in cone(s)
- compare with  $E_{\text{target}}(\text{track})$
- if “good” agreement remove hits and replace them with track

*Please note: dual-readout is used to correct energy of clustered calorimeter hits and improve track-hit matching*

<https://doi.org/10.1088/1748-0221/17/06/P06008>



# jet clustering

<https://doi.org/10.1088/1748-0221/17/06/P06008>

- Jet clustering algorithm\* fed with collection of
  - all photon hits
  - tracks of
    - charged particles not reaching calorimeter
    - tracks swapped with calorimeter hits in previous step
  - All other calorimeter hits (both ECAL and HCAL) not been swapped out
- As result, 4-momentum vectors are clustered into two jets
- Jet energy (“non-swapped hadron” component) is corrected with DRO\*\*

$$E_{jet} = C_{PFA} \cdot \left[ \sum E_{hits,\gamma} + \sum E_{tracks} + \sum E_{hits,left\over,DRO} \right]$$

\*FASTJET package: generalized  $k_T$  algorithm with  $R=2\pi$  and number of jets fixed to 2

\*\*dual-readout used here to correct energy of calorimeter hits with no match to tracks (e.g. neutral hadrons)



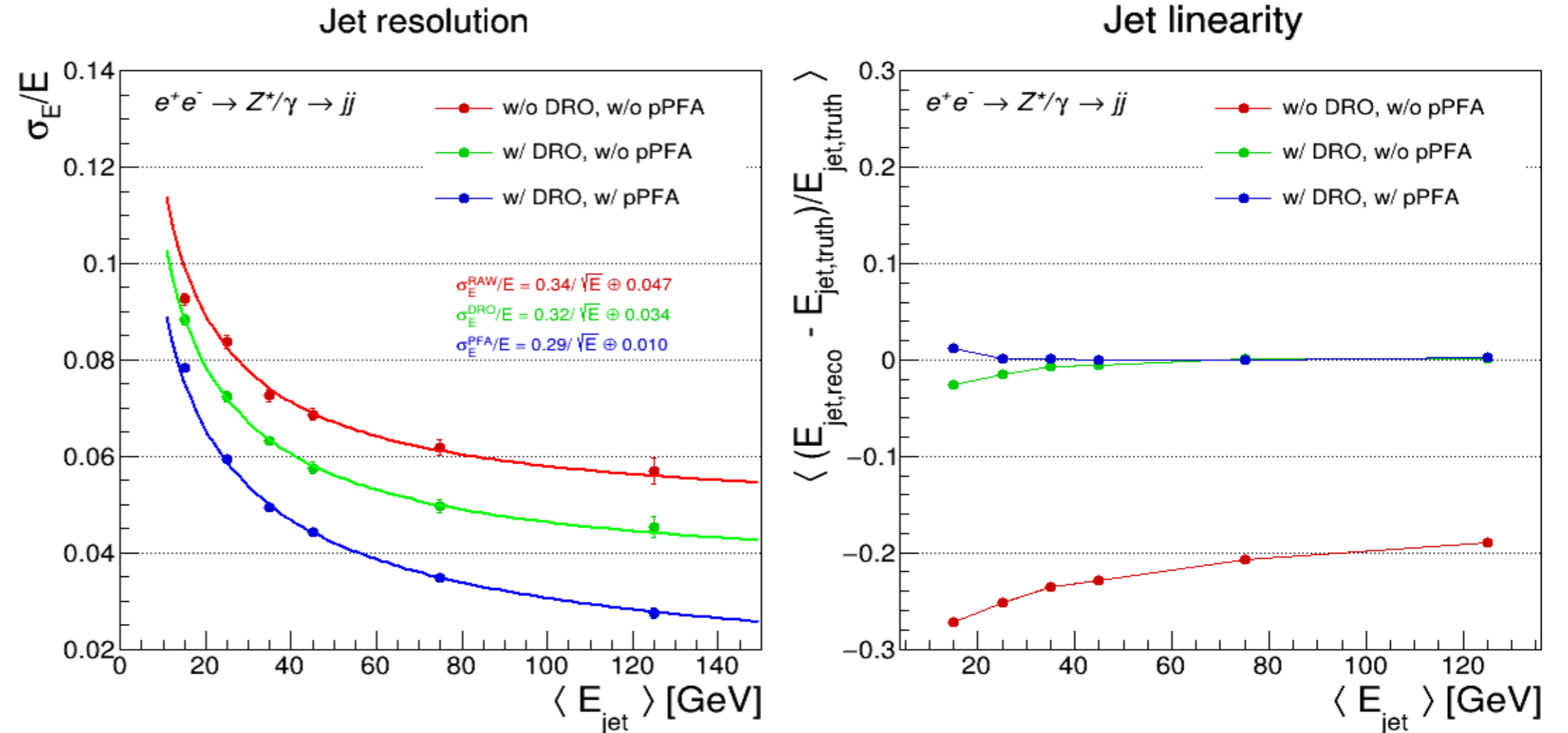
# jet energy resolution w/ and w/o DR-pPFA

<https://doi.org/10.1088/1748-0221/17/06/P06008>

Resolution and linearity as a function of jet energy in off-shell  $e^+e^- \rightarrow Z^* \rightarrow jj$  events (at different centre-of-mass energies):

*More details in: 2022 JINST 17 P06008*

- crystals + IDEEA w/o DRO
- crystals + IDEEA w/ DRO
- crystals + IDEEA w/ DRO + pPFA

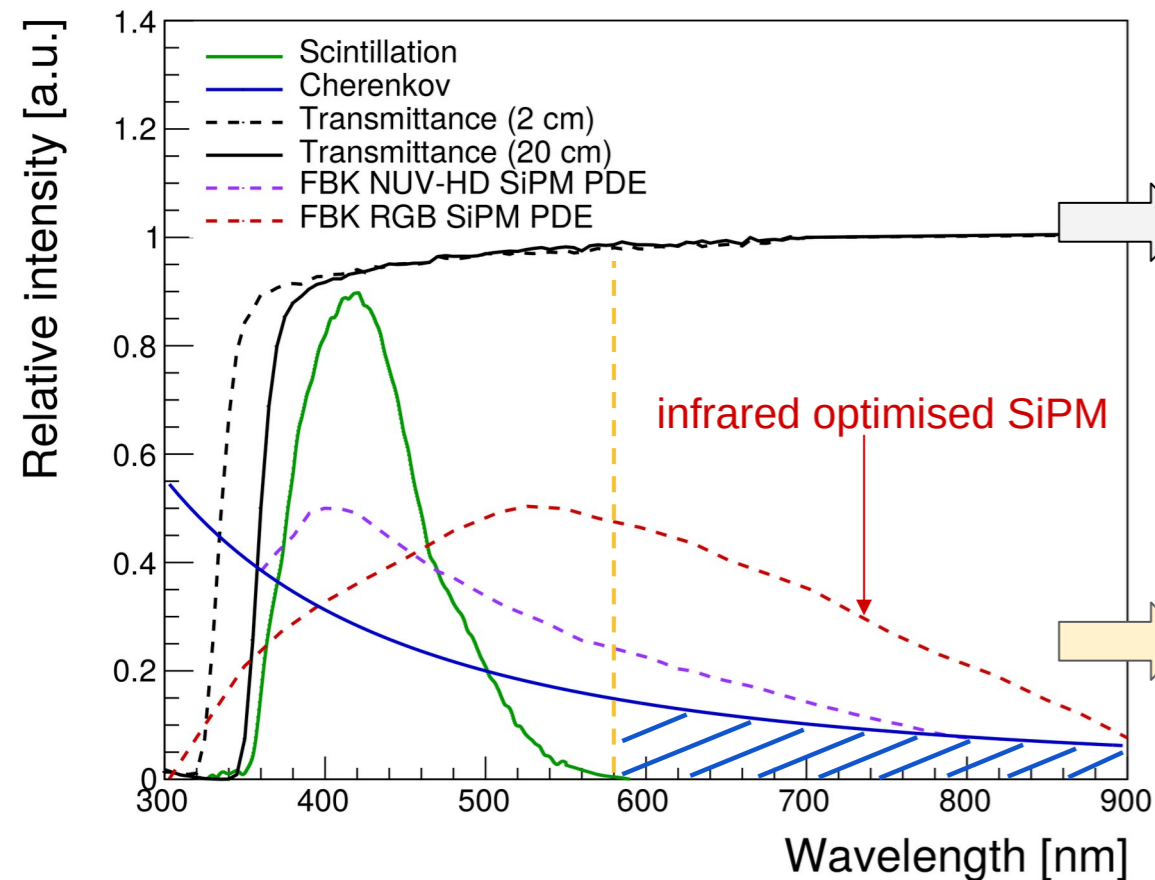


**Sensible improvement in jet energy resolution using dual-readout information combined with PF approach → 3-4% for energies above 50 GeV**

# dual-readout challenge w/ crystals

- Light yield and purity of S and C signals - likely - key discriminant between crystal options
- Different strategies exploitable for different scintillators

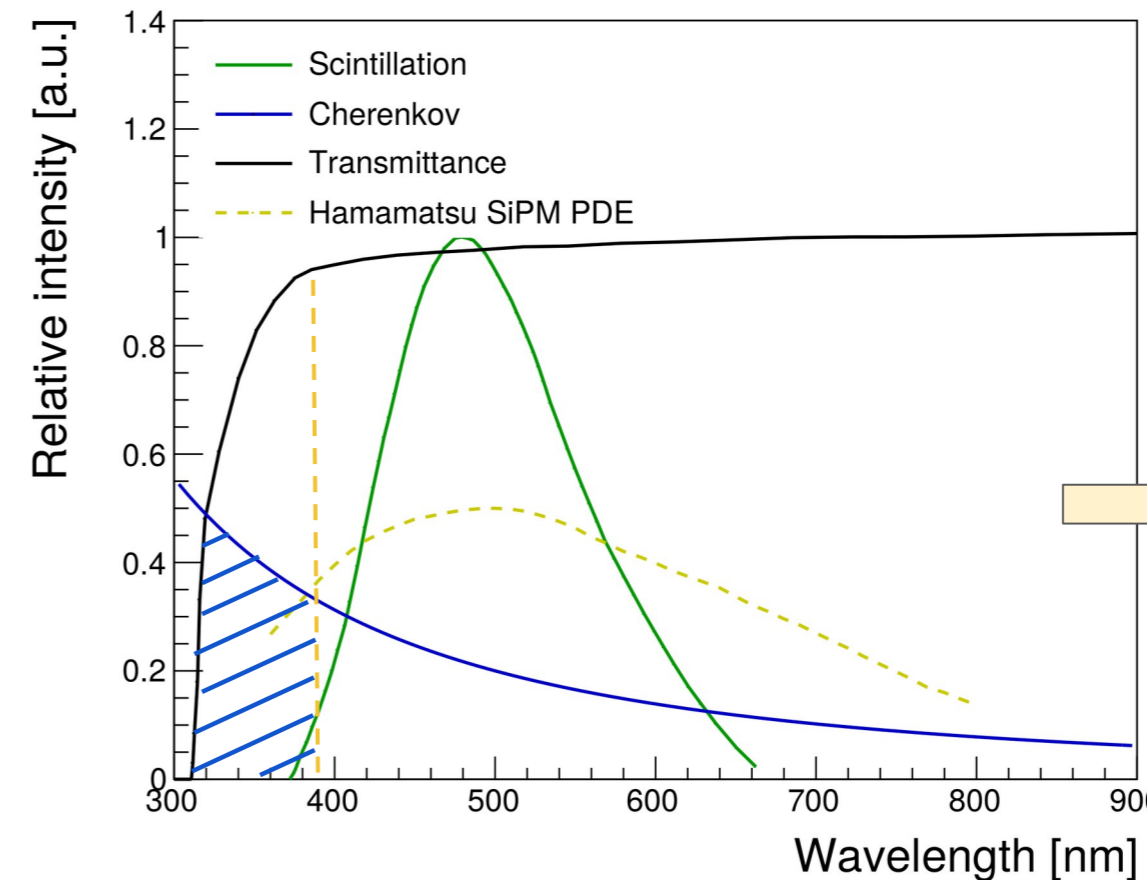
## PWO



Estimated:  
>2000 pe/GeV for  
scintillation photons  
>100 pe/GeV for  
Cherenkov photons

Cherenkov photons  
above scintillation peak  
much less affected by  
self-absorption

## BGO / BSO



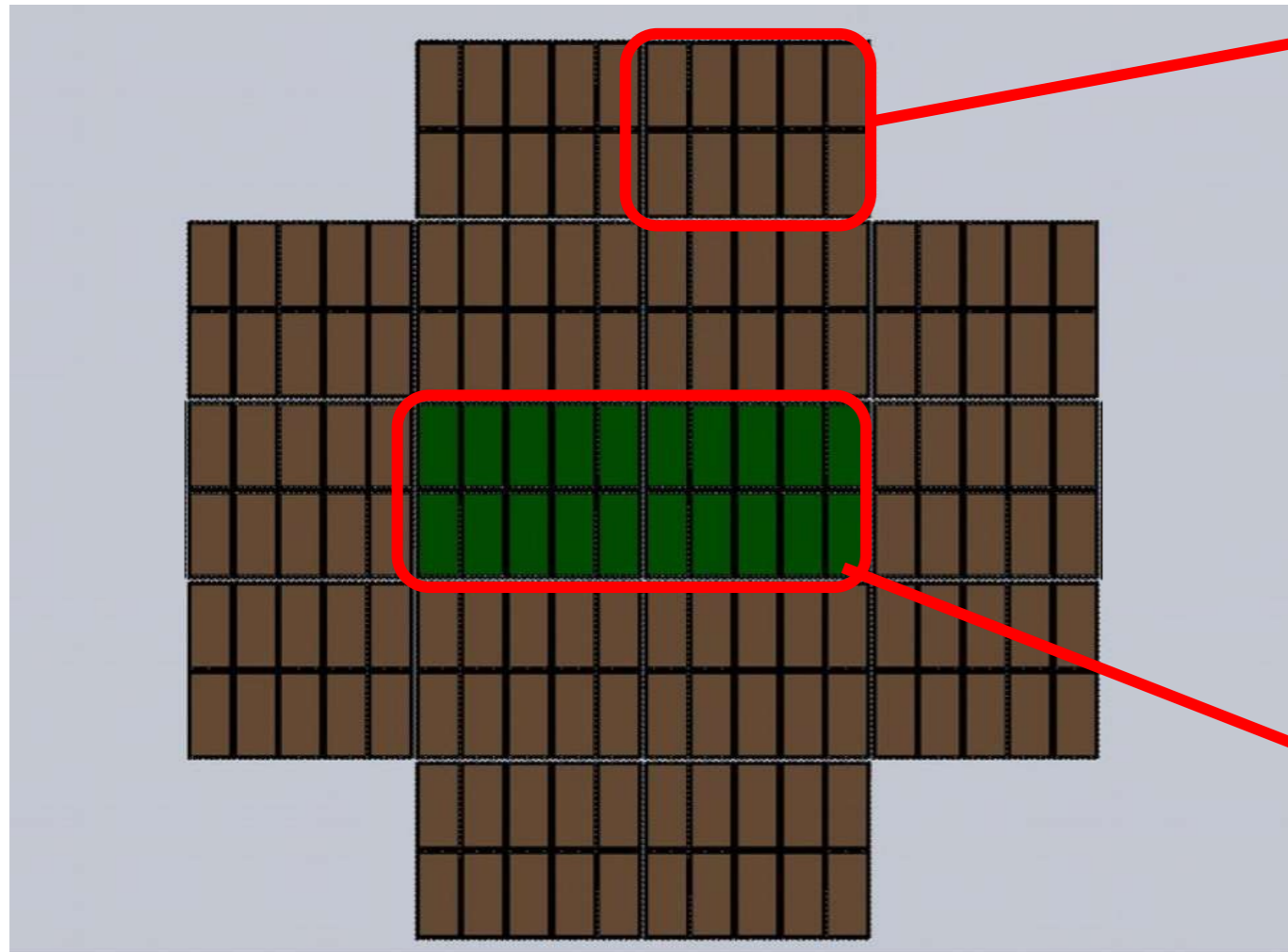
Larger Stokes shift, i.e.  
wider range of  
transparency for  
'Cherenkov UV'  
photons

---

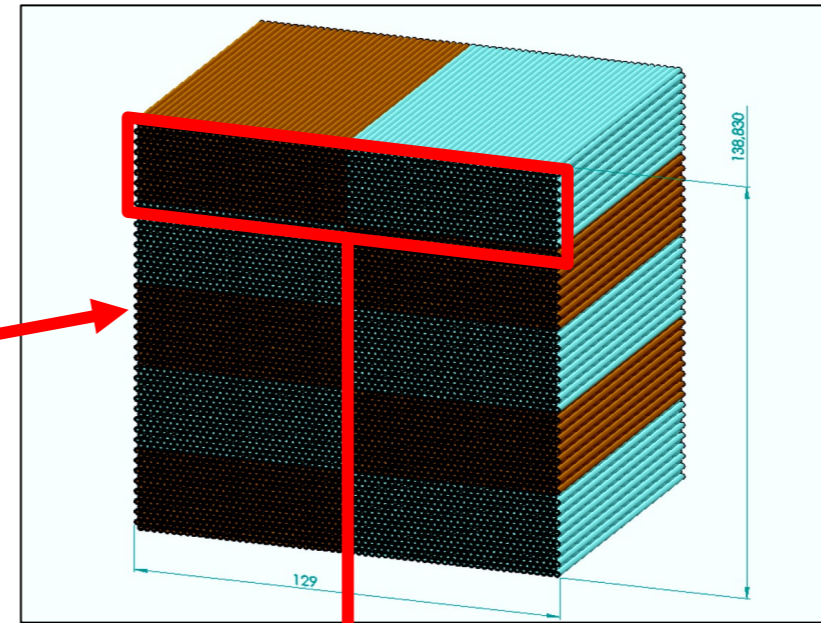
# Hadronic-containment prototype

# HiDRa – Highly granular Dual Readout demonstrator

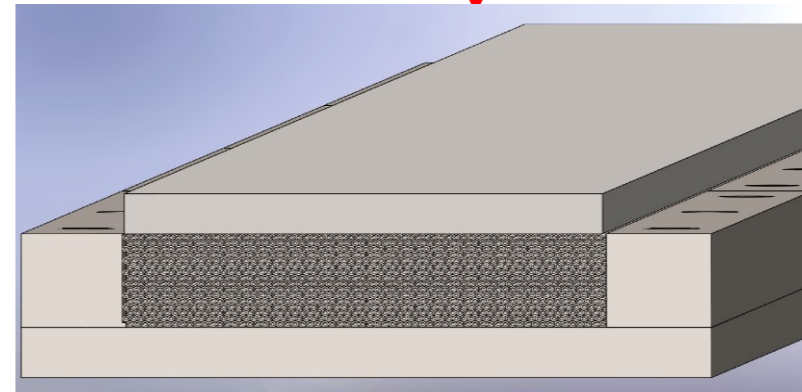
Hadronic-size prototype:  
16 modules w/ highly granular core



~ 65 × 65 × 250 cm<sup>3</sup>



1 Module: 5 MMs  
~ 13 × 13 cm<sup>2</sup>  
5120 fibres



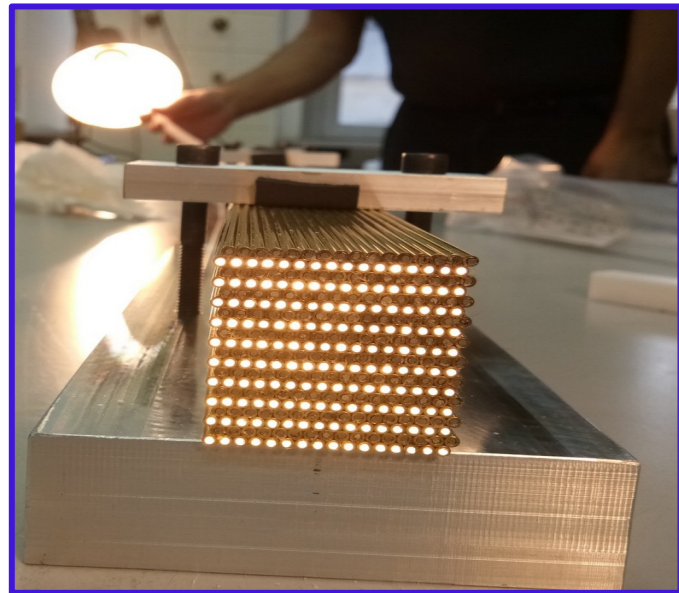
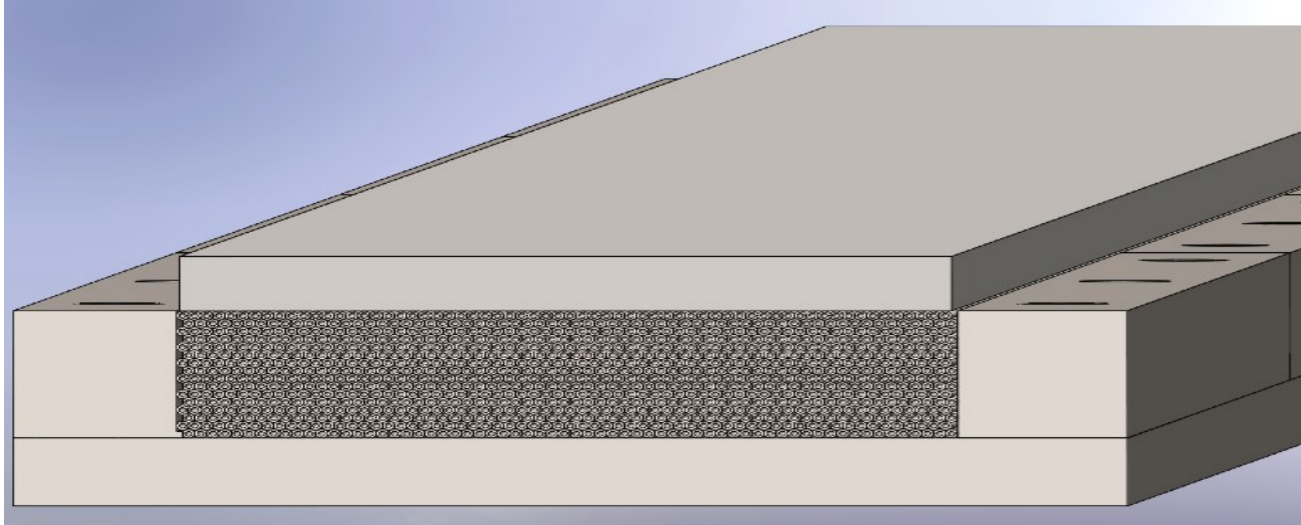
1 MiniModule:  
64 × 16 = 1024 fibres in total  
512 S + 512 C

highly granular core:  
10240 fibres to be read out with SiPMs

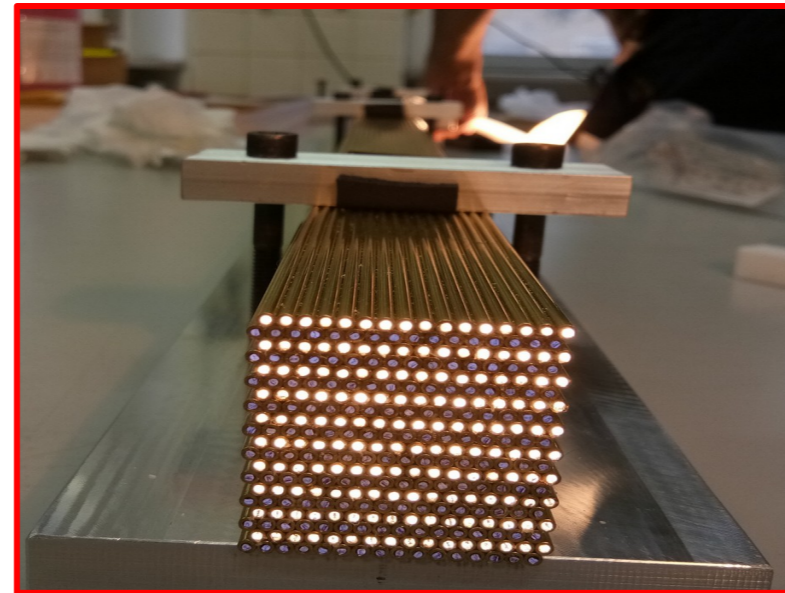


# Work in progress

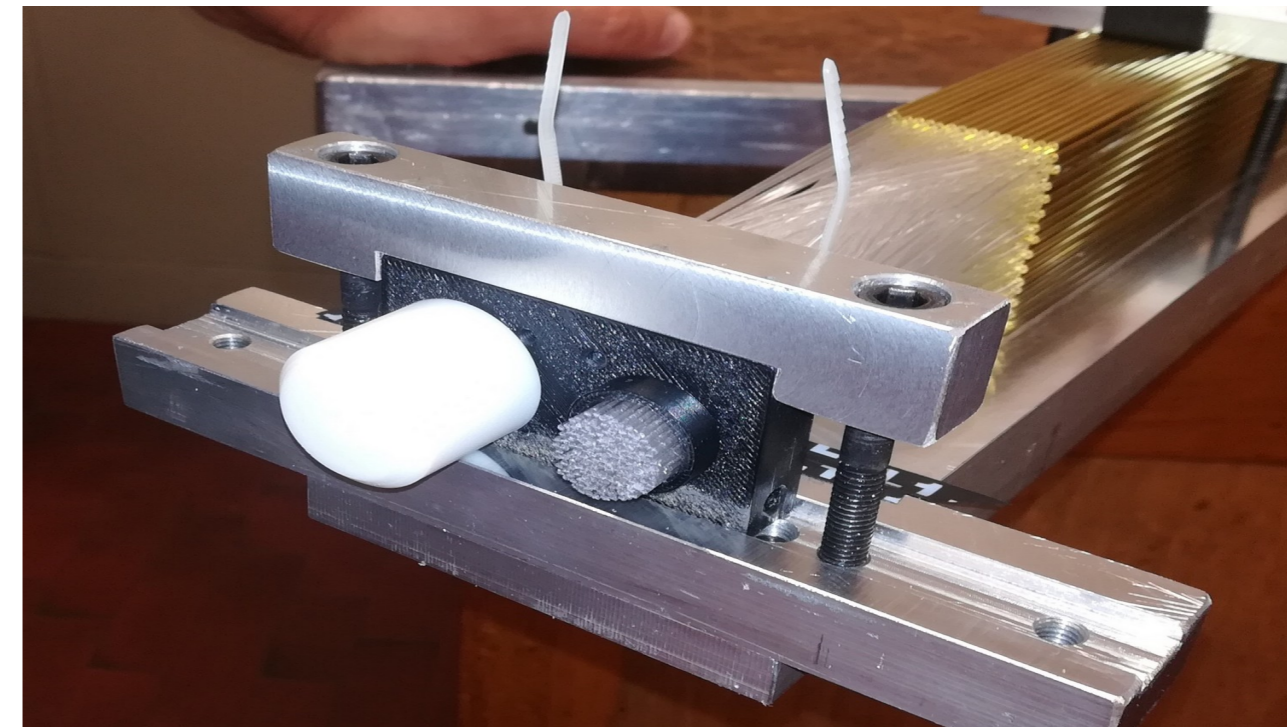
- Stainless steel capillary tubes w/ 2 mm diameter
- C and S fibres positioned per row
- Fibre separation at calorimeter rear end
- Fibre grouping for PMT coupling



scintillating fibres



Cherenkov fibres



Fibre disposal and grouping (pictures from 2020 brass prototype)

# SiPMs for HiDRa

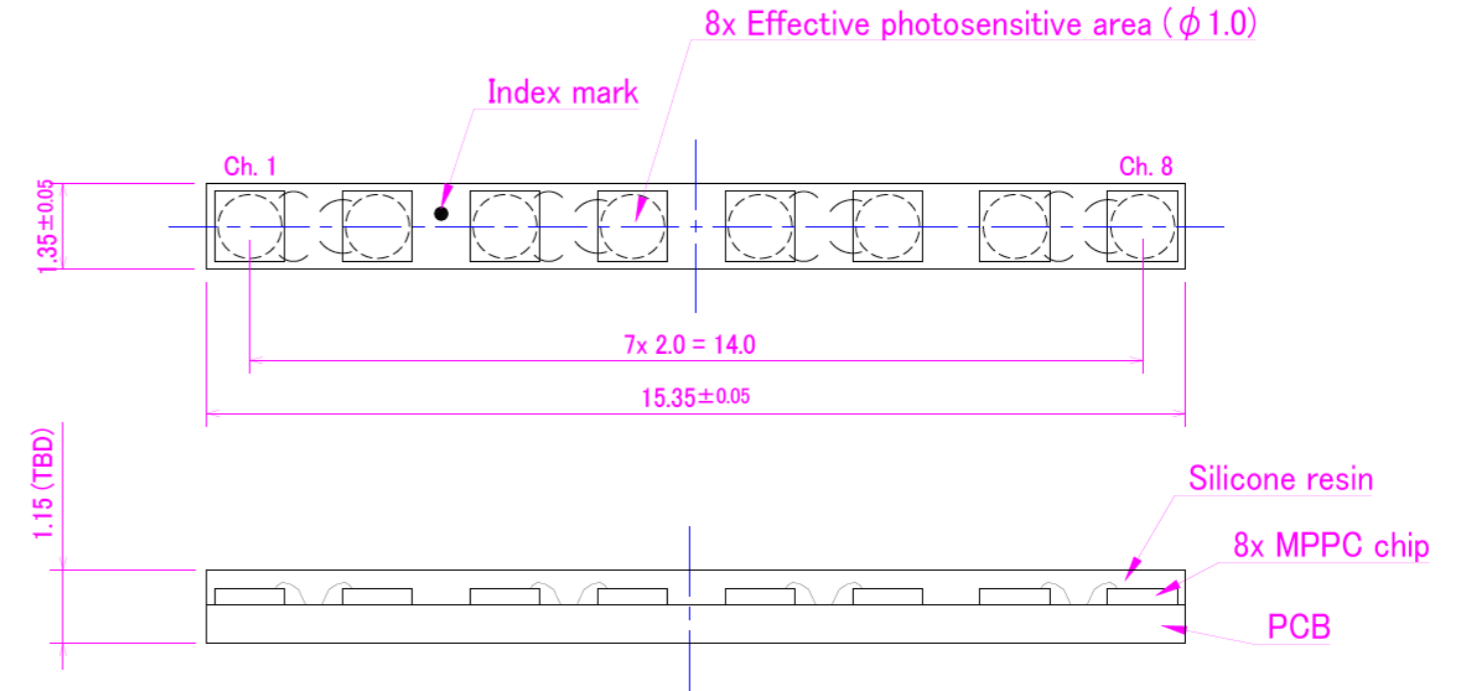
New solution by Hamamatsu:

boards with 8 “in-line” SiPMs

dimension  $1 \times 1 \text{ mm}^2$

10 or 15  $\mu\text{m}$  cell size

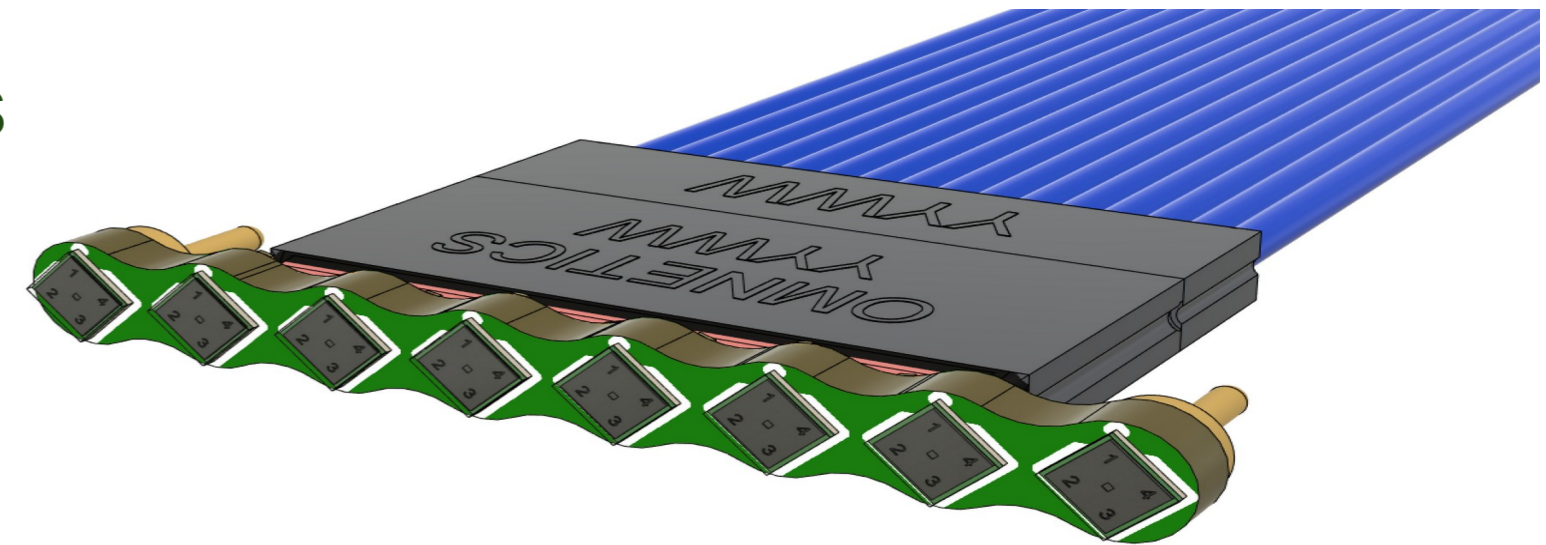
SiPMs selected such that  $\Delta V_{\text{bd}} < 100 \text{ mV}$



Our present best fit:

a) use 10  $\mu\text{m}$  cell-size SiPMs for scintillating fibres

b) use 15  $\mu\text{m}$  cell-size SiPMs for clear fibres

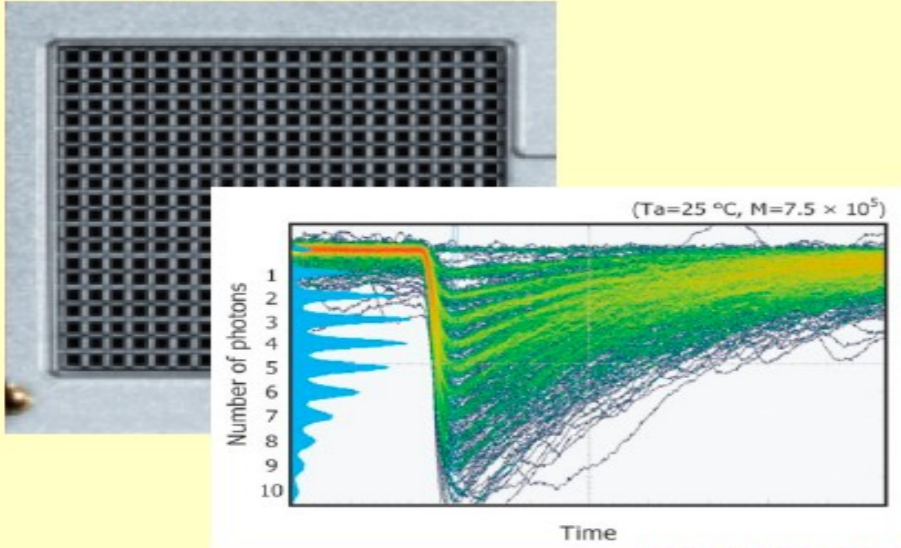


Testing 10 boards per cell-size type



# Alternative photosensors

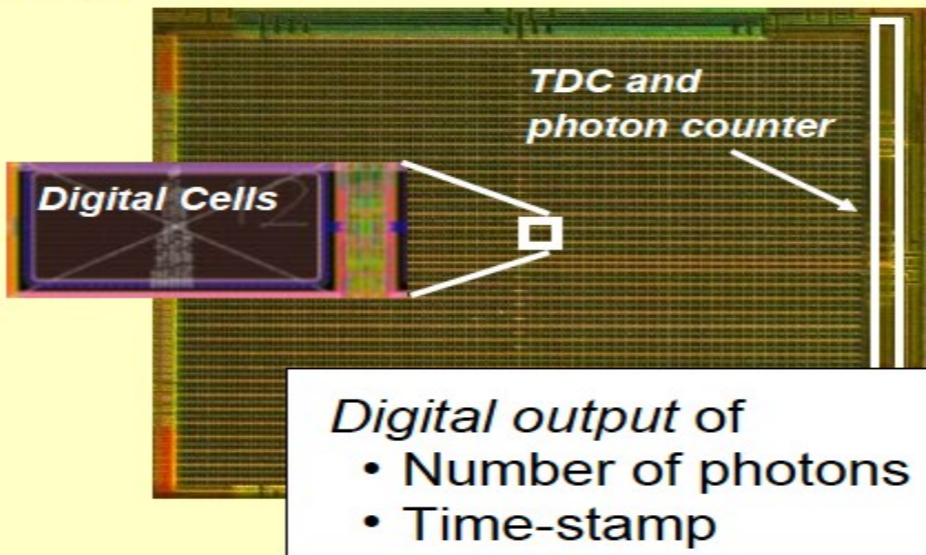
## Analog SiPM



The image shows a physical Analog SiPM sensor on the left, which is a square chip with a grid of small diodes. On the right is a graph showing the signal output. The y-axis is labeled 'Number of photons' and ranges from 1 to 10. The x-axis is labeled 'Time'. The graph shows a series of pulses that increase in amplitude over time, indicating the detection of multiple photons. The conditions for the measurement are given as  $(T_a=25\text{ }^\circ\text{C}, M=7.5 \times 10^5)$ . The source is cited as [www.hamamatsu.com](http://www.hamamatsu.com).

- Cells connected to common readout
- Analog sum of charge pulses
- Analog output signal

## Digital SiPM



The image shows a physical Digital SiPM sensor on the left, which is a square chip with a grid of small diodes. On the right is a graph showing the digital output. The y-axis is labeled 'Number of photons' and ranges from 1 to 10. The x-axis is labeled 'Time'. The graph shows a series of pulses that increase in amplitude over time, indicating the detection of multiple photons. The conditions for the measurement are given as  $(T_a=25\text{ }^\circ\text{C}, M=7.5 \times 10^5)$ . The source is cited as [www.hamamatsu.com](http://www.hamamatsu.com).

*Digital Cells*

*TDC and photon counter*

*Digital output of*

- Number of photons
- Time-stamp

- Each diode is a digital switch
- Digital sum of detected photons
- Digital data output

**digital SiPMs (dSiPMs)**

**no need for analogue-signal post-processing**

- SPAD array in CMOS:
  - complex functions embedded in single substrate (e.g. SPAD masking, counting, TDCs)
  - front-end electronics optimised to preserve signal integrity ( $\rightarrow$  timing)
  - simplified assembly of large area detectors
  - R&D costs relatively low for design over standard process

# Conclusions

---

Growing interest for dual-readout calorimetry

(other activities ongoing on dual- and also triple-readout calorimeters)

IDEA fibre calorimeter: dual-readout + single-fibre light sensors (SiPM) + timing

→ highly granular 3D information

Dual-readout crystal option → may boost em performance without spoiling hadronic one

Highly granular 3D information

→ powerful input for deep-learning algorithms and/or PFA

→ highly performing final-state identification capabilities

Many R&D activities ongoing exploiting all directions → including different readout options (both charge-integrator and waveform sampling ASICs)

Hadronic-scale demonstrators under construction



# Targets

---

Demonstrate (assess) physics performance for both single hadrons and jets (and electrons)

Validate Geant4 shower modeling

Assess scalable solutions concerning construction and signal readout/handling

Exploit DNN architectures for physics analysis

Assess performance in relevant benchmark physics channels

→ **Fully exploit dual-readout potential for physics programme at FCC-ee**

# Further lectures

---

R. Wigmans, Calorimetry: Energy Measurement in Particle Physics, Inter. Series of Mono-graphs on Phys.107, Second Edition, Oxford Scholarship Online (2017)

R.L. Workman et al. (Particle Data Group), Prog. Theor. Exp. Phys. 2022, 083C01 (2022)

W.R. Leo, Techniques for nuclear and particle physics experiments, Springer-Verlag, 1994

C. Fabjan, Calorimetry in high energy physics, in Techniques and Concepts of high energy physics III, T. Ferbel ed., Plenum Press, New York, 1985